In presenting the dissertation as a partial fulfillment of the requirements for an advanced degree from the Georgia Institute of Technology, I agree that the Library of the Institution shall make it available for inspection and circulation in accordance with its regulations governing materials of this type. I agree that permission to copy from, or to publish from, this dissertation may be granted by the professor under whose direction it was written, or, in his absence, by the dean of the Graduate Division when such copying or publication is solely for scholarly purposes and does not involve potential financial gain. It is understood that any copying from, or publication of, this dissertation which involves potential financial gain will not be allowed without written permission.

_____

_____

VAPOR-LIQUID PHASE EQUILIBRIA OF THE BINARY SYSTEM ARGON-HELIUM

A THESIS

Presented to

The Faculty of the Graduate Division

by

William David McCain, Jr.

In Partial Fulfillment

of the Requirements for the Degree

Doctor of Philosophy in the School of Chemical Engineering

Georgia Institute of Technology

April, 1964

54
12-R

VAPOR-LIQUID PHASE EQUILIBRIA

OF THE BINARY SYSTEM

ARGON-HELIUM

Approved:

Date approved by Chairman: May 8 1964

ACKNOWLEDGEMENTS

The author is grateful to his thesis adviser, Dr. Waldemar T. Ziegler, for the suggestion of the research work and his helpful suggestions and constructive criticisms as it progressed.

The advice and encouragement given by the author's fellow students; Mr. David W. Yarbrough, Dr. Bradley S. Kirk, and Mr. Joseph C. Mullins, is gratefully acknowledged. The latter two were particularly helpful in the calculational phase of this research and Dr. Kirk made a large contribution in the experimental phase. The extent of their contribution will be apparent to the reader of their theses.

A portion of this research work was supported by the Engineering Experiment Station of the Georgia Institute of Technology. The experimental work was performed in the facilities of the Experiment Station. Without this help the experimental work would have been extremely difficult.

A large amount of computer time was used in this study and appreciation is expressed to the staff of the Rich Electronic Computer Center for their assistance.

The author also wishes to express his appreciation to the Texas Company for the Texaco Fellowship in Chemical Engineering during the academic year 1959-1960, and to the Air Reduction Company for the Air Reduction Company Cryogenic Fellowship for the academic years 1960-1961, 1961-1962, and 1962-1963. The Air Reduction Company grant furnished subsistence for the author's family and also provided funds for purchase of

equipment. This expression of appreciation seems very small compared to the major effect these grants had on the life of the author.

Finally the encouragement of three fine Mississippians: Dr. W. D. McCain, Dean Harry C. Simrall, and Dr. Eldred W. Hough must be gratefully acknowledged. Dean Simrall and Dr. Hough made the completion of this work much easier than it would have been without their interest.

TABLE OF CONTENTS

LIST OF TABLES

LIST OF FIGURES

SUMMARY

The dew points and bubble points of mixtures of helium and argon were studied at temperatures from 100° K to 150° K and at pressures below 70 atmospheres.

Experimental determinations of dew-point and bubble-point pressures of mixtures of known composition were made at various temperatures. The equipment was of the general type used by researchers at the Institute of Gas Technology in studying several binary mixtures of the components of natural gas.

The method involves the injection of a mixture of known composition into a glass cell held at constant temperature in a cryostat. The pressure at the instant of first visual observation of formation of drops of liquid was designated as the dew-point pressure. The bubble-point pressure was taken as the pressure corresponding to the first visual observation of the formation of a gas bubble in the cell full of liquid as pressure was reduced at constant temperature.

These dew points and bubble points were used to construct the pressure-temperature (P-T) diagram of the binary system. The data were then graphically interpolated to permit construction of equilibrium diagrams of pressure against composition (P-x) and temperature against composition (T-x). The data were further presented in the form of equilibrium vaporization constants, $K = y/x$, against pressure (K-P) at even values of temperature and as enhancement factors against pressure (ϕ-P) at even values of temperature.

At the time that this project was initiated the only other phase equilibrium data for this system were the very limited data of Karasz and Halsey (29). However, Mullins (41) has recently completed an experimental study of the vapor-liquid and vapor-solid phase equilibria of this system from 108° K to 68° K. Mullins obtained only one isotherm above 100° K so the overlap region between his data and the data of this work is limited.

The assigned precision of the pressure and temperature measurements of the dew points and bubble points is ±0.02° K and ±0.15 atm. The uncertainty in the composition of the prepared gas mixtures used is ±2 per cent of the concentration of the minor constituent.

The bubble points have been measured with a precision of ±0.02° K, ±0.15 atm. or ±2 per cent of the helium concentration except below about 110° K where comparison of the data with the results found by Mullins suggests that the uncertainty in the helium concentration may be as much as ±5 per cent, rising to as much as 20 per cent at the lowest temperature (99.92° K).

The dew points have been measured with the same apparent precision in temperature and pressure as given above. However, because of the low argon concentration present at the lower temperatures, the composition of the equilibrium gas is known less accurately. The estimated overall errors, in terms of the composition limits for the assigned pressure and temperature are:

1. ±2 per cent of the concentration of the minor component (helium) at temperatures between 135° K and 145° K.

2. ±5 per cent of the concentration of the minor component (ar-

gon or helium) at temperatures between 125° K and 130° K.

3. ±10 per cent of the concentration of the minor component (argon) at temperatures between 110° K and 120° K.

4. ±15 per cent of the concentration of the minor component (argon) at 105° K.

As a part of the calibration and testing of the equipment, the vapor pressure of argon has been measured in the temperature range 114.5° K to 150.6° K. These measurements agree with the best available vapor pressure data from the literature to better than ±0.02° K and ±0.15 atm. The critical temperature and critical pressure of argon have been determined to be 150.65° K and 47.92 atm. to within ±0.02° K and ±0.15 atm. by visual observation of the appearance and disappearance of the meniscus at the critical point. The only other direct measurement of the critical point of argon appears to be that of Crommelin in 1910 who reported -122.44° C and 47.996 atm.

The vapor phase data were extrapolated through the use of the enhancement factor correlation. These extrapolations indicate that the lower temperature dew-point data of this work does not agree well with the data of Mullins. Computations were made which showed that most of the discrepancy between the two sets of data could be explained by the change of concentration of the vapor when dew was formed. This dew formation, which was essentially pure argon, could have reduced the concentration of argon in the vapor by as much as fifteen per cent.

Prediction of the equilibrium vapor compositions as a function of pressure and temperature for mixtures of helium and argon was made with an enhancement factor approach similar to that described by Kirk, Ziegler,

and Mullins (34), and improved by Kirk (33). The lengthy equation for prediction of enhancement factor used in this work is suitable only for systems in which the liquid may be assumed to contain only one of the components. In order to use this equation one must select a method of estimating the properties of the gas phase and also of determining the properties of the pure condensed phase.

The properties of the gas mixtures were estimated with the virial equation of state truncated after the third virial coefficient. The Kihara core model with a 6-12 potential function was used to estimate the second virial coefficients of the gas mixtures, and the Lennard-Jones 6-12 potential function was used to estimate the third virial coefficients of the gas mixtures. The properties of the liquid phase, which was assumed to be pure argon, were taken from published experimental data.

The calculated values of enhancement factor were graphically compared with the experimental data. Reasonably good agreement was observed at the higher temperatures. However, at the lower temperatures the experimental values of enhancement factor were as much as fifteen per cent higher than the calculated values.

Comparison of the dew-point data with the vapor phase equilibrium data of Mullins below 108^{o} K by use of the enhancement factor as a correlating function showed the two sets of data to be in fair agreement. Computation showed that most of the discrepancy between the two sets of data could be explained by a decrease in concentration of argon resulting when the dew is formed. This dew formation, which was essentially pure argon, could have reduced the concentration of argon in the vapor by as

much as 15 per cent near 105° K.

NOMENCLATURE

a	constant in liquid volume equation constant in thermocouple calibration equation
B	second virial coefficient
b	constant in liquid volume equation constant in thermocouple calibration equation
b_o	volumetric parameter in Lennard-Jones potential function
C	third virial coefficient
c	constant in thermocouple calibration equation
d	constant in thermocouple calibration equation
E	electrical potential
e	constant in thermocouple calibration equation
e/k	energy parameter in Lennard-Jones potential function
I	general interaction coefficient in the enhancement factor equation
K_h	modified Henry's law constant
M_o	parameter of Kihara core
n	number of moles
P	total system pressure
p	vapor pressure
R	gas constant (0.0820545 liter-atm/gm mole-^oK)
S_o	surface parameter of Kihara core
T	temperature, ^oK
t	temperature, ^oC
U	potential energy
U_o	maximum (negative) potential energy

V	molal volume of condensed phase
V_o	volume parameter of Kihara core
v	molal volume of condensed phase
x	mole fraction in condensed phase
y	mole fraction in gas phase
z	compressibility factor, PV/RT

GREEK SYMBOLS

σ	shortest distance between Kihara molecular cores
σ_o	shortest distance between Kihara molecular cores at minimum energy
ϕ	enhancement factor

SUBSCRIPTS

1	condensable component at temperature and pressure
01	condensable component under its vapor pressure
2	non-condensable component at temperature and pressure
12	interaction between components 1 and 2
112	interaction between components 1 and 2
122	interaction between components 1 and 2
b	interaction coefficient containing y and B only
c	interaction coefficient containing y and C only
m	gas mixture

CHAPTER I

INTRODUCTION

Certain binary systems exhibit unusual liquid solubility effects. These systems show an increase of concentration of the lighter component in the liquid phase as the temperature is increased at constant pressure. In the normal system this concentration in the liquid phase of the lighter component would decrease as temperature is increased. We refer to these unusual systems as "reverse solubility" systems.

These reverse solubility systems invariably consist of one component whose critical temperature is well below the triple point temperature of the other component. Thus the temperatures at which vapor-liquid equilibria can exist are well above the critical temperature of one component and below the critical temperature of the other component. A number of investigations of systems of this type have been reported. For instance, the binary system, nitrogen-helium, which has been experimentally investigated by several researchers (31, 19, 6, 23, 11, 6, 12). Although the results of these investigations do not agree particularly well, they do show that this binary system, in which the temperature range for the liquid region of nitrogen is well above the critical temperature of helium, does exhibit reverse solubility. Other systems, such as methane-helium (30, 24) and methane-hydrogen (33, 1, 46, 16, 22), also have the same characteristic.

It should be noted that the reverse solubility effect is not a

result of chemical type, as the components mentioned above are also found in systems which do not show reverse solubility. For instance, the methane-nitrogen system, which has been investigated by a great number of researchers (7, 3, 4, 17, 18, 20, 37, 48, 50), exhibits normal solubility behavior. The temperature range of vapor-liquid phase equilibria is approximately 90°K to 190°K, which is below the critical temperature of methane and includes the critical temperature of nitrogen. There are many other binary systems containing one of these components, such as the nitrogen-ethane system (15, 43), the methane-ethane system (2, 5, 36, 44, 45), and the nitrogen-oxygen system (13), which have normal solubility relationships.

By analogy with other systems, such as the nitrogen-helium binary mentioned above, it was predicted that binary mixtures of argon and helium would also exhibit reverse solubility. That is, it was thought that the concentration of helium in the equilibrium liquid phase would increase as temperature increased at constant pressure. This was found experimentally to be true. The vapor-liquid phase equilibria of mixtures of helium and argon were experimentally investigated at temperatures from 100°K to 145°K over a pressure range of 10 to 70 atmospheres. The only other phase data for this system are those of Mullins (41) at temperatures from 108°K down into the solid-vapor region, which became available after this investigation was completed, and the limited vapor-liquid data of Karasz and Halsey (29).

It is interesting to note that the system ammonia-argon (38) exhibits reverse solubility. However, in this system, unlike the argon-

helium system, argon is the constituent which has a critical temperature much lower than the temperature region of existence of vapor-liquid equilibria. Therefore argon is the minor component in the liquid phase and the composition of argon in the liquid increases with temperature at constant pressure. Also, this system has a vapor-liquid temperature range above room temperature, thus eliminating low temperature as a possible cause of the reverse solubility effect.

As an aid in evaluating the precision and accuracy of the experimental vapor phase data, calculations of the enhancement factor, after the work of Kirk (33), were made. The enhancement factor is defined as

$$\phi = \frac{Py_1}{p_{01}} \tag{1}$$

The equation of Kirk is

$$\ln\phi = \ln \frac{zm}{z_{01}} + \frac{(P - p_{01})}{RT}\left[a + \tfrac{1}{2}b(P + p_{01})\right] + \left[2\frac{B_{11}}{V_{01}} + \frac{3}{2}\frac{C_{111}}{V_{01}^2}\right]$$

$$- \frac{2(y_1B_{11} + y_2B_{22})}{V_m} - \frac{3}{2}\frac{(y_1^2C_{111} + 2y_2y_1C_{112} + y_2^2C_{122})}{V_m^2} \tag{2}$$

The following assumptions were made in the derivation of this equation and in its use in this investigation:

1. The condensed phase contains only one component (component 1).
2. The virial equation of state truncated after the third term

adequately represents the properties of the vapor mixture and the vapor of pure component 1.

3. The Kihara core model with a 6-12 potential function may be used to estimate the second virial and second virial interaction coefficients.

4. The Lennard Jones 6-12 potential function may be used to estimate the third virial and third virial interaction coefficients.

5. Certain simple mixture rules may be used to compute the second and third virial interaction coefficients.

6. An equation linear in pressure may be used to represent the compressibility of the pure condensed phase.

A modified Henry's law relationship defined as

$$K_h = \frac{P - p_{01}}{x_2 \cdot 100} \tag{3}$$

was used as an aid in evaluating the liquid data.

CHAPTER II

INSTRUMENTATION AND EQUIPMENT

The method employed to obtain experimental equilibrium vapor and liquid phase compositions involved the measurement of dew and bubble point temperatures and pressures for gas mixtures of known composition. The reasons for the selection of this method from the several methods which have been used by other investigators are given below.

Selection of Experimental Method

If one major problem in phase equilibria experimentation had to be selected, it most certainly would be the analytical problem. This includes the difficulty of obtaining representative samples, usually of both phases, as well as the complications of precision analysis, and preparation of acceptable standards for calibration and recalibration of analytical equipment. In the dew-bubble-point experimental method, selected in this work, the sampling problem is virtually eliminated, as will be shown later, and the analytical problem is minimized due to the large reduction in required analyses.

Another advantage of the dew-bubble-point method, as applied in this work, which is of interest to the experimenter, is the opportunity to visually observe the conditions in the equilibrium cell. Of primary importance is the possibility of formation of two immiscible liquid phases which could go undetected in techniques which do not permit visual observation.

The question of attainment of equilibrium between the two phases, a question which is necessarily asked of all phase equilibria experimental methods, is completely satisfied, in principle, by the use of the dew-bubble-point method. The procedures used in this experimentation, as will be described in detail later, assure that the primary phase under observation is homogeneous, and therefore that the initial drop of liquid or bubble of gas, as the case may be, is in equilibrium with the primary phase.

The precision measurement and control of temperature and pressure depend primarily on careful design and equipment selection; therefore these are of secondary importance in selection of an experimental method.

Briefly, the experimentation involved obtaining temperatures and pressures at which dew and bubble points occurred for mixtures of helium and argon of known composition. The dew-points were attained by slowly injecting the known composition gas mixtures into the glass equilibrium cell at constant temperature, thereby increasing the pressure, until the first droplets of liquid were observed on the walls of the cell. The temperature and pressure at which this condition first occurred were considered to be the dew-point temperature and the dew-point pressure. In obtaining bubble points the first step was to quickly fill the glass cell with warm gas mixture to a pressure well above the bubble-point pressure. The mixture in the cell then cooled to cryostat temperature, thus resulting in a cell full of liquid at the proper temperature without the formation of two phases. Then the pressure was lowered slowly until small bubbles were observed, usually being formed

along the wall of the cell and immediately rising to the top of the cell. The pressure and temperature at the instant of bubble formation were taken to be the bubble-point pressure and bubble-point temperature.

A schematic diagram of the equipment used is shown in Figure 1. The equipment consisted of two main sections: the cryostat, and the gas mixing and storage section. The equilibrium cell is shown in place in the cryostat.

Equipment of this general design has been used by investigators at the Institute of Gas Technology in investigations of the phase relations of the systems methane-nitrogen (3), ethane-nitrogen (15), and methane-ethane (2). Two basic differences between the equipment of the Institute of Gas Technology and the equipment used in this research are the substitution of precision test pressure gage for the dead-weight gage used to determine equilibrium cell pressure and the elimination of the manual magnetic stirrer from the equilibrium cell. More recently, Kurata and co-workers (35, 11) have described equipment which can be used to obtain dew and bubble points.

To the author's knowledge the present investigation constitutes the only applications of this experimental method to systems which exhibit reverse solubility with such extremes of concentration.

The Equilibrium Cell

The equilibrium cell was constructed of heavy wall pyrex glass tubing of six millimeters inside diameter and 19 millimeters outside diameter, and pyrex glass capillary tubing of $\frac{1}{2}$ millimeter inside diameter and seven millimeters outside diameter. This glass was selected from normal glass stock and had wall thicknesses somewhat larger than

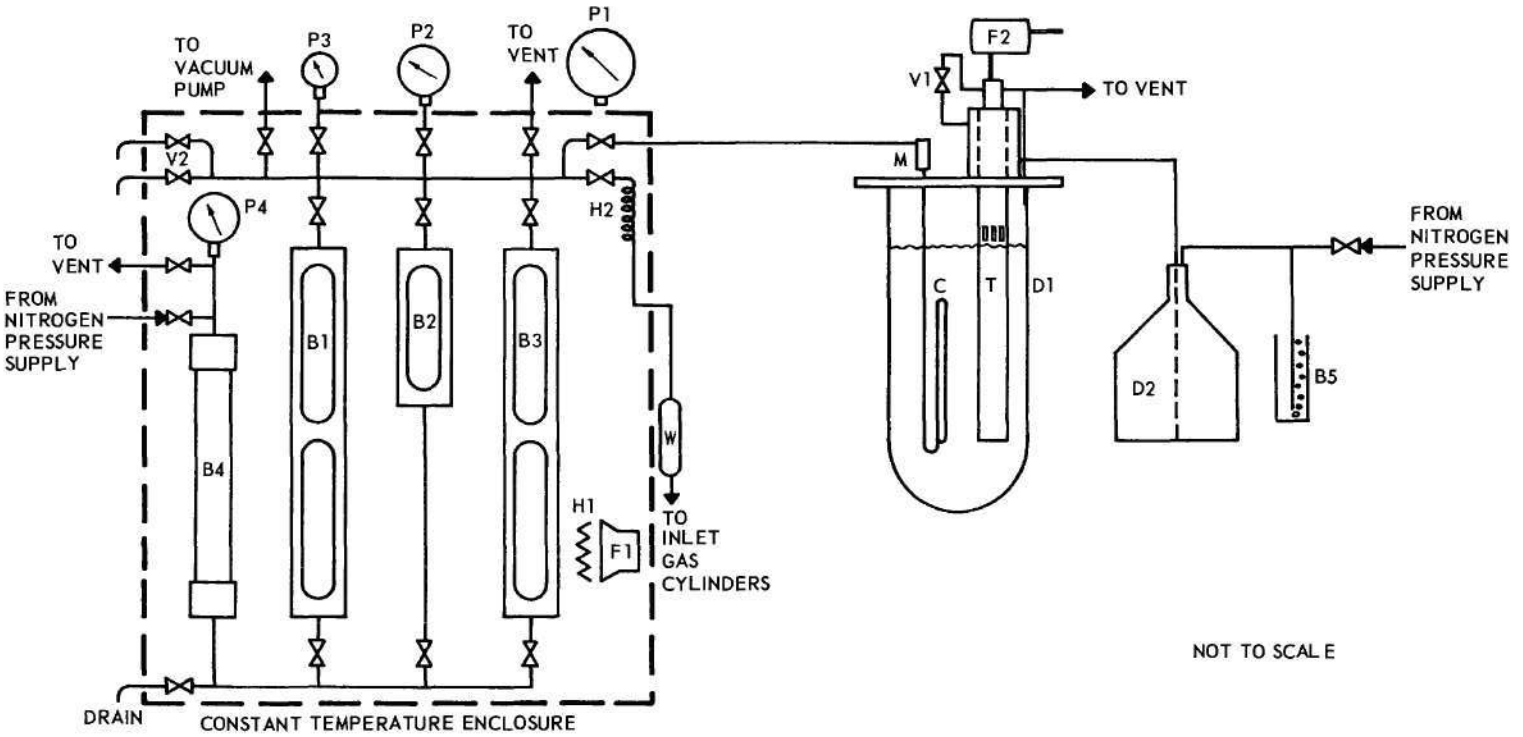

B1 – JERGUSON GAGE GAS BURET
B2 – JERGUSON GAGE GAS BURET
B3 – JERGUSON GAGE GAS BURET
B4 – MERCURY STORAGE VESSEL
B5 – NITROGEN PRESSURE CONTROL "BUBBLER"
C – EQUILIBRIUM CELL
D1 – CRYOSTAT DEWAR
D2 – LIQUID NITROGEN DEWAR
F1 – BLOWER
F2 – CRYOSTAT STIRRER
H1 – CABINET AIR HEATER
H2 – INLET GAS PREHEATER
M – METAL TO GLASS TUBING CONNECTOR
P1 – EQUILIBRIUM CELL PRESSURE GAGE
P2 – MANIFOLD PRESSURE GAGE
P3 – VACUUM PRESSURE GAGE
P4 – MERCURY STORAGE PRESSURE GAGE
T – COOLING TUBE
V1 – LIQUID NITROGEN FLOW RATE CONTROL VALVE
V2 – GAS SAMPLING VALVES
W – INLET GAS DRYER

Figure 1. Schematic Diagram of Dew-Point Bubble-Point Equipment.

the nominal dimensions of the glass stock.

Figure 2 shows the cell design. Two cells of design A (volume about eight cm^3) were constructed: one as a test prototype, and one which was used throughout most of the experimental operation. One cell of design B (volume about four cm^3) was constructed and used during certain of the bubble-point and dew-point determinations. All three cells were tested at pressures over 1000 psig at temperatures from 95° to $150^{\circ}K$. Not one of the cells failed due to excessive pressure, although the prototype model was broken in handling. A scale of ceramic ink was fired onto the outside of each of the cells.

The Glass to Metal Connector

The device used to connect the glass cell to the metal tubing from the gas mixing and storage section is shown in Figure 3. This connector, which was very similar to one described by Eakin (15), was completely satisfactory. No evidence of leakage was detected at any time during testing or experimental operation.

The lower metal piece and the teflon collar were permanently attached on the glass capillary tubing of the equilibrium cell below the flanged end. When the two metal pieces were joined the lower piece forced the glass flange on the upper end of the glass capillary against the rubber o-ring shown in Figure 3. The teflon collar prevented metal-to-glass contact, thereby protecting the glass flange from rotational stresses as the lower piece was screwed in. The undercut on the lower end of the teflon collar was important as it eliminated stress on the glass capillary due to slight misalinement.

The upper metal piece was permanently fixed to the cryostat main

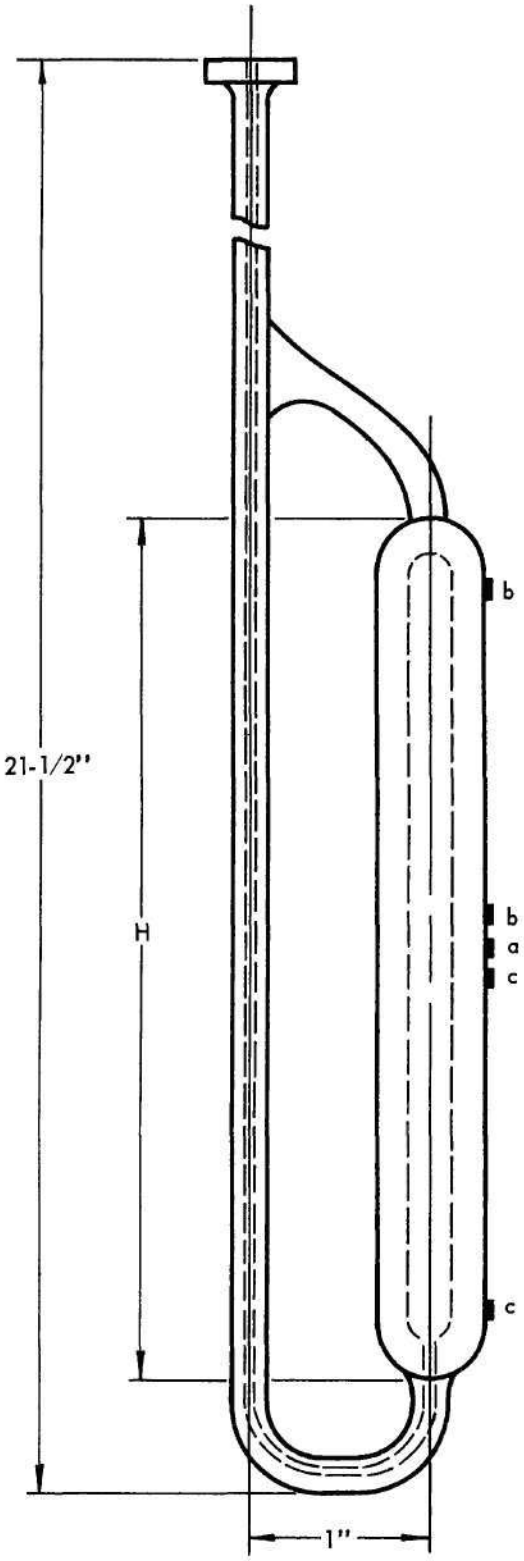

CELL	DIMENSION H INCHES
A	9-1/2
B	4-1/2

SYMBOL	MEANING
▮	indicates position of thermocouple
a	thermocouple used to measure cell temperature
b-b	upper temperature difference thermocouple
c-c	lower temperature difference thermocouple

Figure 2. Glass Equilibrium Cells.

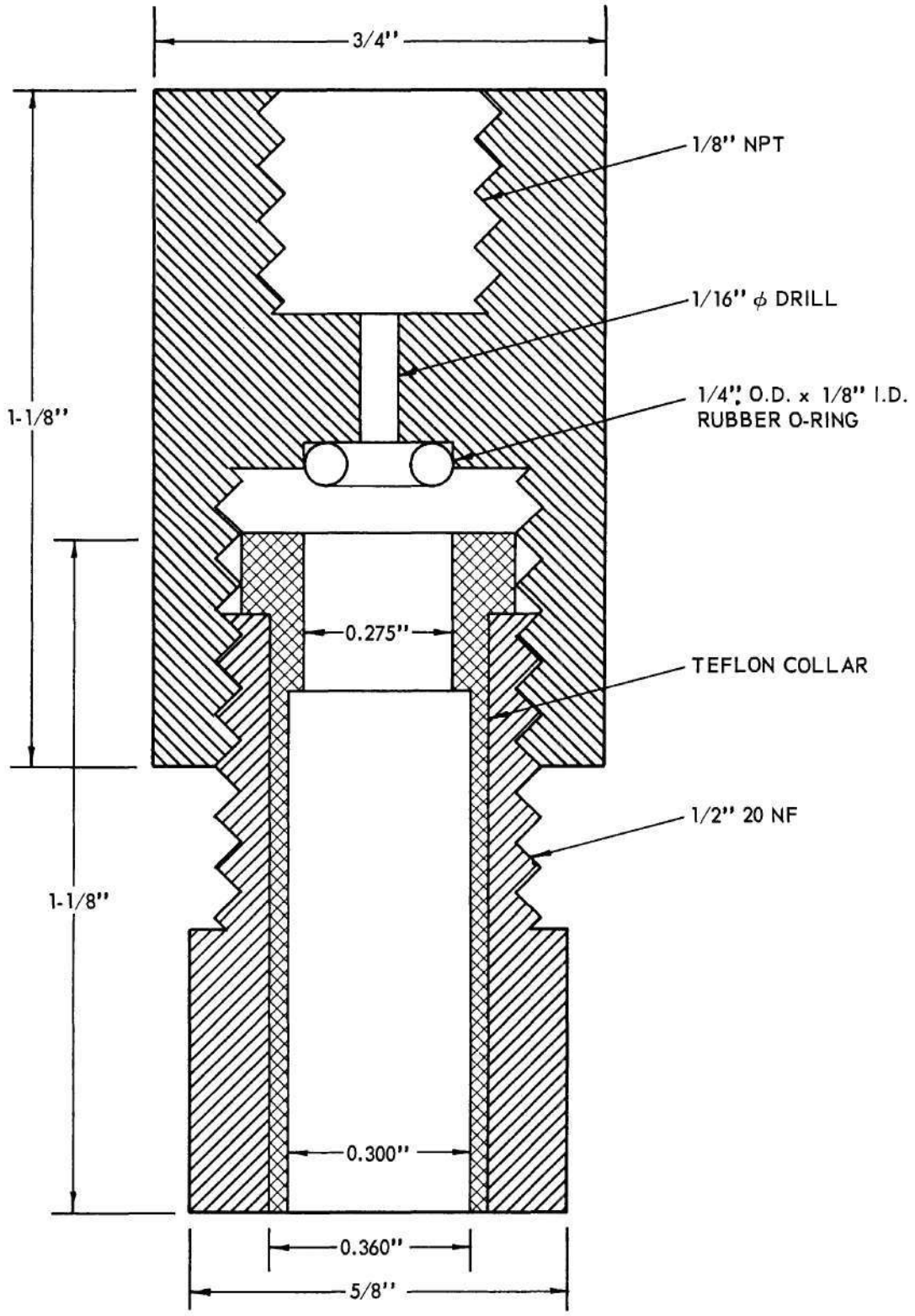

Figure 3. Metal to Glass Connector.

plate. A one-sixteenth inch tubing to one-eighth inch pipe thread adapter was threaded into the upper metal piece to connect to the stainless tubing.

The Cryostat

The construction drawing of the cooling apparatus of the cryostat, less supporting structure, is shown in Figure 4. The main plate and the stirrer motor, not shown, were rigidly fastened to the supporting structure and the remainder of the device was free to expand or contract as required. The dewar which contained the cryofluid, liquid propane, was sealed to the dewar seal sleeve, E, (seven inch brass tubing) extending below the main plate.

The Cooling Tube

Heat was removed from the cryostat through the cooling tube. The cooling tube, see item T in Figure 1 and in Figure 4, was a 24 inch long, one and one quarter inch diameter, extra strong, copper tube. The wall thickness was 0.194 inch. The upper end of the tube terminated in the nitrogen boiler, N in Figure 1, above the main plate. The cryofluid was circulated with the stirrer up the inside of the cooling tube and out the openings near the top of this tube. The cryofluid liquid level was normally maintained just below these openings. This circulation improved heat transfer from the liquid to the cooling tube and also provided agitation to the bulk of the cryofluid to eliminate temperature gradients.

An electric heater, which is not shown in Figure 4, was wound on the upper end of the cooling tube just below the nitrogen boiler to be used when rapid temperature increase was desired. This heater was

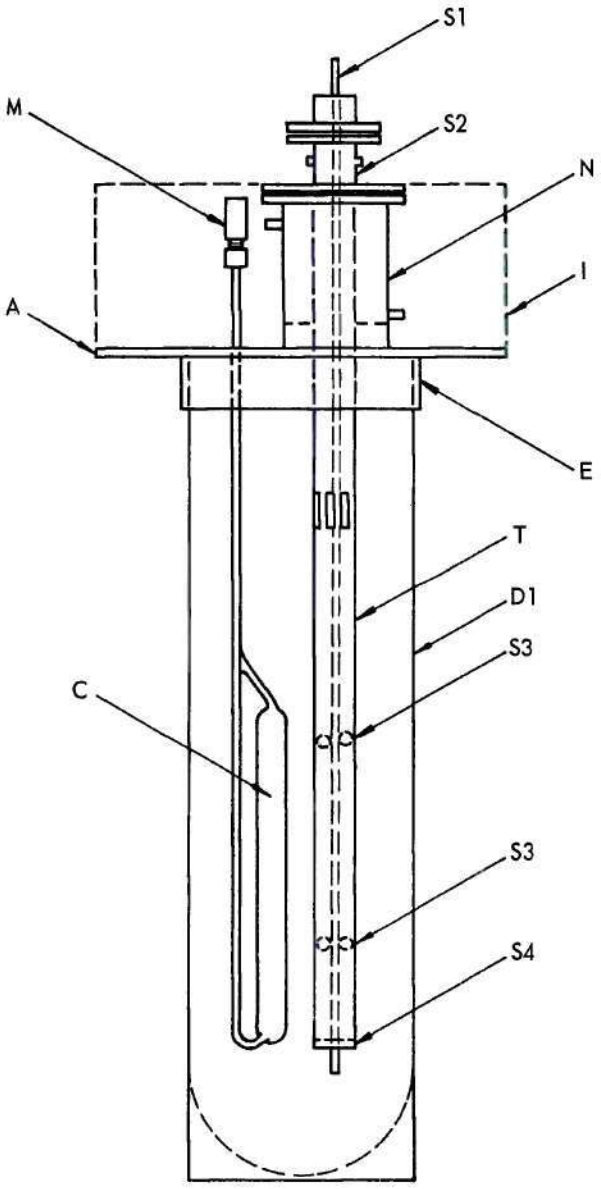

A – MAIN PLATE (BRASS)
C – EQUILIBRIUM CELL (GLASS)
D1 – CRYOSTAT DEWAR (GLASS)
E – DEWAR SEAL SLEEVE (BRASS)
I – INSULATION (POLYURETHANE FOAM)
M – METAL TO GLASS TUBING CONNECTOR (STAINLESS STEEL)
N – NITROGEN BOILER (MONEL)
S1 – STIRRER SHAFT (STAINLESS STEEL)
S2 – SHAFT SEAL AND BEARING ASSEMBLY (BRASS)
S3 – PROPELLER (STAINLESS STEEL)
S4 – SLEEVE BEARING (BRASS)
T – COOLING TUBE (COPPER)

Figure 4. The Cryostat.

controlled with a variable transformer. It could have been used as an aid in temperature control; however, it was not used for this purpose in this work.

Insulation

The main plate was insulated on the underside with styrofoam cut to fit and glued on. The top side of the entire main plate and the nitrogen boiler up to the large flange were insulated with polyurethane foam which was foamed in place to provide good contact with the complex structure. See dotted area, I, on Figure 4. This foam provided excellent insulation for the nitrogen boiler.

The Stirring Mechanism

The shaft seal and bearing assembly, S2, consisted of a double o-ring seal and a ball bearing. This assembly was flanged to the top of the nitrogen boiler. The bearing was a Nice model 1605-SCNS made by Boston Gear Works. The seals were one-sixteenth inch thick teflon o-rings. The two openings between the two flanges, which may be seen in Figure 4, were used to pass warm air through the assembly in event of excessive cooling of the bearing.

The stirrer shaft, S1, was driven by a one-twelfth horsepower, 12,000 rpm motor purchased from Talboys Instrument Corporation. The shaft was connected to the motor with a piece of one quarter inch inside diameter heavy wall rubber tubing. The tubing was clamped on both the motor shaft and the stirrer shaft. This flexible connection eliminated the need for perfect alignment of the two shafts.

Two one-inch diameter, three bladed, stainless steel propellers were clamped to the stirrer shaft. One was three inches above the

lower sleeve bearing, the other six inches higher. These propellers caused the circulation of the cryofluid up the inside of the cooling tube.

The Dewar

The cryofluid was contained in the dewar shown in Figure 4 as item D1. It was made to specification by the H. S. Martin Company. A one and one-half inch wide unsilvered strip was left on each side of the dewar to permit visual observation of the equilibrium cell. The upper end of the dewar fitted inside the seven inch diameter brass tubing extending down from the main plate. The outside of the upper end of the dewar was padded with rubber tape and the top of the dewar was insulated from the main plate by one and one-half inches of styrofoam. The dewar was sealed to the brass tubing with rubber tape. The dewar was supported by a lower plate, not shown, made of brass, which was hung from the main plate by four support rods. This permitted easy removal of the dewar for maintenance of the glass cell or cooling tube assembly.

As Figure 1 shows, the vent line from the dewar was connected into the exhaust line from the nitrogen flow rate control valve. This insured that the vapor space above the cryofluid in the dewar always contained dry nitrogen at slightly above atmospheric pressure. However, during emergency or for shutdown the liquid propane could be safely vaporized without difficulty into the vent system.

Equilibrium Cell Pressure Measurement

Equilibrium cell pressure was measured with the eight-inch diameter, Martin Decker, 1500 psig, precision test pressure gage shown in Figure 1

as item P1. The calibration and precision of this gage is discussed in the Chapter entitled Discussion of Results and in Appendix D.

Equilibrium Cell Temperature Measurement

Temperatures in the cryostat were measured with four Advance alloy-copper thermocouples which were connected to a Leeds and Northrup type K-3 potentiometer. Potentiometer null was detected with a Leeds and Northrup type 9834 DC electronic null detecter. The thermocouples were calibrated in place against a platinum resistance thermometer which had been previously calibrated by the National Bureau of Standards. The calibration procedure is described in Appendix C. Two temperature difference couples were also used in the cryostat. The locations of the thermocouples on the equilibrium cell are shown in Figure 2. Another thermoucouple was attached to the outside of the cooling tube approximately at the mid-point. Two of the four thermocouples were spares. The entire system of thermocouples, switch, potentiometer, and null detector was used intact during thermocouple calibration and experimental operation.

Safety Considerations

As a safety measure the cryostat was contained in a sealed plywood cabinet. A squirrel-cage blower constantly evacuated the cabinet. Clear plastic windows three-eight inch thick were placed in front of and behind the viewing slits on the dewar. The cabinet had sufficient volume to easily contain all the liquid propane should the dewar have ever broken. The blower had sufficient capacity to readily remove propane vapors from the cabinet in this event. The blower exhausted through a vent line to the roof of the laboratory.

The interior of the cryostat was illuminated by two fifteen-watt fluorescent bulbs placed behind the rear window of the cabinet. The light was directed into the rear unsilvered strip of the dewar and nicely illuminated the equilibrium cell.

Liquid Nitrogen System

The upper end of the cooling tube was cooled by liquid nitrogen as has been described. The liquid nitrogen transfer system may be seen in Figure 1. Liquid nitrogen was stored in a 25-liter metal dewar, indicated as D2 in Figure 1. The liquid nitrogen was forced to the boiler by a dry nitrogen pressure system. Constant pressure was maintained at about five feet of water by slowly bubbling a portion of the dry nitrogen pressuring gas through the mercury bubbler shown in Figure 1.

The rate of flow of liquid nitrogen and thus the cooling rate was regulated with a valve, labeled the liquid nitrogen flow rate control valve, V1, in Figure 1, on the exhaust line of the boiler. This valve actually controlled the rate of exhaust of nitrogen vapor, which in turn controlled the pressure difference between the boiler and the liquid nitrogen storage dewar. This controlled the rate of transfer of liquid nitrogen into the boiler.

The liquid nitrogen line from the storage dewar to the boiler was a double-walled vacuum insulated transfer line. The use of this type transfer line reduced the amount of heat absorption into the liquid nitrogen.

The Gas Mixing and Storage Section

A schematic drawing of the gas mixing and storage section of the experimental apparatus is shown in Figure 1. This section of the equipment, as its name implies, was used to prepare and store the gas mixtures, and to trasfer the gas to the equilibrium cell via mercury displacement. The gas burets were constructed of 316 stainless steel and glass. All tubing and tubing fittings were of 304 stainless steel. All original valves were of 303 stainless steel, however, some replacement valves in the upper manifold were of brass.

The Gas Burets

The gas burets were transparent-type liquid level gages purchased from Jerguson Gage and Valve Company. They are shown as B1, B2, and B3 on Figure 1. The two large burets were model number 29-T-30; the small buret was model 19-T-30. The volume of the 29-T-30 burets was approximately 250 cm^3 each and of the 19-T-30 was approximately 125 cm^3. The rated maximum operating pressure of these vessels was 2000 psig at 100°F. Arbitrary scales for gas measuring purposes were attached to the glass face of each gage. The scales, which were prepared by the photographic laboratory of the Georgia Institute of Technology Engineering Experiment Station, were the negatives of a photograph of ten by ten to the half-inch graph paper on Mylar film. Mylar film was selected as it exhibits negligible swelling or distortion with exposure to moderate temperatures and humidities. The calibration of these burets is described in Appendix F.

The gas burets were used to prepare gas mixtures as follows. First one buret was filled with a pure gas component to the desired vol-

ume and pressure, and then a second buret was filled to the desired, not necessarily the same, volume and pressure. The gas volume in the gas burets could be varied by forcing mercury to or from the mercury storage vessel, B4 in Figure 1. After the desired quantities of gases were contained in the burets the upper manifold was evacuated and the gases were mixed by displacing the gas rapidly back and forth between the burets with mercury. The standard mixing procedure which was developed and its results are given in Appendix B.

The mercury storage vessel had the necessary volume to contain enough mercury to fill all three burets at once. Pressure was applied to the mercury from nitrogen cylinders. The mercury storage pressure gage, P4, was an inexpensive and inaccurate gage used only to give approximate pressure readings.

The manifold pressure gage was an Ashcroft five-inch diameter, 3000 psig test pressure gage. See P2 on Figure 1. The calibration of this gage is described in Appendix D.

Gas Sampling

The lower of the two sample valves, V2, shown in Figure 1 was connected directly to the sample inlet valve on the gas chromatograph used to determine gas mixture composition. The upper sample valve was used to vent the sample line. This direct connection to the analytical device completely eliminated sample handling, and thus, reduced sampling errors.

Temperature Control

The entire gas mixing and storage section was enclosed in a sealed plywood cabinet which was approximately five feet by three feet by one foot in size. The interior walls of the cabinet were insulated so that

the cabinet could be maintained at constant temperature.

The temperature control equipment consisted of a heater, a blower, and a thermistor temperature controller. Air from the bottom of the cabinet was forced by the blower past the heater, which was contained in the three-inch diameter exhaust duct of the blower. The warm air was evenly distributed across the top of the cabinet through a sparger at the top of the duct. The blower capacity was sufficient to circulate six times the volume of the air in the cabinet every minute.

The heater was constructed of nichrome heater wire wound around a coil of three-eighths inch diameter copper tubing.

The temperature detecting element, a thermistor, was placed at the top of the cabinet just below the upper manifold. The thermistor acted as one leg of an E. H. Sargent model S-82050 resistance bridge temperature controller (trade name Thermonitor). This controller regulated the voltage applied to the heater. With this control arrangement temperature control to within $\pm 0.01^{\circ}C$. was possible. Tests showed gradients of up to $\pm 0.1^{\circ}C$. within the contents of the cabinet.

Eleven thermocouples, constructed of Advance alloy and copper, were located throughout the cabinet to measure temperature differences. These thermocouples were connected through a switch to the same potentiometer-detector system used with the thermocouples in the cryostat.

Analytical Equipment

Gas chromatography was selected as the analytical technique to be used to determine the concentrations of the various helium-argon mixtures. This instrument was selected primarily because of the short analysis time and minimum of sample handling required. In addition, impurities of var-

ious kinds can be readily detected through the use of gas chromatography.

There are a number of disadvantages to any analytical technique, and gas chromatography is no exception. There are many variables, such as temperature, pressure, fluctuations in electrical supply voltage, carrier gas flow rate, and others, that adversely affect the analysis. Precautions can be taken to control these variables; however, some drift in these instruments is usually present. To eliminate this drift as a factor on the results of this experimental work an instrument calibration was undertaken every time an analysis was made. The calibration procedure is described in Chapter III entitled Procedure.

The Chromatograph

The chromatograph was a Perkin-Elmer Model 154D Vapor Fractometer, which had been used in previous phase equilibria work (33) in this laboratory. Several modifications, which are described in detail by Kirk (33), had been made to improve the precision of the instrument. The potentiometer recorder could be manually standardized against a standard voltage by adjusting rheostats which were added to the battery circuit. The detector cell voltage could be standardized with the potentiometer recorder through a switching system. Also a reversing switch could be used to reverse the polarity of the detector circuit during analysis if necessary.

The column used in this instrument was constructed of a two meter, one-quarter inch tube containing 42/60 mesh, Linde 5A Molecular Sieve. Gas mixtures used in the bubble-point measurements, containing low helium content, were analyzed with argon as the carrier gas. The dew-point gas mixtures, containing up to 45 per cent helium were also analyzed with

argon as the carrier gas. Helium carrier gas was used for gas mixtures containing over 50 per cent helium. The above procedure was selected as the most precise, as the gas under direct study was always the one of lower concentration. The gases used as carrier gases were the same as were used in preparing the experimental gas mixtures. The purity of these gases is discussed in Chapter V.

In all cases only one peak appeared on the chromatogram. The height of the peak, rather than the included area, as is sometimes used, was taken to be representative of the concentration. At least two, and sometimes three, precisely prepared gas mixtures were used to calibrate the chromatograph for each unknown gas mixture analyzed. These known calibration mixtures usually bracketed the unknown in composition. At least one of the known mixtures was within two per cent of the unknown in concentration.

The known calibration mixtures were prepared in a special precision gas mixing apparatus constructed and carefully tested by Kirk (33). On the basis of Kirk's experience with this mixing apparatus it is believed that the mixtures were prepared with a precision of about one per cent of the stated value of the minor component.

Sampling

A simple stopcock manifold for admitting the gas sample to the chromatograph gas sample inlet valve had been added to the instrument by Kirk. A one-eight inch tube was used to connect the sample valve on the gas mixing section of the phase equilibria equipment directly to this stopcock manifold. The stopcock manifold was arranged to permit purging the gas sample inlet valve either by flow or by vacuum. The sample inlet

valve and manifold were constructed so that a controlled volume of gas mixture could be sampled at atmospheric pressure.

CHAPTER III

PROCEDURE

Dew and Bubble Points

The development of procedures for obtaining dew and bubble points required some experimentation. Several methods were tried; the methods described below were selected as the ones which produced the most reliable results.

Dew-Point Observations

Dew points were obtained by slowly displacing the gas mixture from the gas burets into the equilibrium cell until droplets of moisture were observed on the walls of the cell. The gas mixture was injected in increments at time intervals of not less than one minute. The pressure increase in the cell due to an incremental injection was normally less than two pounds per square inch.

Temperature and pressure readings were made once every minute while dew points were being obtained. Usually no discernable temperature change was noted during this operation and in no case was the temperature permitted to vary by more than $\pm 0.005^{\circ}K$.

Just before every dew point operation at least one gas mixing cycle as described in Appendix B was performed. This was to insure that a uniform gas mixture was injected into the cell, and that the cell contained gas of this same uniform composition.

During the initial runs every dew point was checked at least once.

These checks were performed by lowering the pressure slightly until the dew disappeared and then increasing the pressure until the dew reappeared at the same pressure, within ± 0.5 psig, as it had previously. During later runs this check was not performed for every dew point.

Bubble-Point Observations

The method of obtaining bubble points was similar except that the cell was initially filled with liquid mixture and the pressure was reduced incrementally until bubbles appeared. These bubbles usually appeared along the walls of the cell and quickly rose to the top of the cell. The pressure reduction rate was on the order of two psig per minute or slower. This was done slowly to eliminate the possibility of adiabatic expansion of the liquid which might have caused a temperature reduction in the cell liquid.

The equilibrium cell was filled with liquid by the following procedure. While the cryostat temperature was being changed to a new level, and after at least one, and usually two, mixing cycles (see Appendix B) were performed, the warm gas from the gas burets was quickly injected into the cell to a pressure of over 1000 psig. The contents of the cell quickly cooled; however additional gas injections were made to prevent the pressure from falling below 1000 psig. These injections were continued until finally the temperature of the fluid in the cell became equiliberated. In this manner the cell was filled with liquid with no observable vapor-liquid interface being formed. This was important as it was found that if the interface occurred, persistant concentration gradients were set up which greatly affected the bubble-point pressure.

A slow loss of gas to the atmosphere through leakage was observed.

This is a possible source of error which applies to both the dew-point and bubble-point measurements. It is to be emphasized that this loss was slight as all external connections were double blocked and plugged. Also, several extensive pressure tests were made during the course of the experiments. Possible selective diffusion through small leaks was reduced by completing all operations with a particular gas mixture within 24 hours. However, to further reduce the possibility of change in composition of the gas mixtures due to selective loss of helium the gas was always immediately mixed following every dew-point and bubble-point operation.

Cryostat Temperature Control

An example of the type of temperature control obtained with the manual control system on the cryostat liquid nitrogen supply may be seen in Figure 5. This particular set of data was selected as an example since in this run it was necessary to hold the temperature control for a longer than normal period of time. Usually lineout was held only about ten minutes, however the control shown is typical. The figure shows the various valve settings which were used. A good bit of experience was necessary to anticipate the necessary changes in valve setting.

Temperature control procedure was simple. When cryostat temperature reduction was desired the nitrogen valve was set at full open. When the temperature neared the desired value the valve was partially closed to a setting which was thought to be about correct. Then the valve was adjusted, usually not more than once in five minutes, until

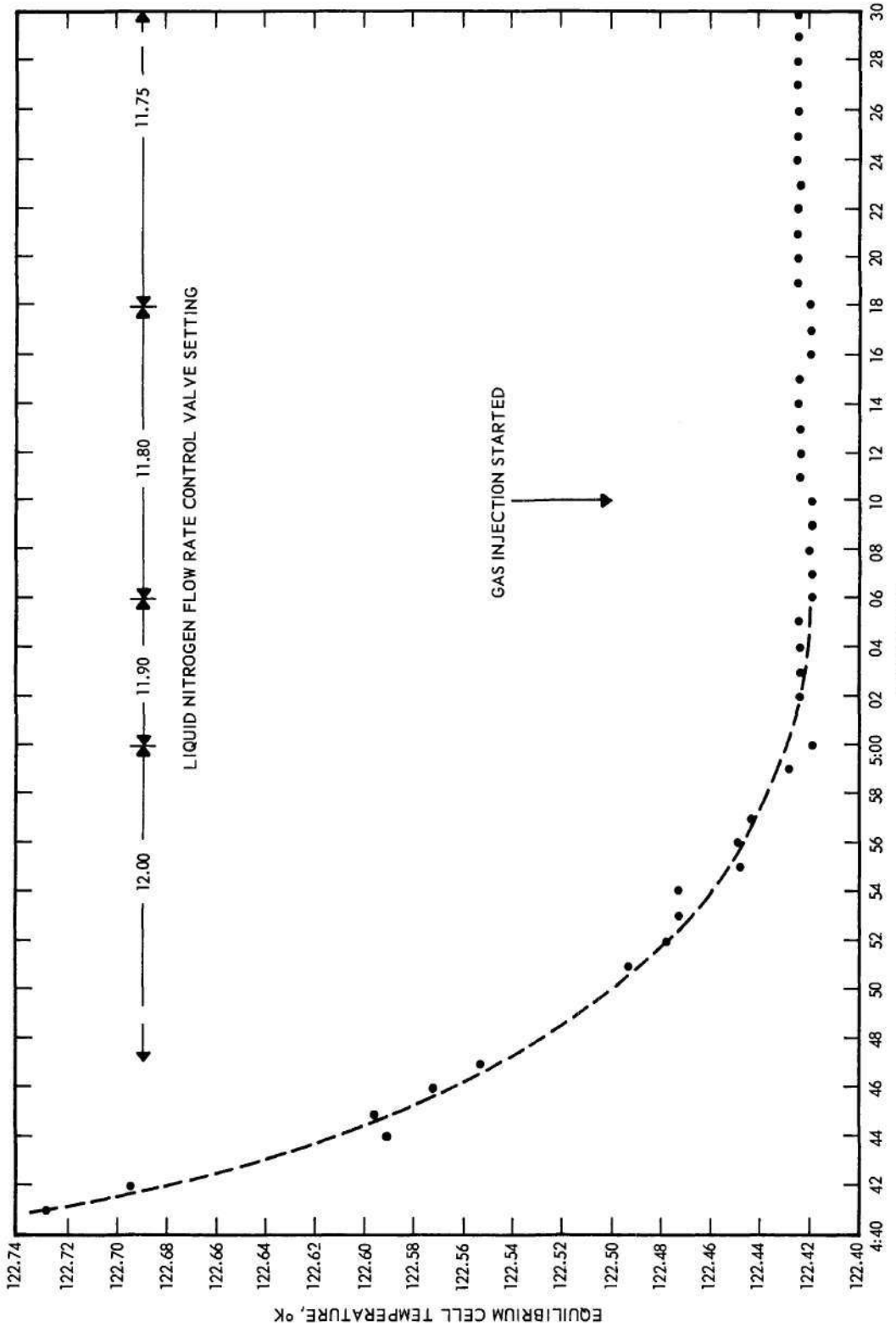

Figure 5. Cryostat Temperature Control, Fifty Minutes During Dew-Point Observation in Run 16.

temperature control was achieved.

If a temperature increase was desired the heater on the upper end of the cooling tube was used. The valve setting was usually not changed, thus when the heater was turned off the nitrogen flow rate was stable and temperature control was readily achieved.

Preparation of Gas Mixtures

The gas mixing section of the apparatus was used to prepare the gas mixtures. This equipment was maintained at a constant temperature throughout the gas measuring operation. After evacuation of the upper manifold and burets, helium was introduced into one of the burets to the desired volume and pressure. After evacuation of the remaining buret and the manifold, argon was introduced to the desired volume and pressure.

The quantities of the gases were calculated using the compressibility equation. Compressibility factors for argon were obtained from National Bureau of Standards Circular 564 (25). The compressibility factors of Stroud, et al. (47) were used for helium.

Following evacuation of the manifold the gases were thoroughly mixed. The gas mixing procedure is described in Appendix B. Several repeats of the mixing procedure were used when a fresh gas mixture was being prepared.

After a short period of operation the valves in the gas mixing and storage section began to leak and the above procedure became quite inaccurate. The later gas mixtures were prepared by injecting each of the gases to a precalculated pressure. In calculating the pressure of injection for each gas, it was assumed that the gases formed a perfect

solution.

After mixing, a quick, approximate analysis was made of the gas mixture using the gas chromatograph described in Chapter II. This gave an indication of the amount of one or the other of the pure gases which had to be added to bring the gas mixture close to the desired concentration. This gas was added, again by following the pressure rise during addition.

The gas mixtures prepared in this manner were approximately the desired composition. Since each mixture was carefully analyzed after its use in experimentation this was sufficient.

Sampling Procedure

The lower of the two gas sampling valves, V2, shown in Figure 1 was connected directly to the sample inlet valve of the gas chromatograph used for analysis of the gas mixtures. The upper of the two valves was used as a vent. A representative sample was obtained by permitting the gas from the gas burets, B1, B2, and B3, to flow slowly through the sampling valve on the chromatograph for at least five minutes prior to sampling.

Since the sample line was connected directly to the upper manifold, an attempt had to be made to obtain a gas sample which was representative of the gas in each gas buret. This was done by raising the mercury level in a buret to the top, thereby forcing the gas from the buret into the upper manifold. The gas from the manifold was thus forced into the remaining buret. This gas was allowed to purge through the sample line and was then sampled. Gas from each buret could be sampled in this manner.

Analytical Procedure

In spite of the care that was taken to control all possible variables, the chromatograph used to determine the gas compositions exhibited some long term drift. However, it was noted that this drift was negligible over a two to three hour period. Therefore it was decided that the chromatograph would be calibrated every time an analysis was required, and that the entire period of calibration and analysis would be limited to less than three hours.

The known composition gas mixtures used for calibration of the chromatograph were prepared in a special precision gas mixing apparatus designed, constructed, and tested by Kirk (33). Kirk showed that gas mixtures could be prepared with more precision than could be obtained with the chromatograph used to analyze them.

At least two, and sometimes three, precisely prepared gas mixtures were used to calibrate the chromatograph for each unknown gas mixture analyzed. Initially a gas mixture was prepared which was the same as the estimated composition of the experimental gas. This known gas mixture was analyzed with the chromatograph at least three times in a ten to fifteen minute period. Then at least six samples of the unknown composition experimental gas mixture, taken at various places in the gas burets as described above, were analyzed in a twenty to thirty minute period. If any of the results deviated from the mean of all the results by more than two per cent the analysis was voided and the experimental gas was mixed using the mixing procedure given in Appendix B.

Following the analysis of the unknown gas mixture, at least two, usually more, additional chromatograms were run for the known mixture. If these differed by more than one per cent from the previous runs the

analysis was voided.

Only two analyses were voided for the reasons given above. It was discovered that in both of these cases the fault was not due to the chromatograph or the analytical procedure, but was a result of the varying electrical load in the laboratory, which caused some variation in the operation of the electrical circuits of the chromatograph. All future analytical work was performed after normal working hours to eliminate this problem.

The comparison of the two sets of chromatograms was then used to determine a new estimate of the composition of the unknown gas mixture. A new calibration mixture was prepared at this estimated composition and the procedure given above was repeated. In most cases the composition of this second known mixture was within two per cent of the unknown mixture, based on chromatogram peak height, and linear interpolation was used to determine the composition of the unknown gas mixture.

In a few cases a third calibration mixture had to be prepared in order to come within two per cent of the unknown. In these cases graphical interpolation was used to determine the composition of the unknown.

It was found that chromatogram peak height was less sensitive to concentration for gas mixtures with the higher helium compositions. In order to compensate for this the following changes were made in the analytical procedure.

At 29.70 and 45.36 per cent helium the peak height of the final known gas mixture was held to within one per cent of the peak height of the unknown mixture. At 69.52, 75.41, and 84.84 per cent helium a three-point calibration of peak height against helium concentration was prepared

by using three known gas mixtures. In each case this calibration bracketed the peak height of the unknown mixture. The composition of the unknown was determined graphically.

Thus the error due to analytical technique was held to within two per cent of the concentration of the minor component even though the sensitivity of the gas chromatograph changed as helium concentration changed.

CHAPTER IV

CALCULATIONS

The prediction of the compositions of the vapor phase of a system such as the one under study from the properties of the pure components is a quite interesting problem. The oversimplified approach is to assume that the vapor phase is a mixture of perfect gases and the vapor pressure of the condensed phase is that of the saturated phase. This results in the following equation for the concentration of the less volatile component in the gas phase.

$$\frac{Py_1}{p_{01}} = 1 \qquad (4)$$

This equation is, of course, greatly in error in that the actual value of y_1 is much larger than this equation predicts.

The Enhancement Factor Equation

A modification of this equation, which has found recent favor, involves the enhancement factor, ϕ , which is defined (14) as follows:

$$\phi = \frac{Py_1}{p_{01}} \qquad (1)$$

Dokoupil (14) gives the following equation for the enhancement factor.

$$\ln\phi = \ln \frac{PV_m}{p_{01}V_{01}} + \frac{1}{RT}\int_{p_{01}}^{P} v_1 dP + \frac{1}{RT}\int_{v_{01}}^{\infty} \left[\left(\frac{\partial P_1}{\partial n_1}\right)_{V,T} - \frac{RT}{V_1}\right] dV_1$$

$$- \frac{1}{RT}\int_{V_m}^{\infty} \left[\left(\frac{\partial P_m}{\partial n_1}\right)_{V,T,n_2} - \frac{RT}{V_m}\right] dV_m \qquad (5)$$

This equation may be derived by equating the chemical potential of the condensable component in the gas mixture with its chemical potential as a pure condensed phase. The assumption involved in the derivation is that the condensed phase, solid or liquid, is a pure phase containing only the condensable component.

An examination of equation 5 above indicates that an equation of state for the gas mixture, and an equation of state for the pure condensed phase, are necessary for one to perform the indicated mathematical operations. Also necessary in the computations is a knowledge of the properties of the condensed phase as a function of pressure and temperature.

Equation of State, Vapor Phase

The virial equation of state, truncated after the third virial coefficient term, was selected to represent the properties of the vapor mixture.

$$PV_m = RT\left(1 + \frac{B_m}{V_m} + \frac{C_m}{V_m^2}\right) \qquad (6)$$

where

$$B_m = y_1^2 B_{11} + 2y_1 y_2 B_{12} + y_2^2 B_{22} \quad (7)$$

and

$$C_m = y_1^3 C_{111} + 3y_1^2 y_2 C_{112} + 3y_1 y_2^2 C_{122} + y_2^3 C_{222} \quad (8)$$

The terms B_{11} and B_{22} are the second virial coefficients of pure components 1 and 2, respectively. The quantity B_{12} represents the second virial coefficient calculated from a potential function which describes the interaction between molecules of species 1 and species 2; hereafter called the second virial interaction coefficient. B_{12} may be estimated from the properties of the pure components by use of mixture rules to be described below. The third virial coefficients are represented by the symbol C with subscripts of similar meaning.

Equation of State, Liquid Phase

The compressibility of the pure liquid phase was described by a linear equation,

$$v_1 = a + bP \quad (9)$$

where the coefficients, a and b, are temperature dependent.

Integration of Enhancement Factor Equation

Kirk, et al., (34) and Kirk (33) have discussed the evaluation of

the enhancement factor by solution of equation 5. Insertion of the assumptions outlined above into equation 5 leads to the expression for enhancement factor presented by Kirk (33) and used in the present work, namely,

$$\ln\phi = \ln\frac{1}{z_{01}} + \frac{(P - p_{01})}{RT}\left[a + \tfrac{1}{2}b(P + p_{01})\right]$$

$$+\left[2\frac{B_{11}}{V_{01}} + \frac{3}{2}\frac{C_{111}}{V_{01}^2}\right] + \frac{I_b}{V_m} + \frac{I_c}{V_m^2} + \ln z_m \qquad (10)$$

where

$$I_b = -2(y_1B_{11} + y_2B_{12}) \qquad (11)$$

and

$$I_c = -\frac{3}{2}(y_1^2C_{111} + 2y_1y_2C_{112} + y_2^2C_{122}) \qquad (12)$$

Determination of Parameters

In order to use equation 10 one must select a procedure for obtaining the second and third virial coefficients for the pure gases and a method of estimating the second and third virial interaction coefficients. Also, the parameters a and b of the liquid volume equation and the properties of saturated pure component 1 must be obtained.

The methods of estimating these parameters were selected as being the best available after a study of the results of Kirk (33). Kirk has evaluated a number of equations of state and methods of estimating the virial interaction coefficients by comparing calculated enhancement factors with his very good experimental data for the methane-hydrogen system. Among the methods examined by him was the method used in this thesis. Kirk found that this method gave good results for the methane-hydrogen system. However, he found that the best agreement with his experimental results came from the use of "hybrid" equations of state.

It is felt that the method chosen for computing the enhancement factor in this thesis is adequate since the possibility exists that the better results obtained by Kirk from the "hybrid" equations may be a result specific for the methane-hydrogen system.

Calculation of the Second Virial Coefficients

In this investigation the second virial coefficients were estimated by the method developed by Prausnitz and Myers (42) using the core model suggested by Kihara (32).

The Kihara core model with a 6-12 potential function is based on an impenetrable core model for the molecule. The dimensions of the core may be taken from known intermolecular distances for the molecule; however, Prausnitz and Myers showed that these cores should be somewhat smaller than the corresponding molecule.

The Kihara potential function retains the six-twelve form of the well-known Lennard-Jones 6-12 function; however, it is written in terms of separation of molecular cores rather than separation of molecular centers.

$$U = U_o \left[\left(\frac{\rho_o}{\rho} \right)^{12} - \left(\frac{\rho_o}{\rho} \right)^{6} \right] \qquad (13)$$

Prausnitz and Myers give values of the Kihara parameters, ρ_o and U_o; and M_o, S_o, and V_o; which are derived from the size and shape of the core for sixteen fluids of cryogenic interest. They also give relations for determining the quantum and quadrupole deviations of the second virial coefficient which are significant for some gases. In addition, a set of mixture rules for the combination of the Kihara parameters for use in calculation of the second virial interaction coefficients are given along with a method of making quantum corrections to the interaction coefficient. The mixture rules are:

$$\rho_{o_{12}} = \frac{1}{2}(\rho_{o_1} + \rho_{o_2}) \;, \quad U_{o_{12}} = \sqrt{U_{o_1} U_{o_2}} \qquad (14)$$

The second virial coefficients for both gases, helium and argon, and the second virial interaction coefficients were calculated using the Kihara 6-12 core model with the parameters of Prausnitz and Myers. For a discussion of the details of making the quantum conectious see Kirk (33). Figure 6 shows a comparison of the calculated second virial coefficients of argon with the data of Michels, et al. (39), and Fender and Halsey (21). Figure 7 gives a comparison of the calculated second virial coefficients of helium with the data of White, Rubin, Camky, and Johnston (51). In both cases the agreement appears to be within experimental error. The data used in the above comparisons were selected as being the best avail-

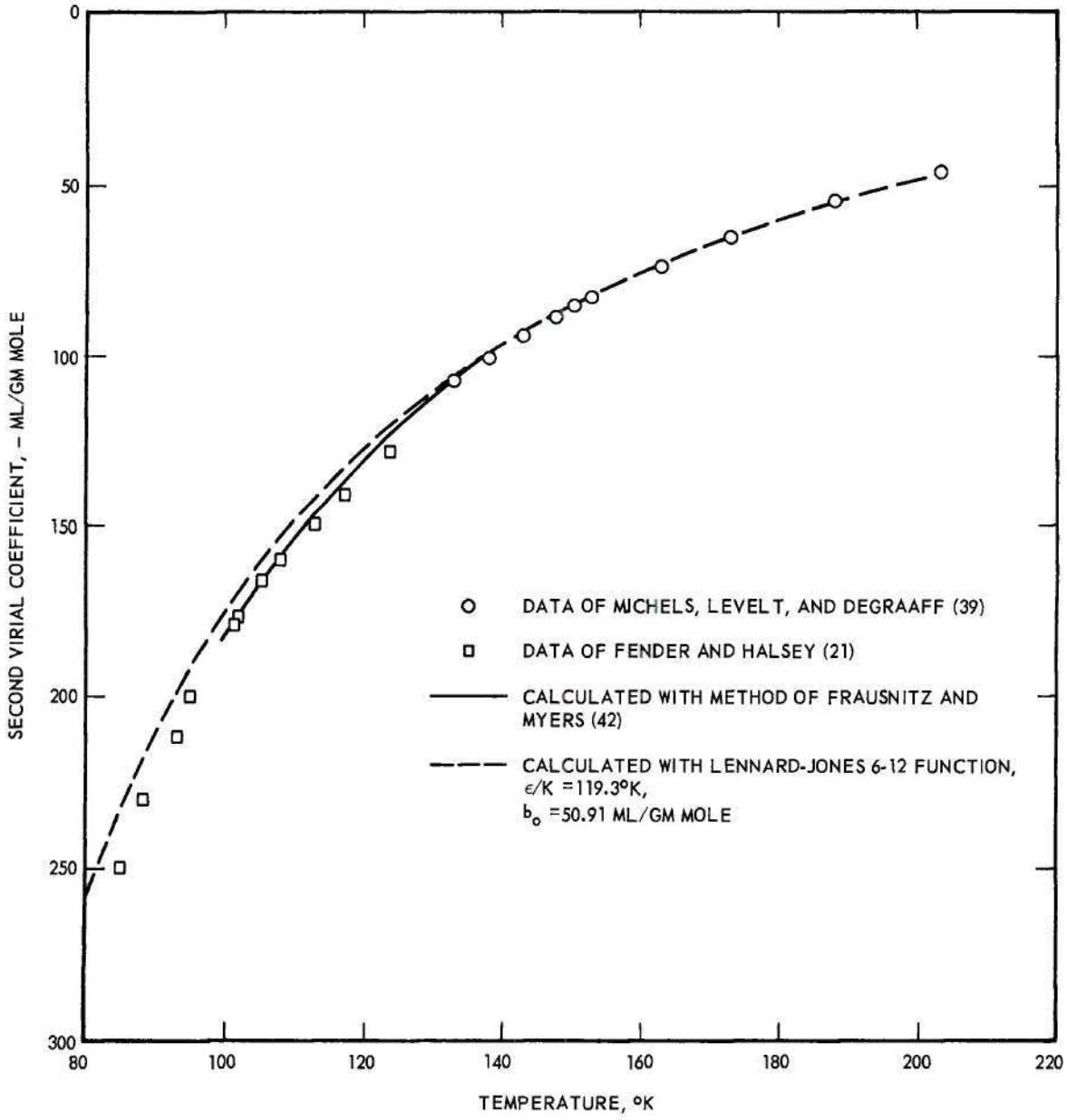

Figure 6. Comparison of the Second Virial Coefficients of Argon Calculated by the Method of Prausnitz and Myers (42) with the Kihara 6-12 Core Model, and Calculated with the Lennard-Jones 6-12 Model, Against the Experimental Measurements of Michels, et. al. (39), and of Fender and Halsey (21).

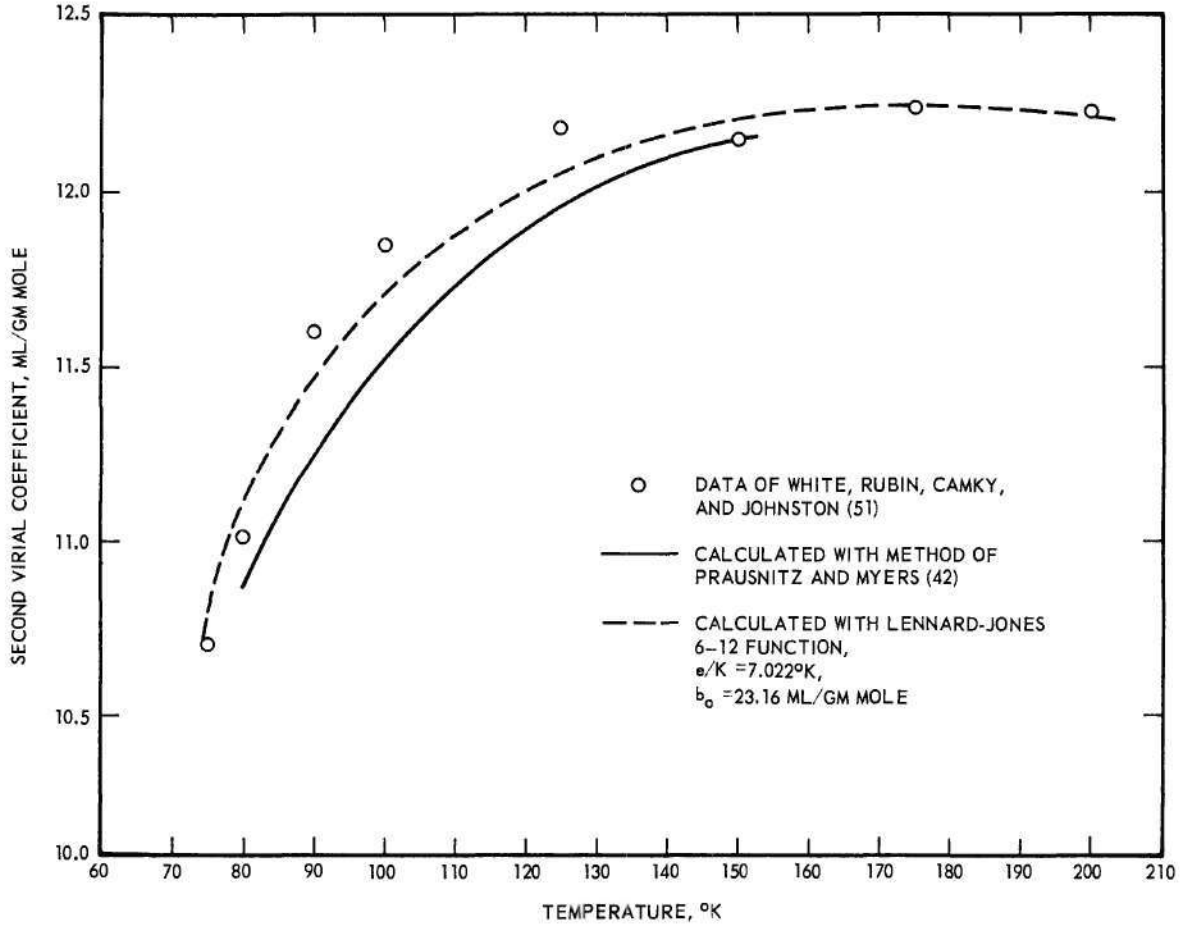

Figure 7. Comparison of the Second Virial Coefficients of Helium Calcualted by the Method of Prausnitz and Myers (42) with the Kihara 6-12 Core Model, and Calculated with the Lennard-Jones 6-12 Model, Against the Experimental Measurements of White, et. al. (51).

able in the temperature range of interest. The numerical values of all parameters used in the enhancement factor calculations are listed in Appendix G.

Calculation of the Third Virial Coefficients

The Lennard-Jones 6-12 potential function was used to compute the third virial coefficients. The calculational method is given by Hirschfelder, Curtiss, and Bird (26). Values of Hirschfelder's term $C^*(T^*)$ were computed with Hirschfelder's equation 3.6-10 using values of $c^{(j)}$ given in their Table I-E. In order to compute the third virial interaction coefficients, C_{112} and C_{122}, values of $b_{o_{112}}$ and $b_{o_{122}}$, and $(e/k)_{112}$ and $(e/k)_{122}$ were determined using the following relations.

$$(e/k)_{ijk} = (e/k)_i^{1/3}(e/k)_j^{1/3}(e/k)_k^{1/3}$$

$$b_{o_{ijk}} = \left[\frac{b_{o_i}^{1/3} + b_{o_j}^{1/3} + b_{o_k}^{1/3}}{3}\right]^3 \qquad (15)$$

An e/k of 119.3° K and a b_o of 50.91 ml/gm mole were used for argon. These values were the selected values of Ziegler, Mullins, and Kirk (53). A graphical comparison of the second virial coefficients of argon calculated using these parameters with experimental data is given in Figure 6.

The values of e/k and b_o given in the literature (27, 28) for helium produce values of the second virial coefficient which are not in agreement with the available experimental data. Thus, using the second virial coefficient data of White, et al. (51), the author derived the

values of 7.022° K for e/k and 23.16 ml/gm mole for b_o which were then used to determine the third virial coefficients. A graphical comparison of the second virial coefficients of helium calculated using these parameters with the data of White is given in Figure 7. White compared his data with those of a number of other investigations; his data were selected for use in this work as they appeared to be the best available in the temperature range of interest.

Equation of State of Liquid Argon

An examination of the available data (49, 39) of the compressibility of liquid argon revealed that the data could be adequately represented with a linear equation in the temperature range of interest.

The data of van Itterbeek, Verbeke, and Staes (49) and of Michels, Levelt, and De Graaff (39) were compared graphically and found to be in good agreement. These data were then graphically interpolated to give the relationship between liquid volume and pressure at even values of temperature, as shown in Figure 8. An equation of the form of equation 9 was fitted to each isotherm. The constants are given in Table 1.

Table 1. Constants for Calculation of the Volume of Liquid Argon

Temperature °K	a cm^3/gm mole	b cm^3/gm mole, atm	v_{01}(39) cm^3/gm mole
100	30.49	0.00850	-----
105	31.36	0.01050	-----
110	32.33	0.01309	-----
115	33.45	0.01639	33.30
120	34.72	0.02034	34.48
125	36.24	0.02630	35.83
130	38.29	0.03920	37.51
135	41.08	0.05779	39.62

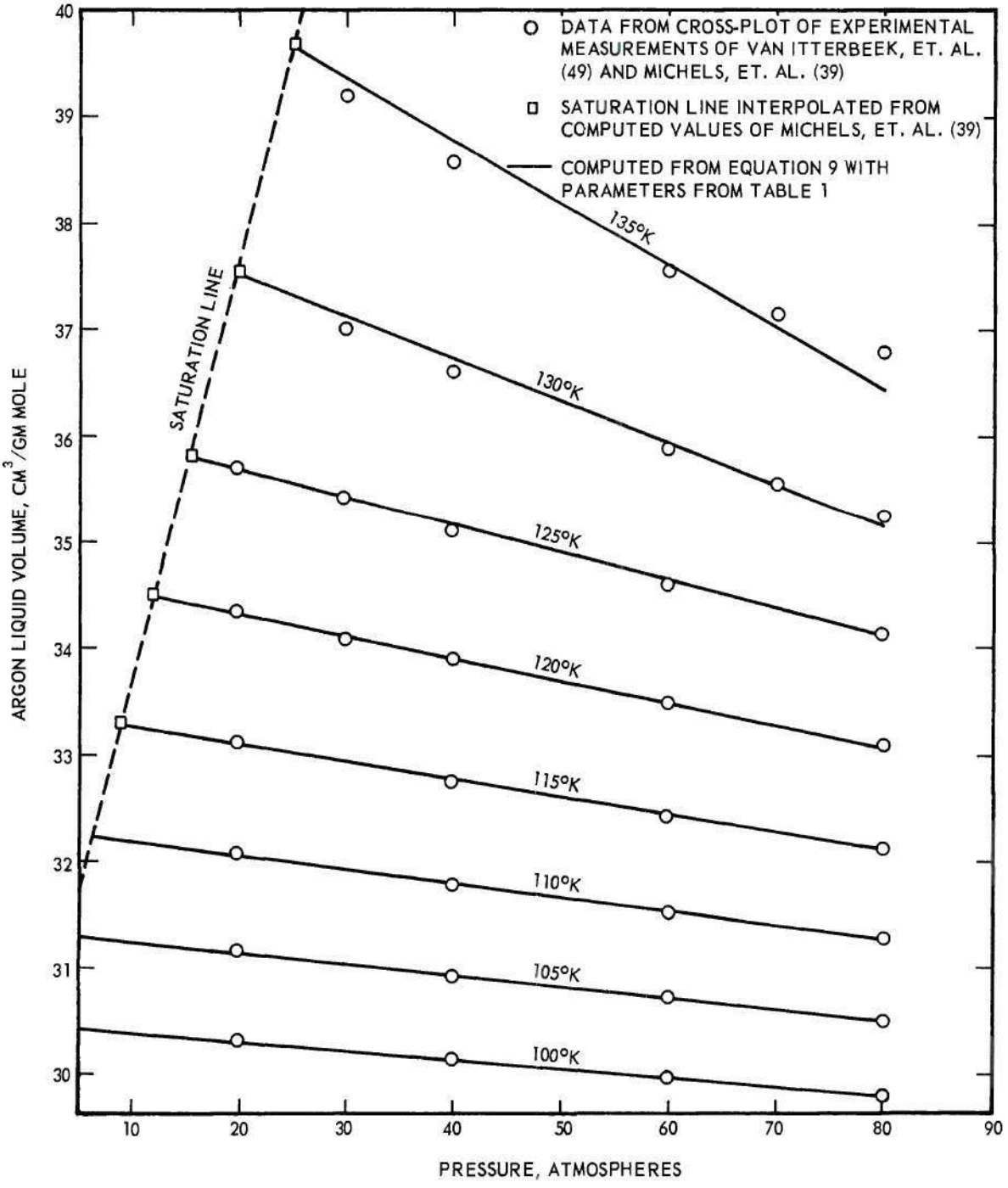

Figure 8. Volume of Liquid Argon as a Function of Pressure.

The values of volume calculated from these equations are shown as the lines on Figure 8. The round points in the figure represent the volumes as interpolated from the above mentioned data of van Itterbeek and of Michels. The square points represent graphically interpolated values of the saturated liquid volume at the vapor pressure from the computed values of Michels (39). One can see that the correlation lines were forced to fit exactly at these points.

The coefficients given in Table 1 were used in calculations with equation 10.

Vapor Pressure of Argon

The equation derived by Michels, Wassenaar, and Zwietering (8) from their argon vapor pressure measurements is given in Chapter V of this thesis, as equation 17. This equation was used to calculate the vapor pressure, p_{01}, needed in the enhancement factor calculations. The saturated vapor volume of argon, V_{01}, also appears in equation 10. The data of Michels, Levelt, and De Graaff (39) were used for V_{01}. The compressibility of argon vapor at saturation, z_{01}, is also needed. This quantity was calculated from V_{01}, using a virial equation truncated after the third term.

$$z_{01} = 1 + \frac{B_{11}}{V_{01}} + \frac{C_{111}}{V_{01}^2} \qquad (16)$$

The calculated values, compared with experimental data may be found in Figure 9.

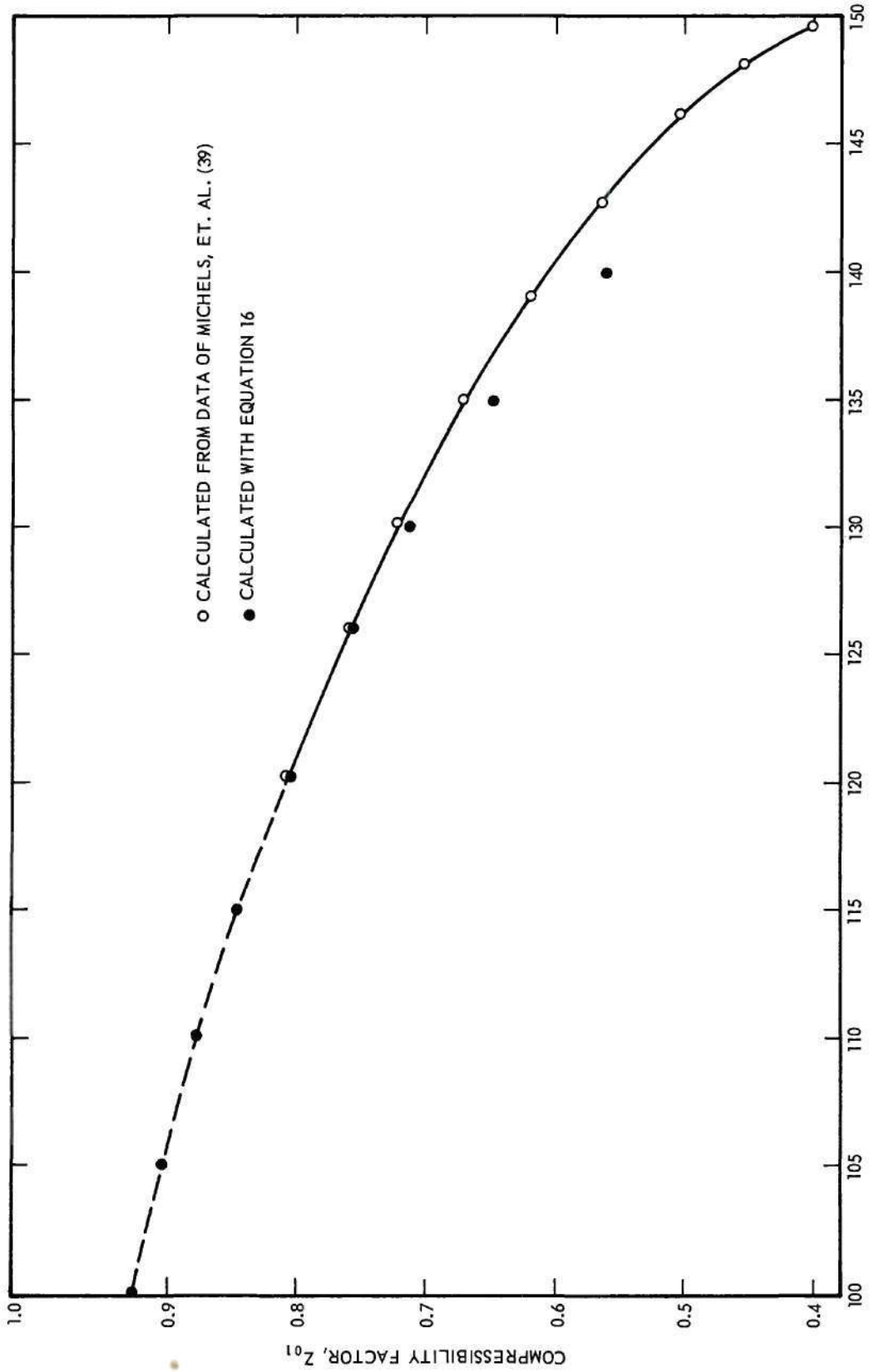

Figure 9. Compressibility of Saturated Argon Vapor as a Function of Temperature.

The Calculations

The calculations were performed using a Burroughs 220 digital computer. The computer program used was written by Kirk (33) and further refined by Mullins (41).

Computer Program

The computational procedure is illustrated by the block flow chart given in Figure 10 taken from Kirk (33). The overall program consists of the driver program and three program independent sub-programs called procedures. These procedures are used to compute z_{01}, to evaluate the equations for V_m, and to compute the interaction terms, I_b and I_c, of the enhancement factor equation.

Each of these three procedures is divided into three parts: LOADHEAD, which reads the necessary input data; TCALC, which performs the calculations which are dependent only on temperature; and RUN, which performs those calculations which are dependent on y_1 and P or V_m.

Kirk describes the calculational procedure as follows:*

> Briefly, the program initially reads the necessary parameters (equation of state parameters, etc.) into the procedures. A temperature parameter card (T CARD) is read; the enhancement factor is computed and printed for each of a series of pressures which are listed in the driver program; another T CARD is read; and so forth. This continues until a value of T = 0 is read; at this time, the program enters a selective reset routine by which any selected parameter in the driver program or procedures can be changed by reading in the desired new values together with certain logic parameters. The evaluation of the enhancement factor at selected pressures along isotherms then resumes.
>
> The driver program and the volume and interaction procedures also respond to another logic parameter which dictates whether the exact $y_1 \neq 0$ or the approximate $y_1 = 0$ calculation is to be performed.

---

*The reference, 61, to Aitken's method of interpolation which appears within the quotation, refers, of course, to Kirk's bibliography. See reference (40) in the bibliography of this work for this information.

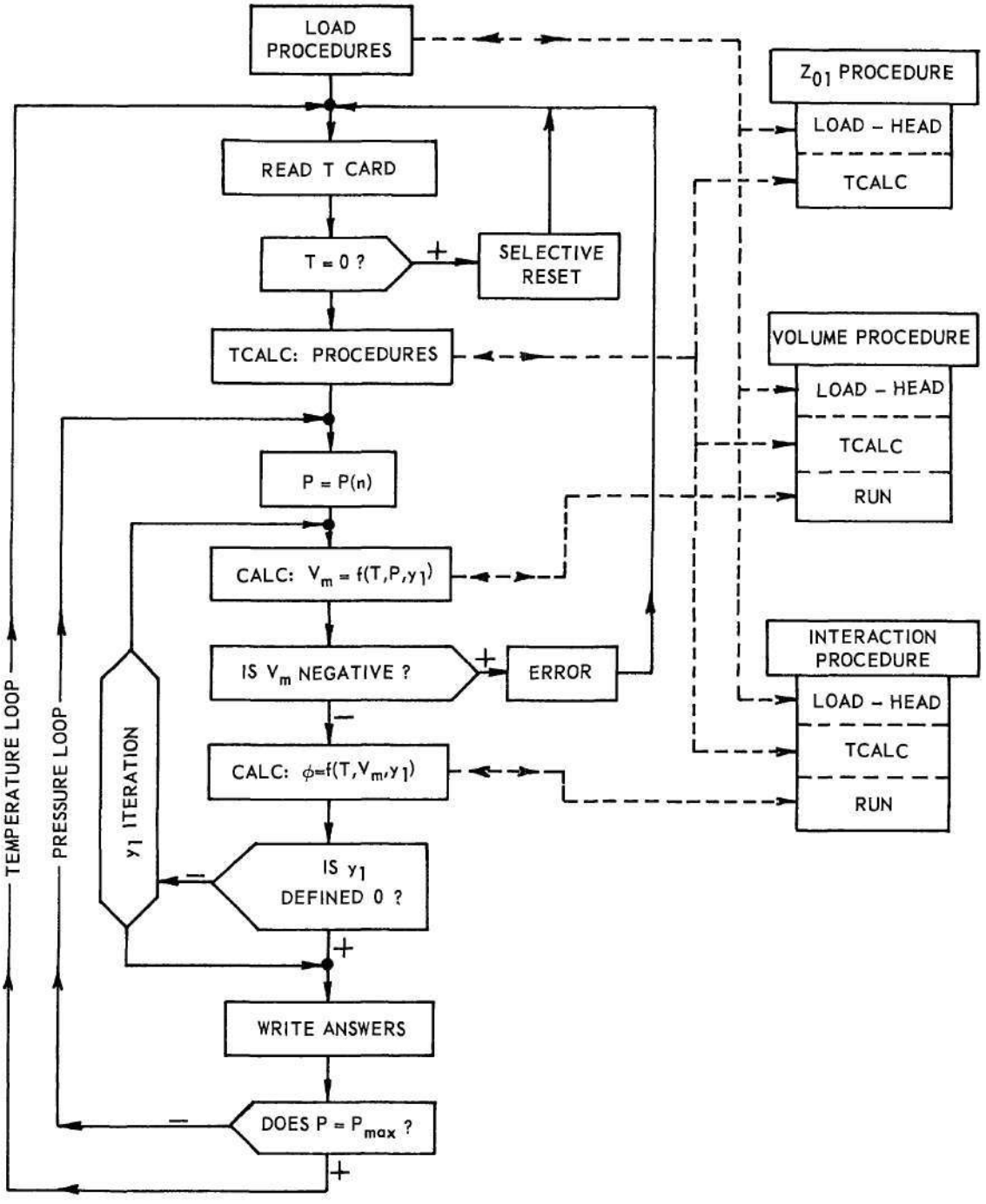

Figure 10. Flow Chart for Computing Enhancement Factors.

For a given pressure and gas composition, the corresponding value of V_m is determined in the volume procedure from the volume implicit equation of state by an iterative process which continues until the pressure computed from the value of V_m differs from the given pressure by less than one part in 100,000.

The iterative process is a quite flexible but apparently not widely used one which is based on Aitken's method of polynomial interpolation.[61] It involves retaining the values of the relative pressure error corresponding to each of the trial values of V_m and, after the first two trials, interpolating (or extrapolating) for the next trial value of V_m (for which the relative pressure error should be zero) by fitting a n-th degree polynomial through the n + 1 previously computed computed relative pressure error - V_m points. If the relative pressure error is not reduced below 10^{-5} in eleven trials, the iteration is abandoned, and V_m is assigned a negative value which is sensed by the driver program as a signal to begin calculations for the next isotherm. Computations for an isotherm start with the lowest pressure, usually 5 atm; the first trial value of V_m is obtained assuming $z_m = 1$. After the iteration is completed, the corresponding value of z_m is saved and used to calculate the first trial value of V_m for the next highest pressure. The second trial value of V_m for each pressure is obtained by a simple delta scheme.

The interaction procedure is given T, V_m and y_1 as input variable and calculates as output to the driver program the interaction terms for the particular enhancement factor relation.

The iteration on y_1 is not executed in the approximate calculations in which y_1 is defined to be zero. In the more exact case, $y_1 \neq 0$, V_m is first evaluated using a trial value of y_1 which is taken from the ideal gas relation for the first, lowest pressure on an isotherm and is taken as the value computed from the enhancement factor for the preceding pressure for all higher pressures. This first value of V_m is used to evaluate ϕ from which y_1 is evaluated and which is used to calculate a new value of V_m which is, in turn, used to compute a new value of ϕ and y_1, and so on. This iteration is continued until the change in y_1 between successive iterations is less than one part in 100,000 or until ten trials have been made. Failure to converge will initiate the computation of the next isotherm.

In this work the $y \neq 0$ calculations were used.

Calculation Results

The results of the enhancement factor calculations are shown in Figure 11. A comparison of these results with the experimental data of this work may be found in Figure 15. Appendix G gives a discussion of the contribution of the various terms in the enhancement factor equation (equation 10) on the calculated value of the enhancement factor.

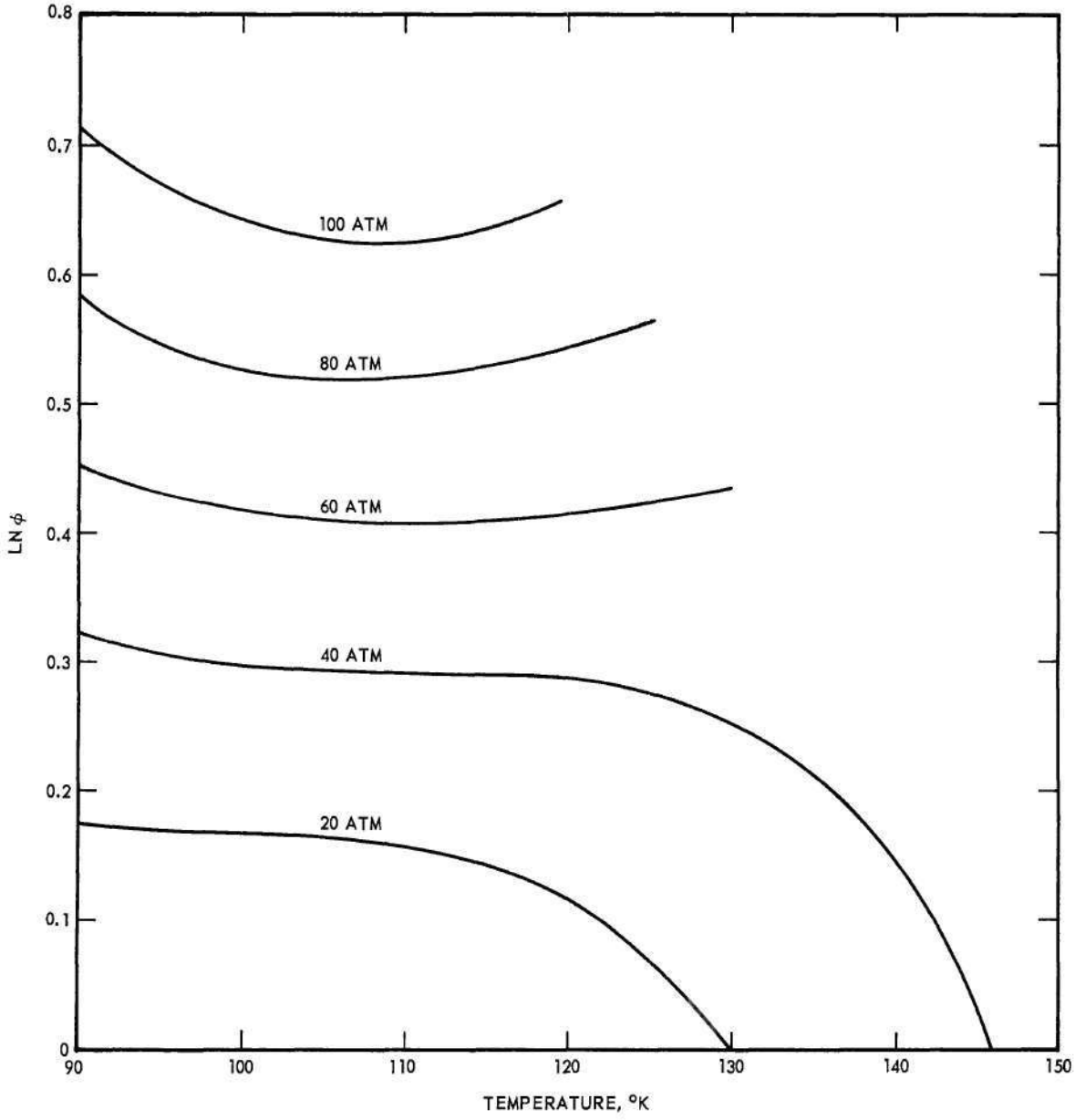

Figure 11. Calculated Values of Enhancement Factor vs. Temperature.

The shapes of the computed enhancement factor isobars, and the magnitudes of the enhancement factors, are considered to be close to those to be expected from the experimental data. The following analysis explains the basis for this statement.

1. The assumption that the condensed phase is pure is not greatly in error for the helium-argon system, since the concentration of the helium in the liquid is not greater than 2.5 mole per cent in the temperature and pressure ranges of the calculations.

2. The use of the Lennard-Jones potential function to estimate the third virial coefficients could produce some error. However, the term which is most affected by the third virial coefficients, I_c, contributes less than five per cent to the enhancement factor. Therefore an error in the third virial coefficients probably will not greatly affect the calculated value of the enhancement factor. This may be verified by a comparison of columns three and four in Table 19.

3. The mixture rules used to compute the second virial interaction coefficient do not adequately represent the physical situation and this could lead to some error. However, the computed value of B_{12} for this system is small compared to B_{11}, contributing less than twenty per cent to the I_b term and less than ten per cent to the value of B_m. Thus for this system the form of the mixture rule chosen is not particularly important. The contribution of these terms to the value of the enhancement factor may be observed by a comparison of columns three, four, and five in Table 19.

4. The linear equation for liquid volume represents the data very well as can be seen from Figure 8. Also the properties of argon along

the vapor pressure line are well known. Therefore the second term of equation 10 should not be greatly in error.

5. The agreement between the calculated and observed values of z_{01} is very good as can be seen in Figure 9.

6. The use of the Kihara potential function and the Prausnitz parameters to compute the second virial coefficients directly affects the value of V_m, which is a major contributer to the magnitude of the enhancement factor. These second virial coefficients agree well in shape and magnitude with the available experimental data as may be seen in Figures 6 and 7.

The contributions of each of the major terms in equation 10 are of interest as an aid in understanding fully the affect of each of the quantities discussed above. The contribution to ϕ of first three terms of equation 10;

$$\ln \frac{1}{z_{01}} + \frac{P - p_{01}}{RT}\left[a + \tfrac{1}{2}b(P + p_{01})\right] + \left[2\frac{B_{11}}{V_{01}} + \frac{3}{2}\frac{C_{111}}{V_{01}^2}\right]$$

vary from ninety per cent of the value of ϕ, at the lowest temperatures and pressures, to sixty per cent at the highest temperatures and pressures. The I_b term contributes approximately ten per cent at the lowest temperatures and pressures to about forty per cent at the highest temperatures and pressures. The I_c term has little effect at low pressure, up to about five per cent at 100 atmospheres, essentially independent of temperature. Appendix G gives a more detailed discussion of these contributions.

It is felt then, that these calculations can be used with considerable confidence to predict the proper shape of the experimental enhancement factor curves and also to provide a reasonably good estimate of the magnitude.

Calculational Limit

Unfortunately the iteration procedure between y_1 and V_m in the computer program diverges at the higher temperatures. Thus the upper limit of the calculations was about 125° K, except at the lower pressures. The isobars below the critical pressure can be extended with some confidence since the logarithm of the enhancement factor must be zero at the vapor pressure line.

Liquid Phase

No prediction calculations were attempted for the liquid phase. One of the correlation techniques used involved the computation of a modified Henry's law constant from the experimental data with the following equation.

$$K_h = \frac{P - p_{01}}{x_2 \cdot 100} \qquad (3)$$

The term $P - p_{01}$ was used as an estimate of the partial pressure of helium rather than other possible relations because it does not depend on the composition of the vapor phase. The quantity K_h thus depends only on liquid composition (and pressure and temperature) and can be used as a guide in the estimation of the precision of the experimental data. A typical ex-

perimental Henry's law constant isobar (at sixty atmospheres) is given in Figure 16.

CHAPTER V

DISCUSSION OF RESULTS

Experimental Data

The dew-point curves, or phase boundary curves, of six mixtures of helium and argon, the bubble-point curves of six mixtures of helium and argon, and the vapor pressure curve of pure argon were experimentally determined. The temperature range covered was 100° K to 150° K; the pressure range was 10 to 70 atmospheres. The compositions of the experimental mixtures were varied from zero to 85 per cent helium in argon.

The dew-point curves, presented on a pressure-temperature diagram, are shown as Figure 12. The bubble-point curves, also on a pressure-temperature diagram, are shown as Figure 13. The experimental data are shown as points on the curves in Figures 12 and 13 and are tabulated in Appendix A, Table 2.

Figure 14 shows one complete phase boundry curve exhibiting dew-point line, bubble-point line, and the estimated critical point. The bubble-point line was interpolated from the data shown in Figure 13; the dew-point line was taken from the experimental data given in Table 2. All mixtures should exhibit complete closed curves of this type; however mixtures with helium contents greater than three per cent have critical points and bubble-point lines at pressures higher than 70 atmospheres and therefore, due to the pressure limitation of the glass equilibrium cell, the phase boundry curves for these mixtures could not be closed in this

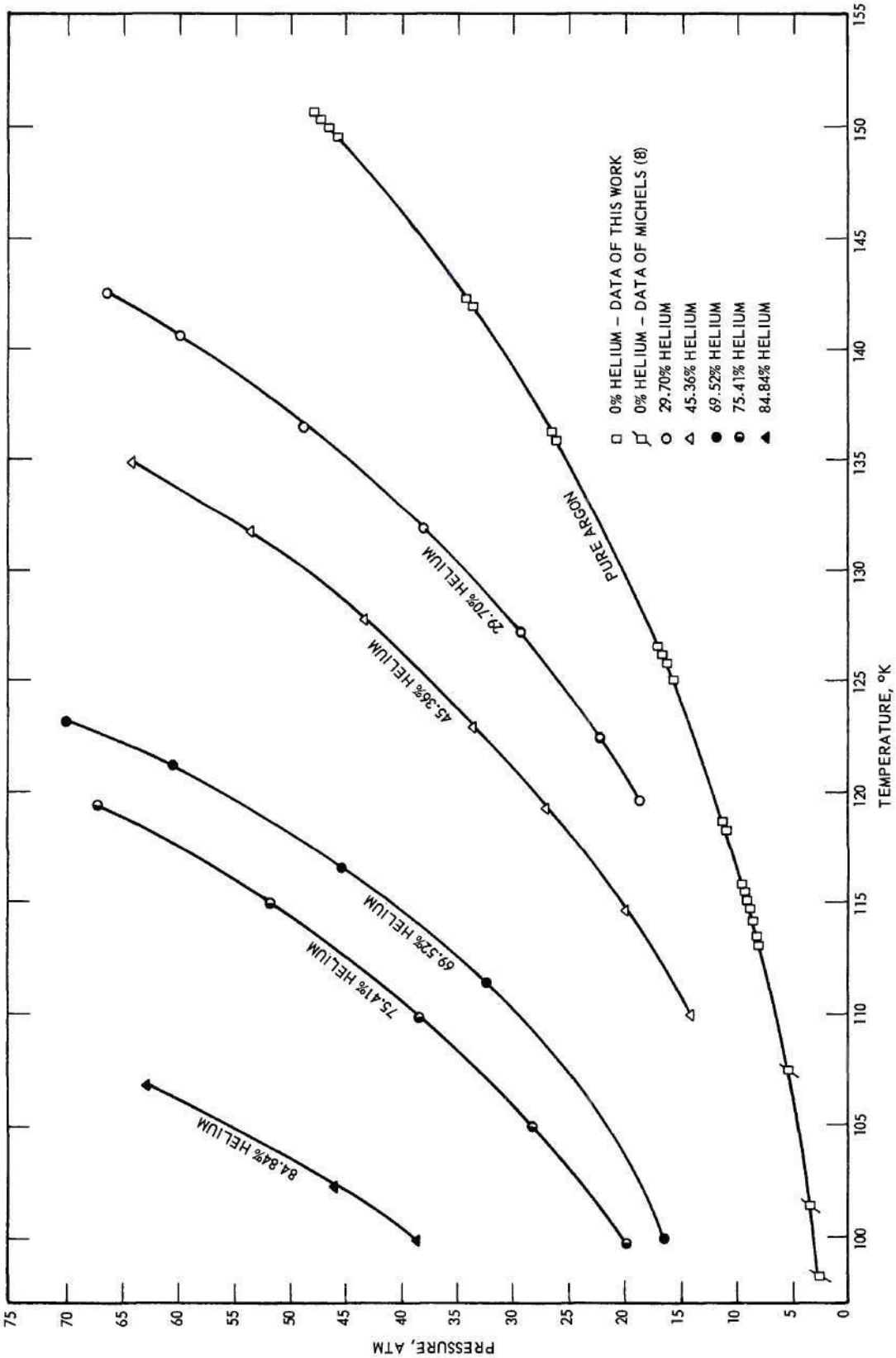

Figure 12. Dew-Point Lines, System: Helium-Argon.

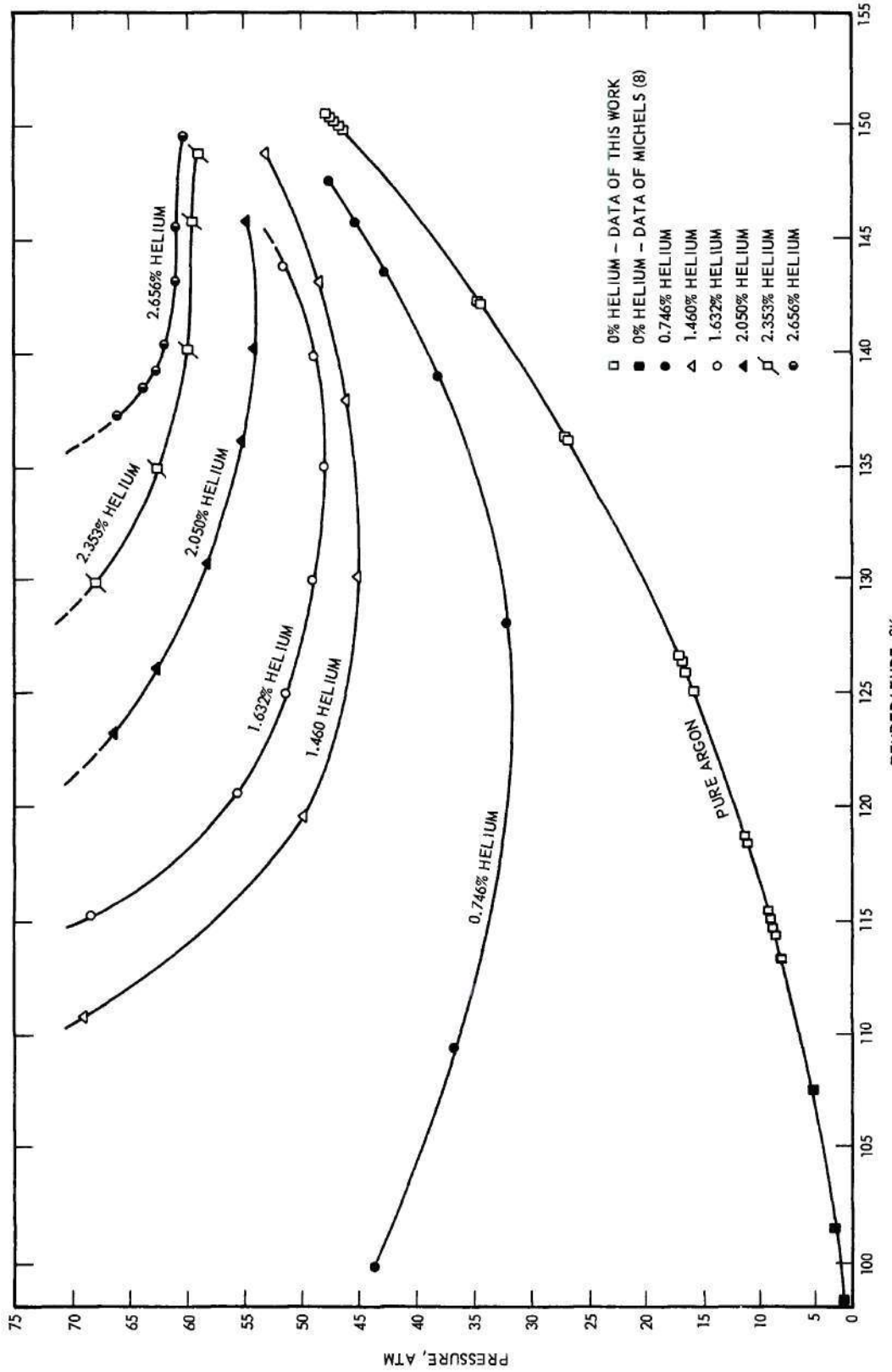

Figure 13. Bubble-Point Lines, System: Helium-Argon.

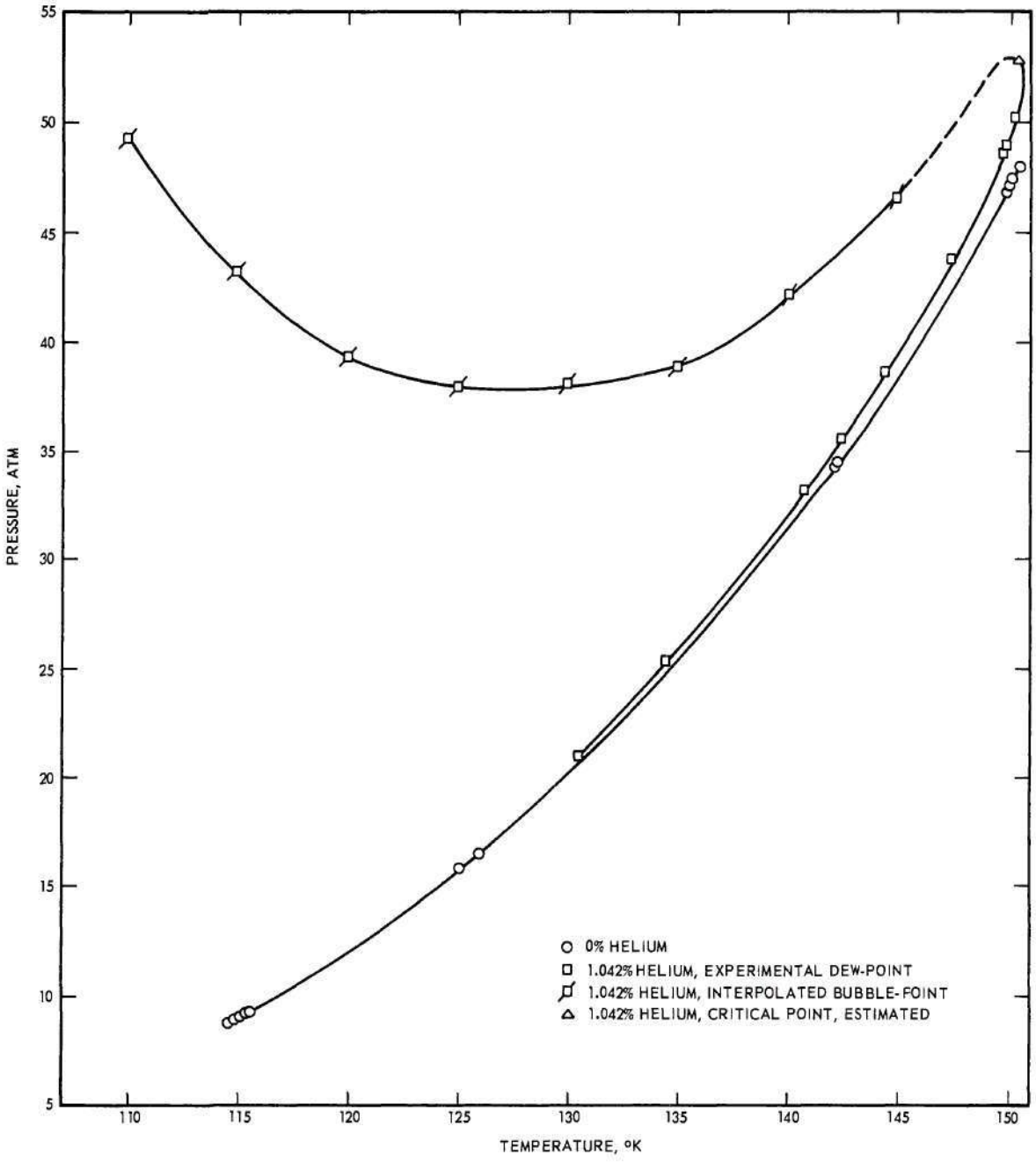

Figure 14. Phase Boundry Curve, System: Helium-Argon.

work. Closed phase boundry curves could have been obtained for the gas mixtures of less than three per cent helium; however, the dew-point portion of the curves was not of particular interest in this work.

The Gases Used

The helium used in preparing the experimental gas mixtures was produced and bottled by the United States Bureau of Mines helium plant in Amarillo, Texas. The manufacturer's stated purity was 99.999 per cent. The purity of this gas was tested by Gas Chromatographic analysis as described in Chapter II with helium eluent at the instrument's highest sensitivity and no impurities were detected.

The argon was purchased from Marks Oxygen Company of Atlanta, Georgia. The manufacturer certified a purity of 99.999 per cent, excepting water. This gas was also analyzed by Gas Chromatograph and no impurities were detected. In addition, dew and bubble points were experimentally observed on three samples of this gas at temperatures between 114° K and 150° K. In most cases the dew and bubble point pressures, at constant temperature, $\pm 0.02^{\circ}$ K, were identical. In no case did these pressures differ by more than 0.03 atm. These data may be found in Table 16. This attests the high purity of the argon gas. Due to the method of bottling the argon there was some water vapor present which was removed by passing the gas through a dryer containing Linde 5A Molecular Sieve at room temperature.

Precision Limits for the Experimental Data

The experimental data have been measured to within temperature precision limits of $\pm 0.02^{\circ}$ K and pressure limits of ± 0.15 atmospheres. A careful discussion of the basis for the assignment of the above values

may be found in Appendices C and D.

The precision limits of composition of the dew-points, vapor phase data and crossplot data in per cent of reported value of the minor component, are given below.

1. ±2 per cent of the concentration of the minor component (helium) at temperatures between 135° K and 145° K.

2. ±5 per cent of the concentration of the minor component (helium or argon) at temperatures between 125° K and 130° K.

3. ±10 per cent of the concentration of the minor component (argon) at temperatures between 110° K and 120° K.

4. ±15 per cent of the concentration of the minor component (argon) at 105° K.

The assigned concentration limit of ±2 per cent for the highest temperatures is based primarily on the estimated precision of the analytical method as described in Chapter III. The increasing larger errors at the lower temperatures are not considered to be due to the analytical method, but rather to an inherent weakness of the dew point method for systems such as the one under study here. Computation showed that the formation of the droplets of liquid, which signified the dew-point, may have caused a reduction in concentration of argon in the vapor of as much as fifteen per cent at the lowest temperatures. In these computations the volume of liquid was estimated to be 0.013 cm^3.

The precision limits of the vapor composition as assigned above were selected after a careful study of the size and effect of drop formation, the shape of the theoretical enhancement factor curves given in Chapter IV, and of the lower-temperature argon-helium phase equilibrium

data of Mullins (41), which became available after these measurements were completed. Figure 15 gives the comparison of the experimental and computed enhancement factor isobars.

Calculation shows that the formation of bubbles in the observation of bubble-points would be expected to produce only small errors (one per cent above 115° , three per cent at 100° K) in the composition of the liquid phase. (In these calculations the bubble was assumed to be spherical with an estimated diameter of approximately $\frac{1}{2}$ of the inside diameter of the cell. This gave a bubble volume of about 0.01 cm^3.) The assigned precision limits for the bubble-point compositions are presumed to depend primarily on the precision of the analytical method, namely, ± 2 per cent of the helium concentration, except below about 115° where the uncertainty is greater. Comparison of the bubble-point data of this investigation with the unpublished liquid phase equilibrium data of Mullins (41) is limited to the bubble points at 110.86° , 109.46° and 99.92° K, since Mullin's data does not extend above 108° K. The disagreement between the two sets of data is within about 5 per cent at 110° , but amounts to about 20 per cent at 99.92° K, the helium concentration found by Mullins being lower than that found in the present study. The modified Henry's law constants, calculated as discussed in Chapter IV, were used to extrapolate the two sets of data to permit comparison. An example of this correlation, calculated from the cross-plot data of this work, is given in Figure 16.

It is also interesting to note the smooth fit of the cross-plot data. This gives an indication that the cross-plot procedure did not introduce any scatter in the data.

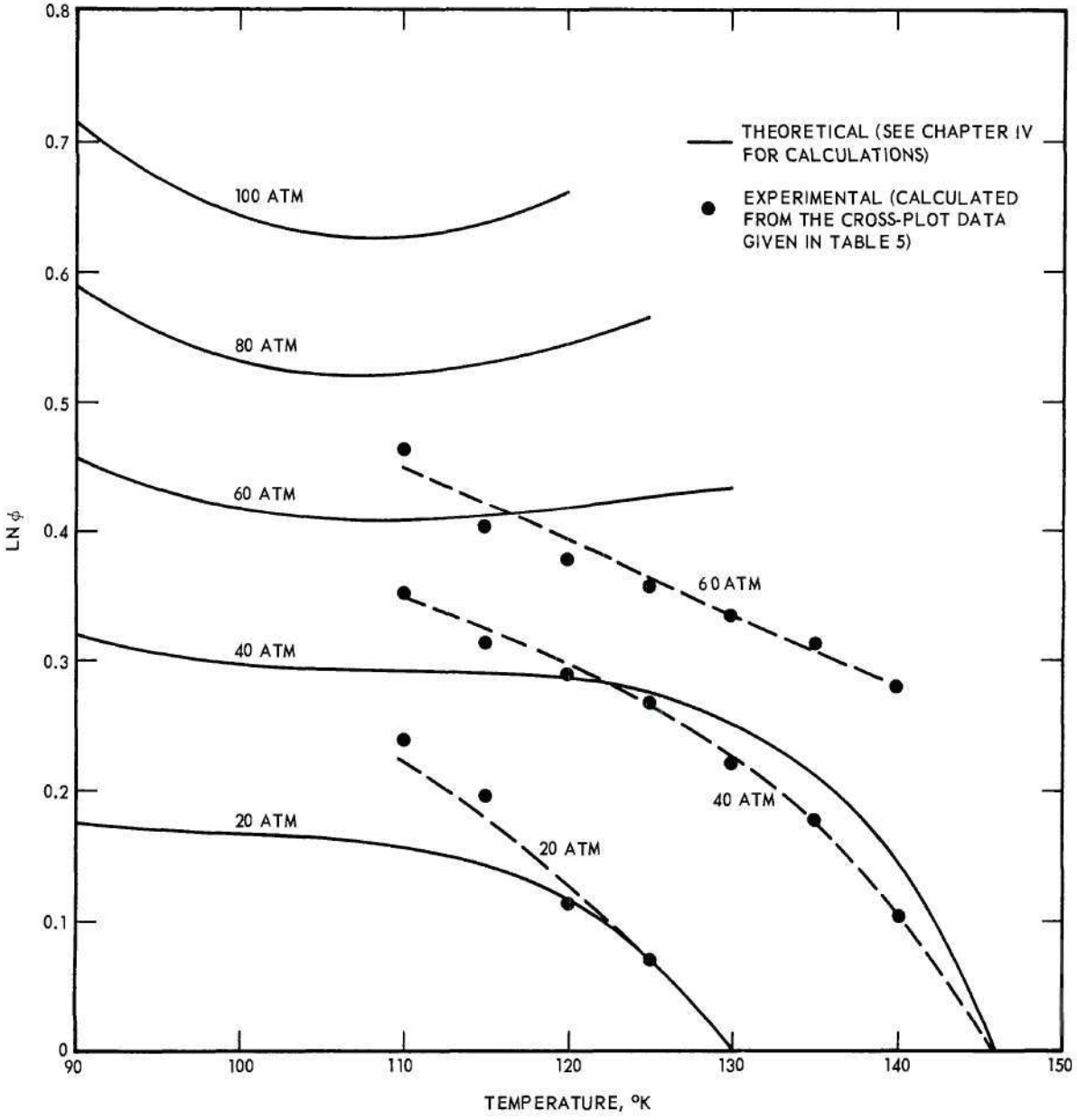

Figure 15. Calculated Values of Enhancement Factor vs. Temperature with Experimental Measurements Included.

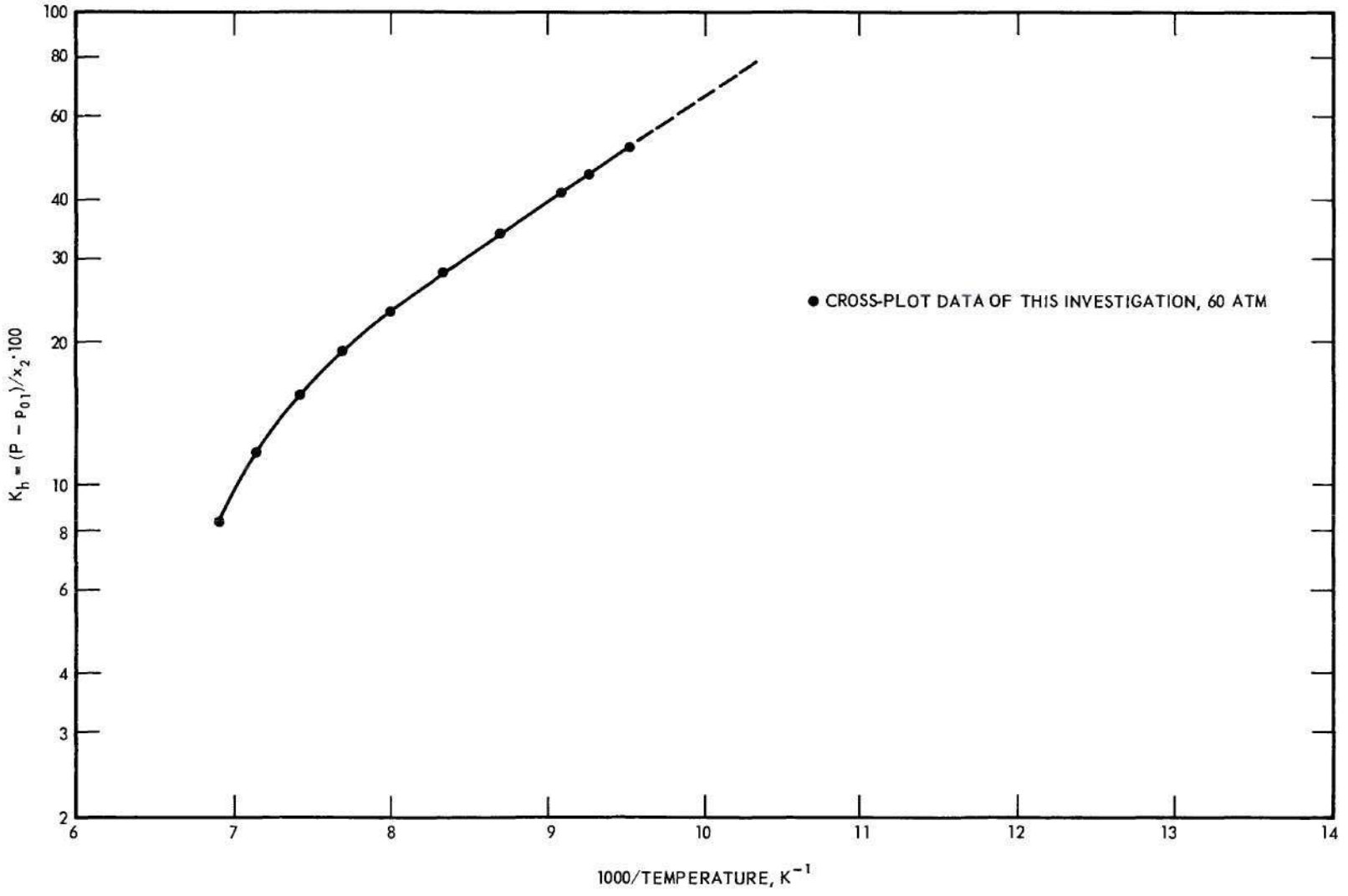

Figure 16. Isobaric Henry's Law Constants vs. Reciprocal of Temperature at Sixty Atmospheres.

Vapor Pressure of Argon

Following the tests and calibrations on each individual instrument, a final check of the operability and precision of the entire experimental system was performed by determining the vapor pressure of pure argon at various temperatures from 114° K to 150° K. The experimental equipment and procedures used on the vapor pressure determinations were deliberately exactly the same as were used throughout the dew-and bubble-point determinations on the binary mixtures.

The vapor pressure-temperature relation of argon has been determined in three other investigations; by Crommelin (10), Clark, et al., and Michels, et al. (8), and again by Michels, et al. (39). Michels et al., (8) fitted the following equation to their data

$$\text{Log}_{10}P = -550.8211/T - 8.7849395 \log_{10}T + 0.0174713T + 21.8379 \quad (17)$$

This equation is used here merely as a means of comparing the various data.

Michels et al., also presented a graph showing deviations of their data, as well as those of the other investigators, from this equation. A reproduction of this deviation plot with the data of this investigation added is presented in Figure 17. The numerical values of the data shown in this Figure are tabulated in Appendix E. One may readily see that the results of all four investigations compare to well within the precision limits of ± 0.15 atm assigned to the measurements of this investigation. Thus no attempt was made to select the best of the three sets of data for comparison purposes.

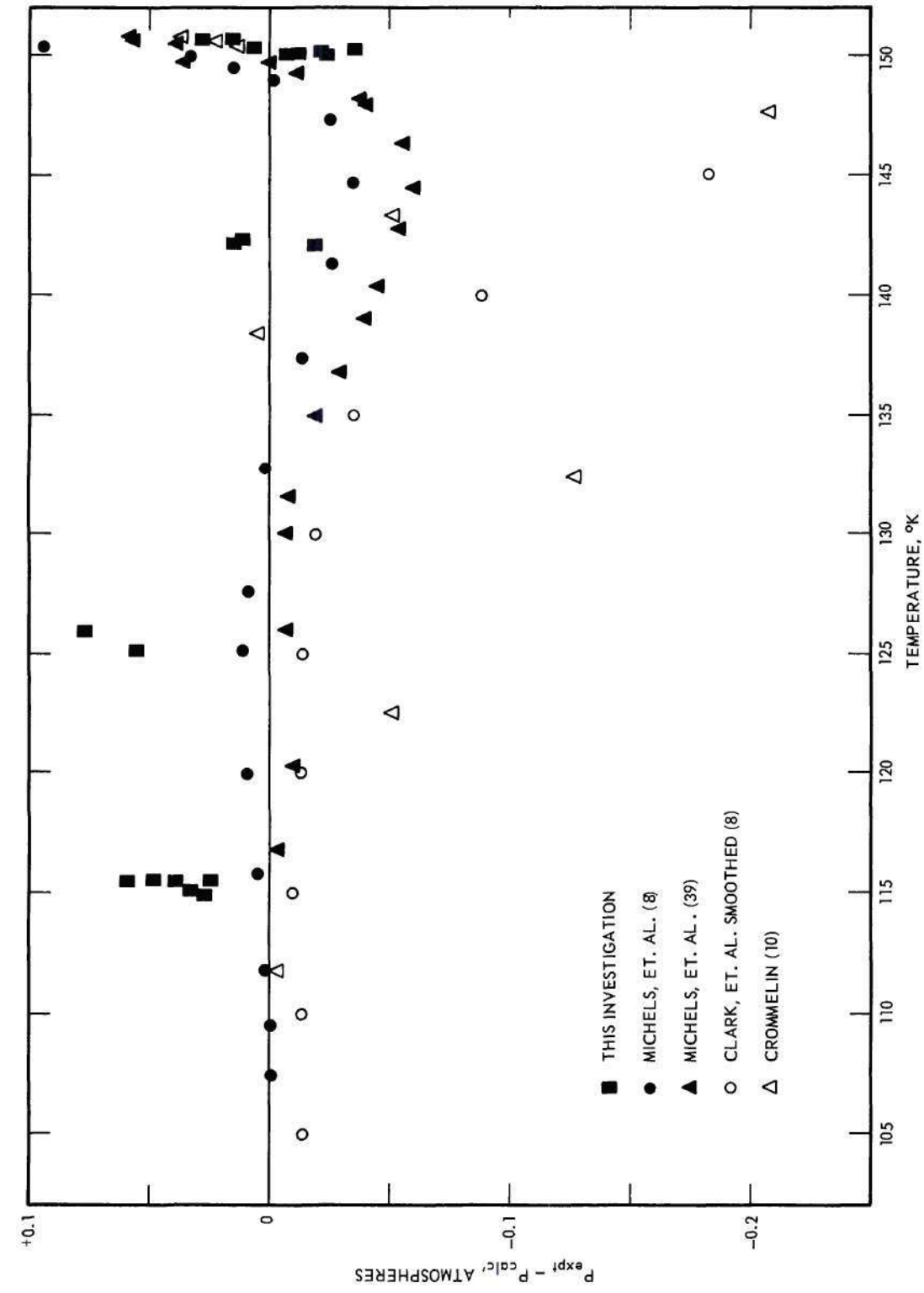

Figure 17. The Deviation of Experimental Argon Vapor Pressure from Michels Equation.

These vapor pressure determinations and favorable comparison with the data of other investigators indicate that the pressure and temperature measurements were as precise as noted above and that the proper experimental procedures were being used. They, of course, shed no light on the effect of drop formation on vapor composition. Also the negligible pressure difference between dew and bubble points as shown in the data tabulated in Appendix E provided a second test which showed the argon to be of high purity.

Other Data Presentations

Isothermal pressure-composition diagrams provide useful presentations of phase equilibria data. These diagrams may be constructed from the pressure-temperature curves of Figures 12 and 13. The pressure values taken from the intersection of given constant temperature lines and the dew-and bubble-point curves for each mixture are tabulated in Appendix A. These values were used to construct the pressure-composition diagram of Figure 18. The curves to the right in Figure 18 correspond to the vapor phase compositions at the indicated pressures and temperatures; the curves to the left correspond to the liquid phase compositions. The compositions of both the liquid and vapor phases at equilibrium conditions may be determined by locating the points at which the selected pressure line intersects each of the isotherms corresponding to the desired temperature.

In order to demonstrate the shape of the vapor and liquid curves without undue crowding Figure 18 shows only three selected isotherms. Figure 19 shows the vapor isotherms at five degree intervals. The liquid phase isotherms are given on an expanded scale in Figure 20. Thus in or-

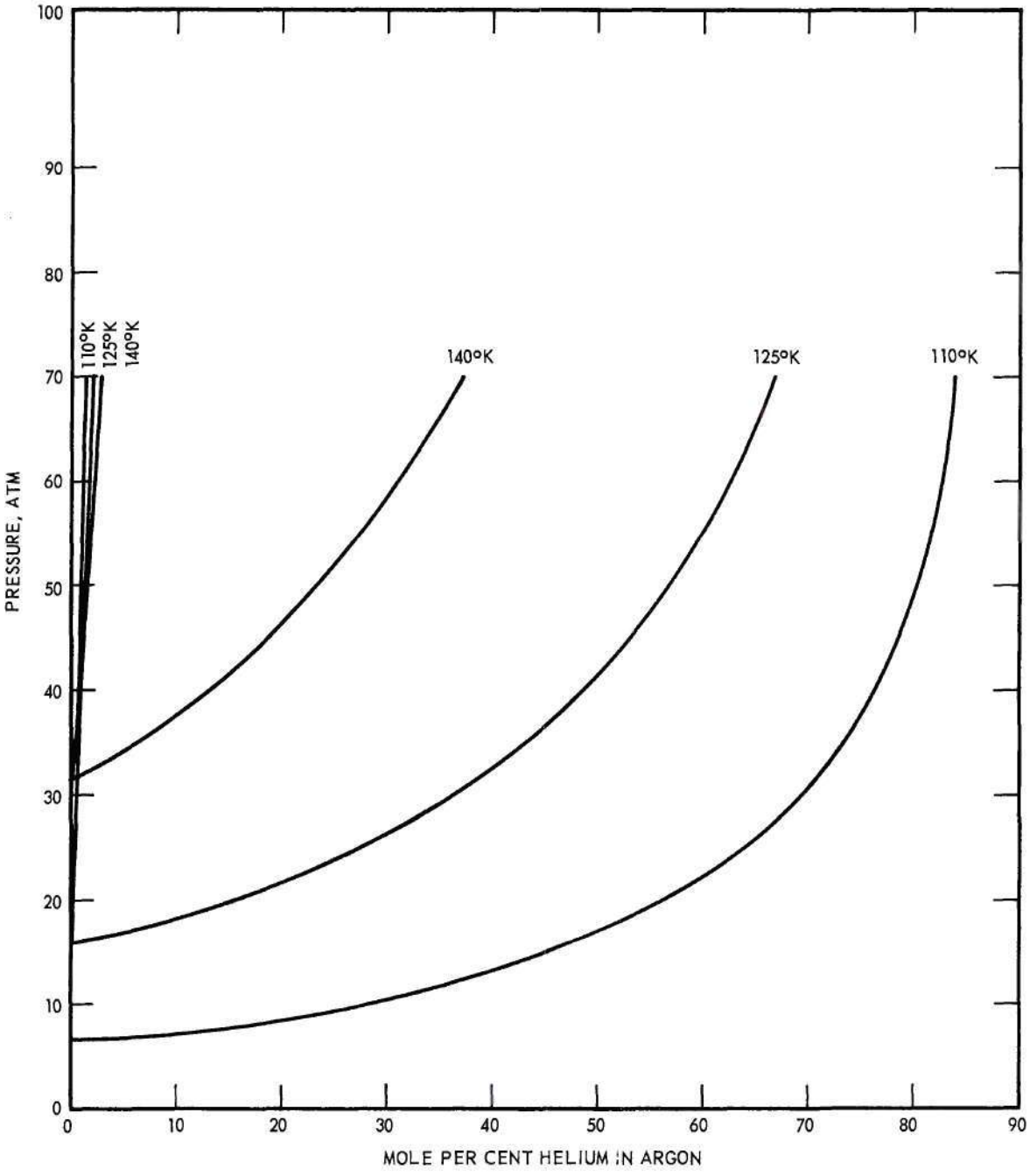

Figure 18. Pressure vs. Helium Content in the Liquid and Vapor Phases.

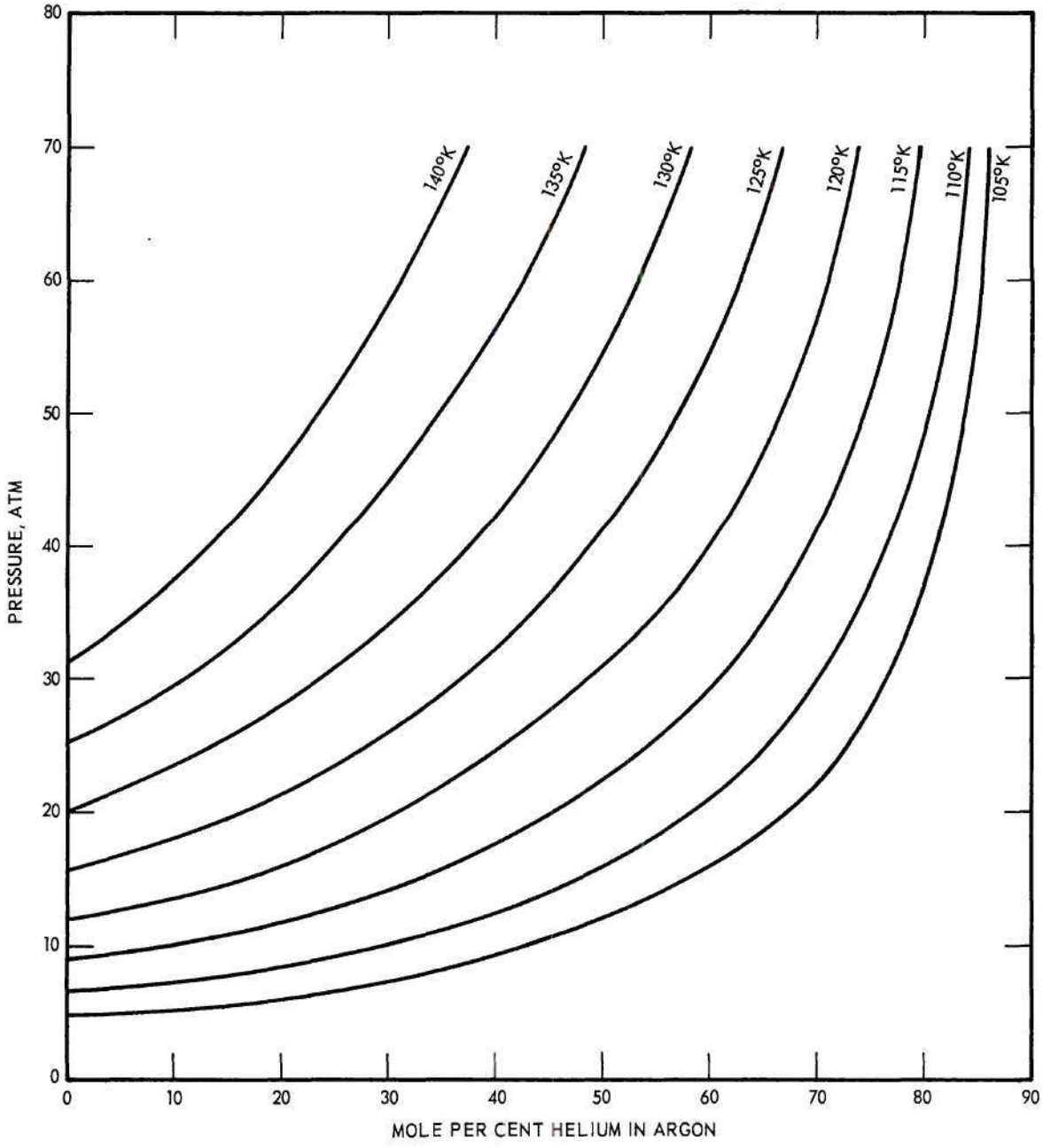

Figure 19. Pressure vs. Helium Content in the Vapor Phase.

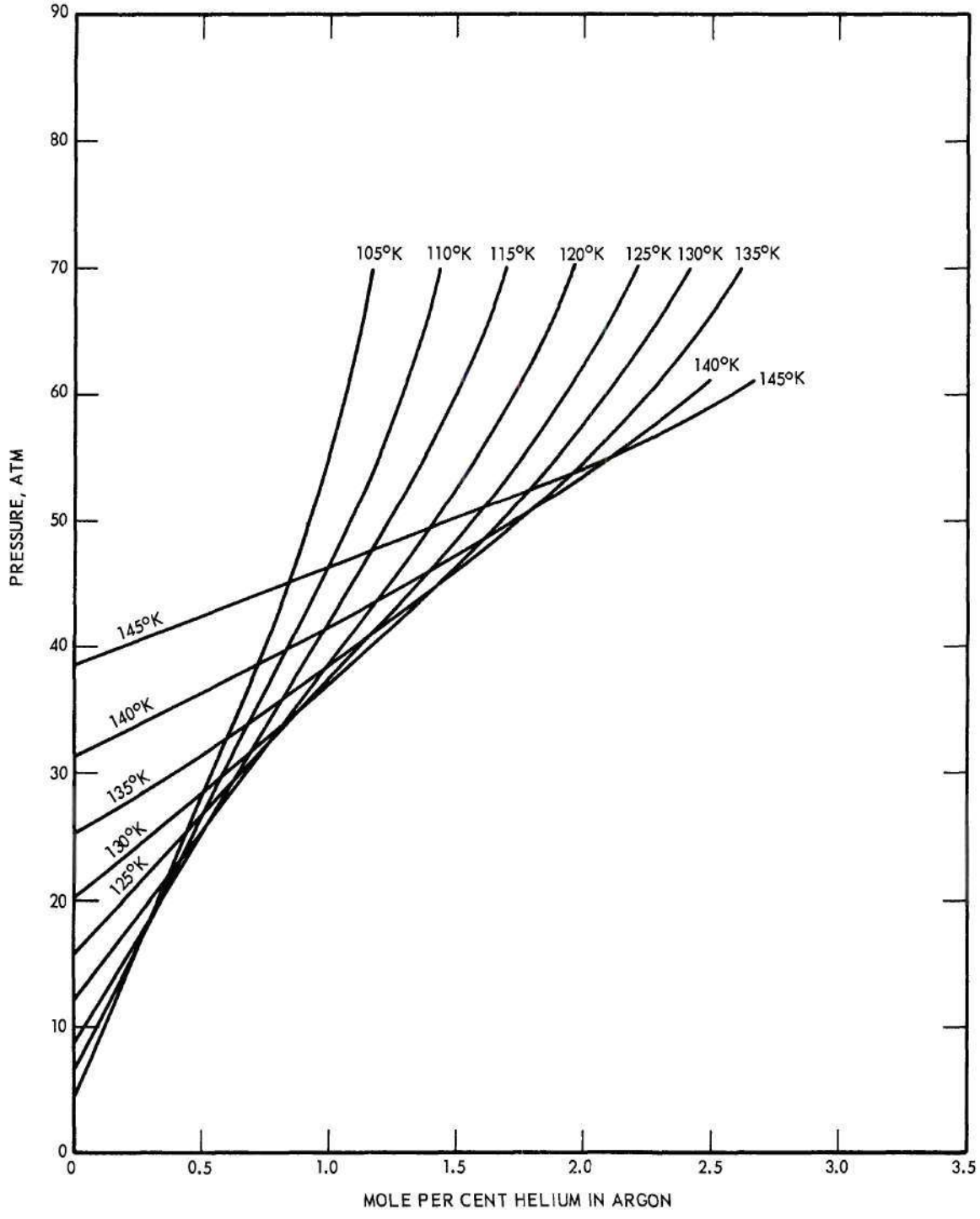

Figure 20. Pressure vs. Helium Content in the Liquid Phase.

der to determine the phase compositions at given temperature and pressure Figure 20 must be used to obtain the liquid phase composition and Figure 19 to obtain the vapor composition.

The isobaric temperature-composition diagram given in Figure 21 was constructed from the pressure-temperature diagram in a manner similar to that described above. Only three selected isobars are shown to illustrate the shape of the temperature-composition curves. The curves to the right give vapor compositions and the curves to the left give the liquid compositions. A complete set of curves for the vapor side of the isobaric envelope is given in Figure 22; for the liquid in Figure 23. The data used to construct these figures was taken from Figure 12 and 13 and is given in Appendix A.

A phase equilibria data presentation which is convenient for the engineer is the equilibrium constant-pressure diagram. The equilibrium constant, K, is defined as equal to the ratio of the composition in the vapor phase to the composition in the liquid phase. Figures 24 and 25 give the equilibrium constant-pressure diagrams for the helium-argon system. Another method of presenting the data is the enhancement factor-pressure graph given in Figure 26.

Cryostat Operation

Temperature Control Operation

The temperature control operation of the cryostat must be evaluated as successful. Temperatures as low as 91° K were attained. Temperature gradients in the liquid bath were very small during line-out operation, the temperature gradient along the equilibrium cell from top to bot-

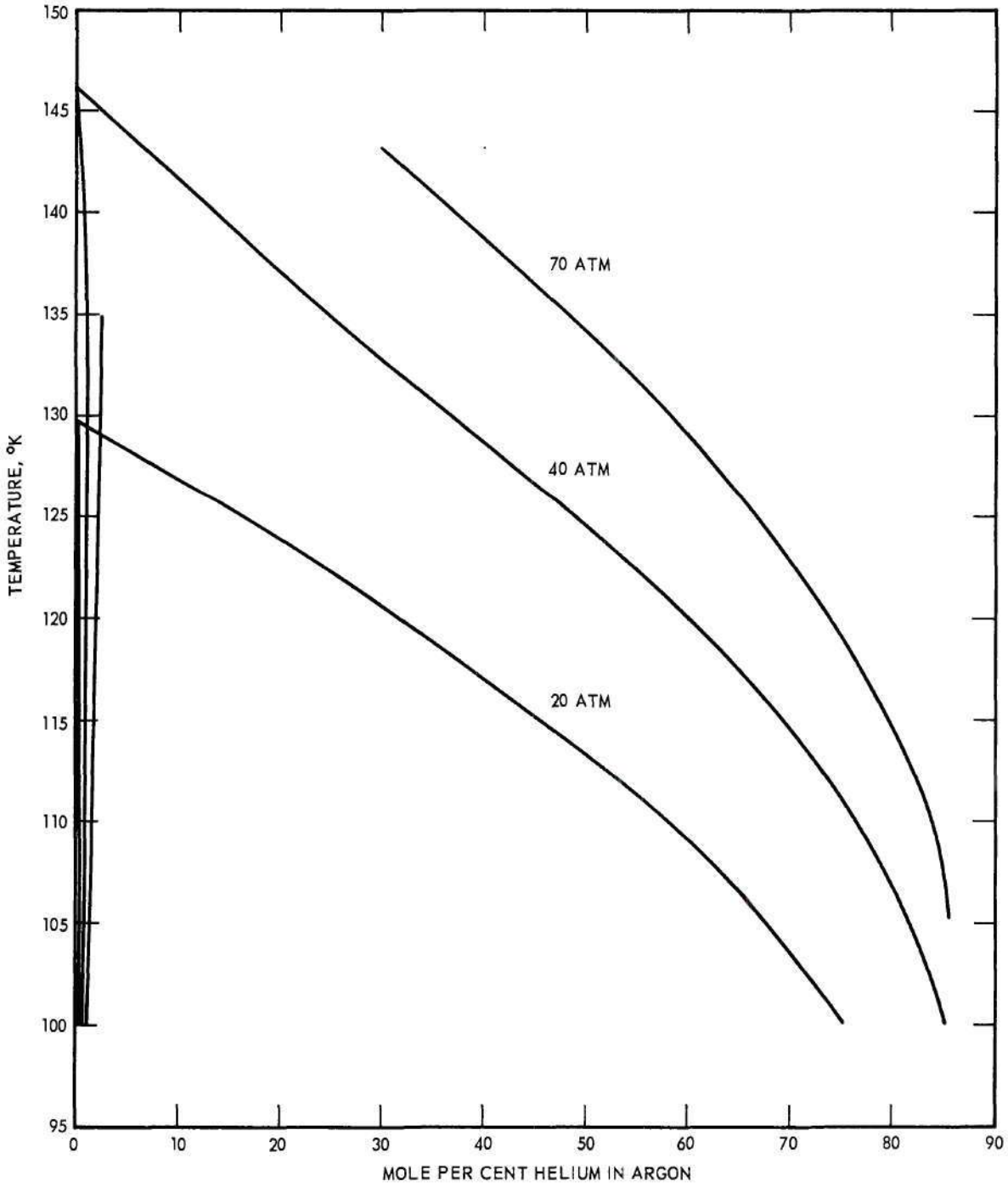

Figure 21. Temperature vs. Helium Content in the Liquid and Vapor Phases.

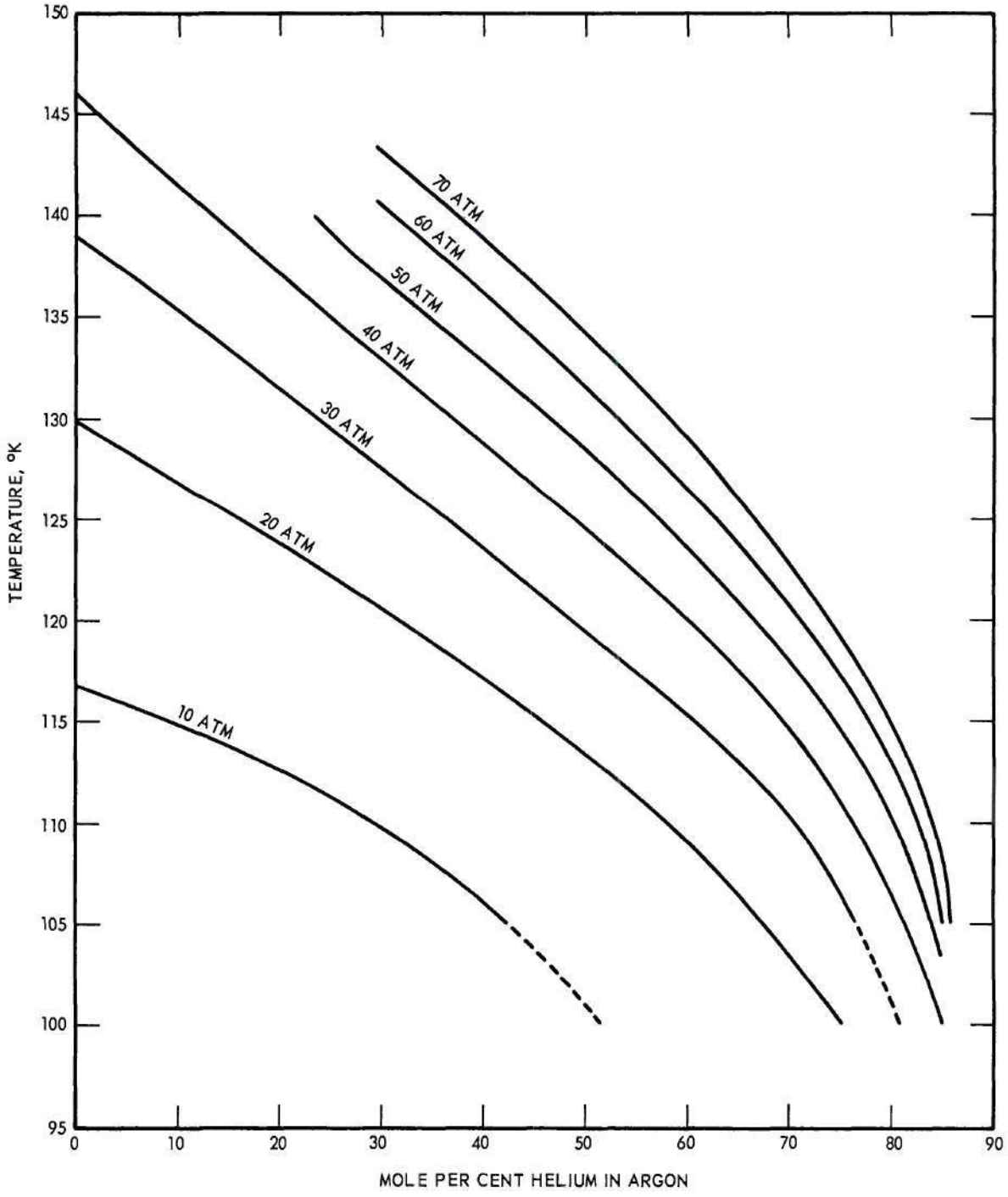

Figure 22. Temperature vs. Helium Content in the Vapor Phase.

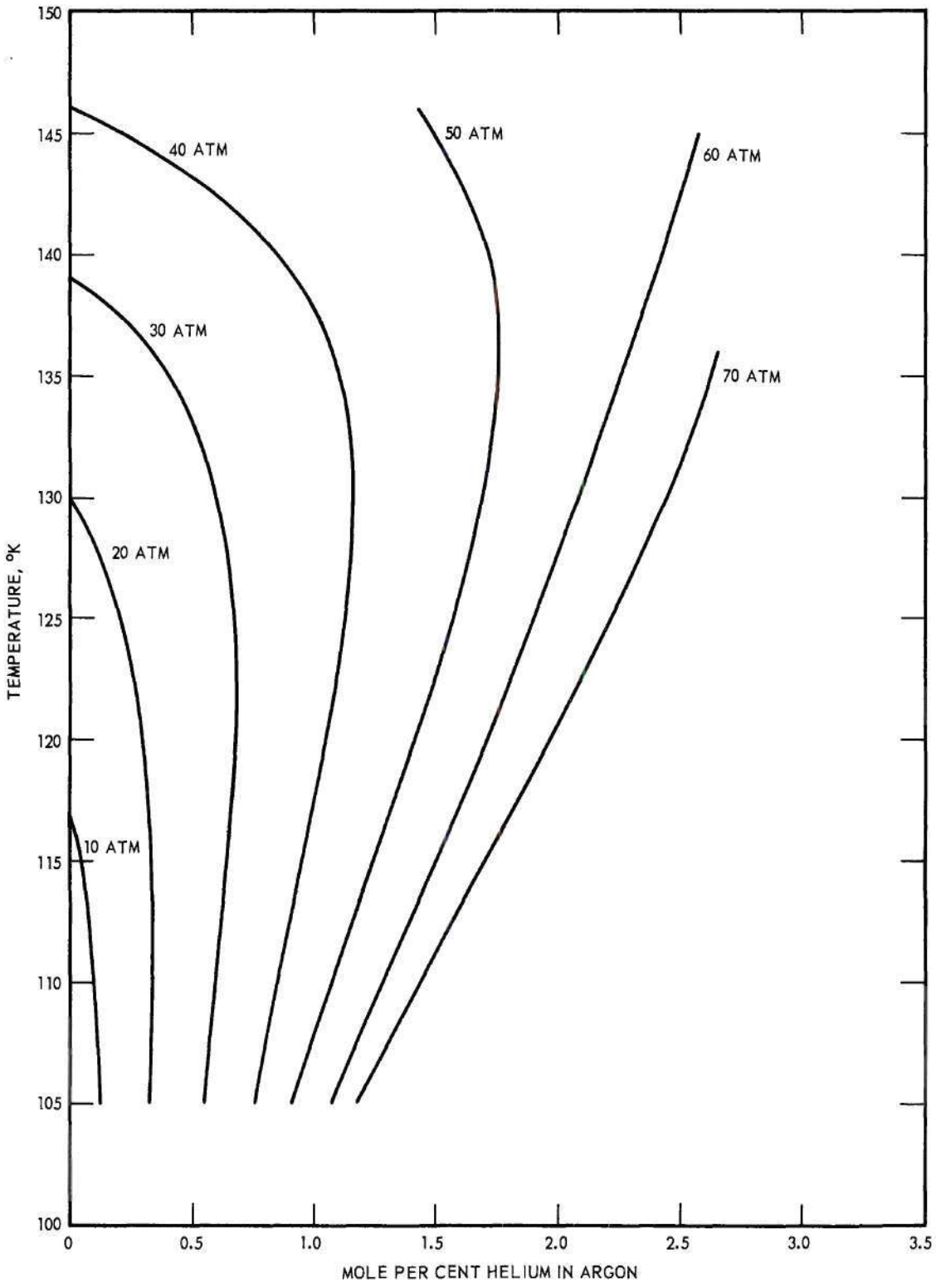

Figure 23. Temperature vs. Helium Content in the Liquid Phase.

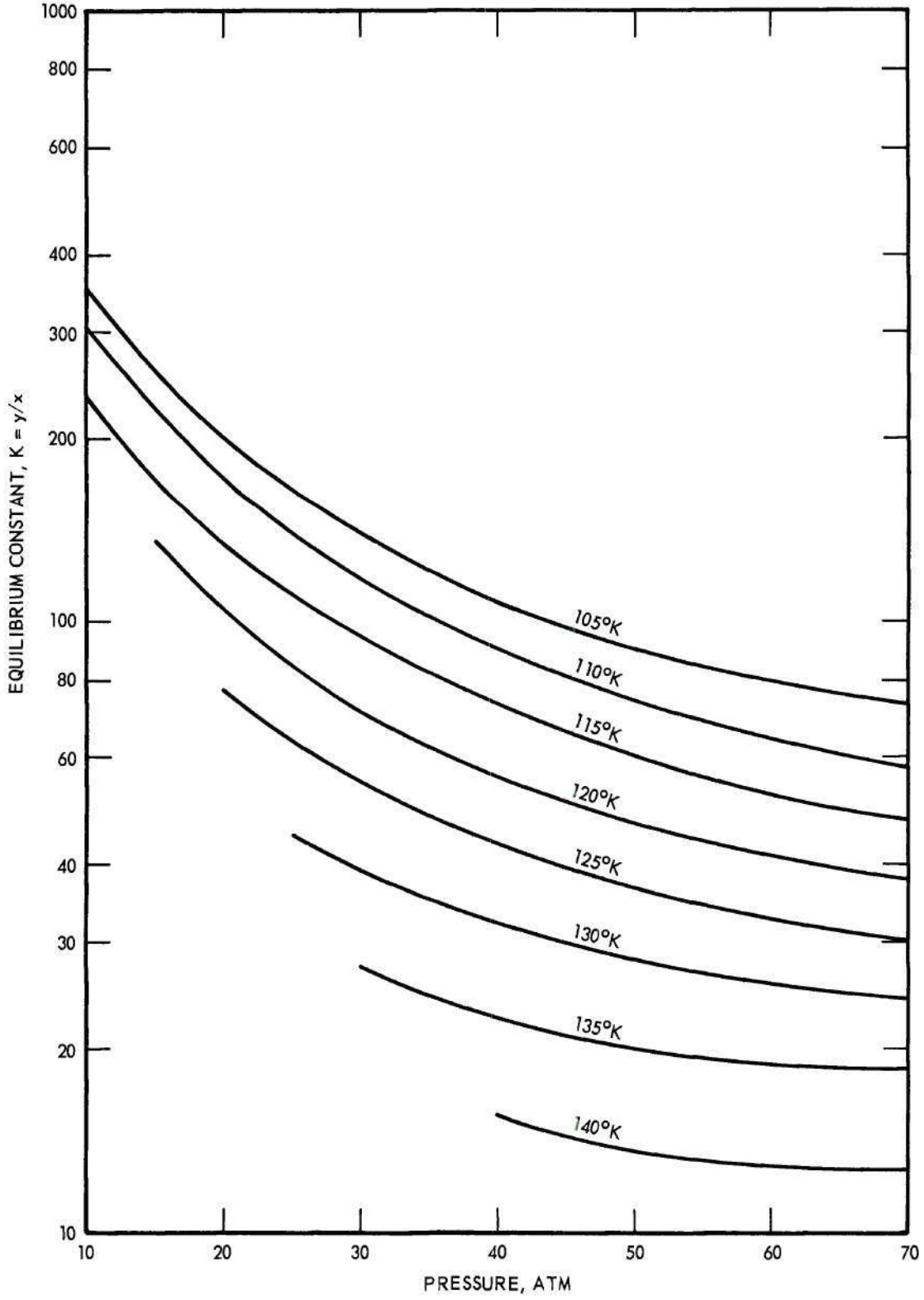

Figure 24. Equilibrium Constant vs. Pressure for Helium in Argon.

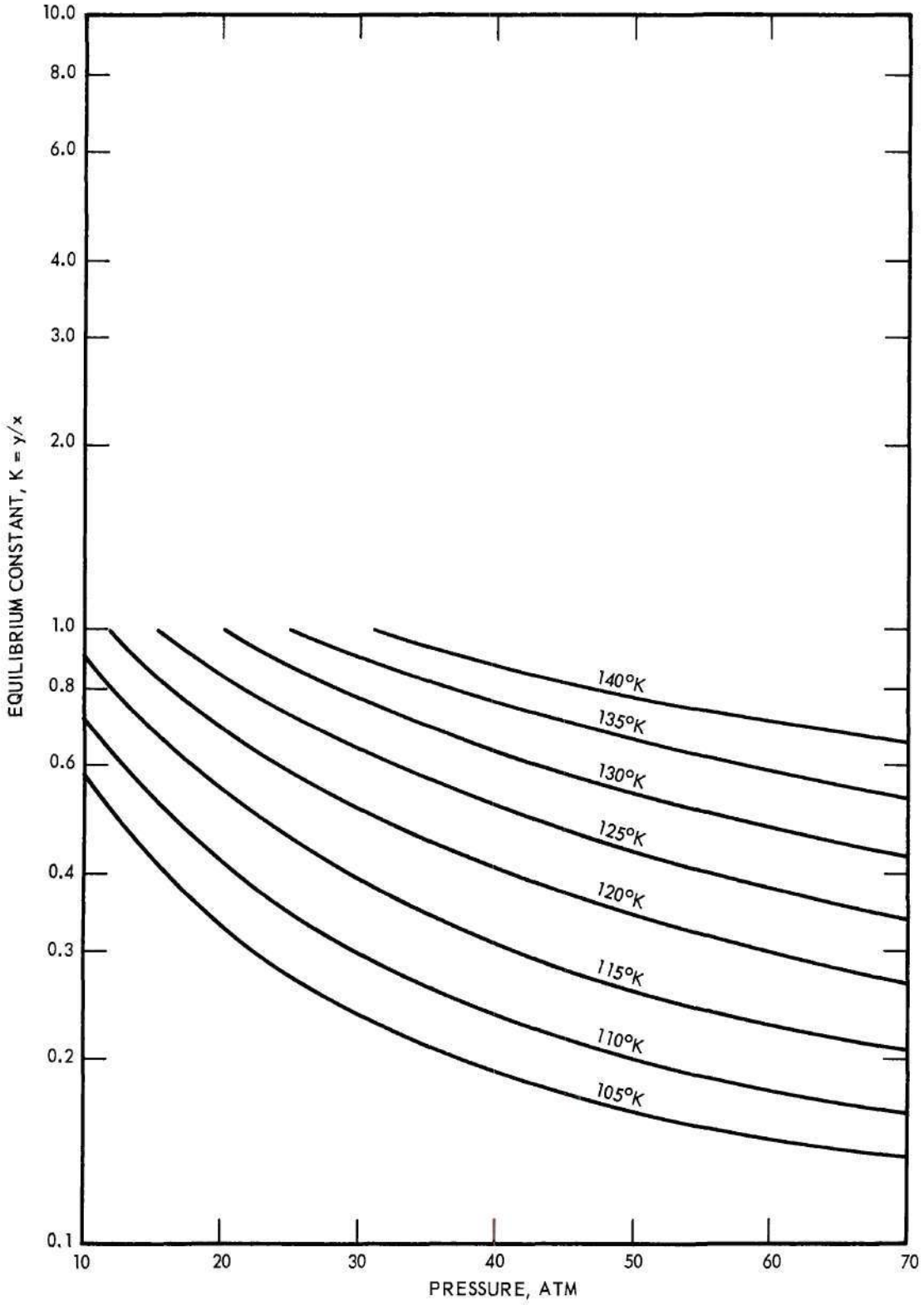

Figure 25. Equilibrium Constant vs. Pressure for Argon in Helium.

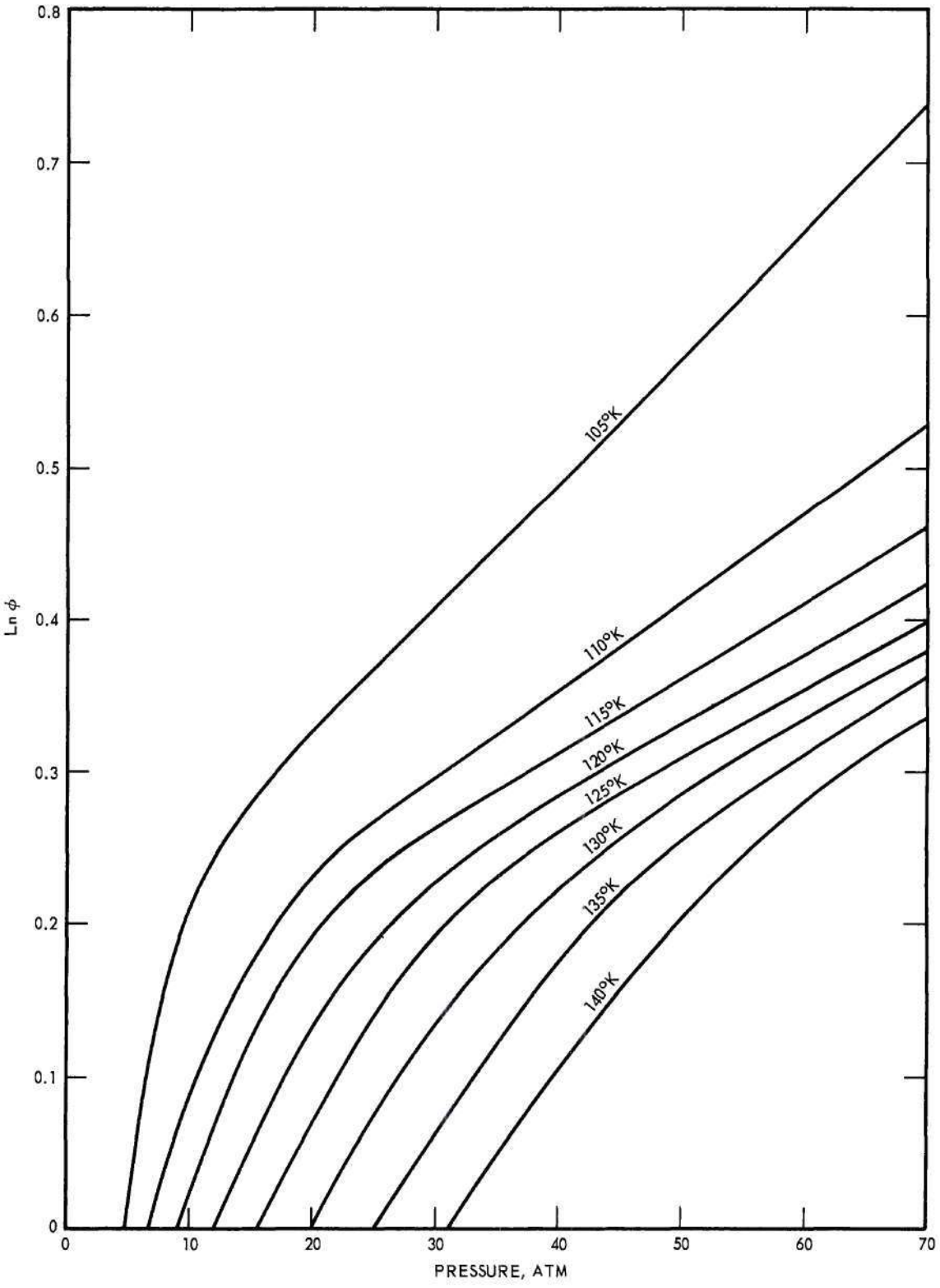

Figure 26. Enhancement Factor vs. Pressure for Argon in Argon-Helium System.

tom never exceeding $\pm 0.003^{\circ}$ K during controlled operation. The cell temperature could be controlled to $\pm 0.005^{\circ}$ K within thirty minutes after desired temperature was reached. This temperature control could be held for as long as one hour if necessary. Figure 5 gives an example of the normal temperature control.

Stirrer Operation

As in all new equipment design some operational difficulties developed. These difficulties will be discussed in some detail below so that future investigators may derive some benefit from the experience gained in initial operations.

The major operational problems were concerned with the stirring mechanism. This was not unexpected. Upon initial start-up the bearing was permitted to become much too cold and it promptly wore out, probably due to contraction stresses. Future trouble was reduced by heating the bearing assembly with heat lamps; however this caused some increase in liquid nitrogen consumption. A favorable effect on bearing operation was obtained by running it dry with graphite lubrication.

The stirrer circulated the liquid propane extremely well. The motor speed was greatly over-designed, as the motor was never operated at over one-quarter of its rated speed. The motor power was satisfactory.

The liquid propane used in the bath was commercial propane prepared for domestic use. The propane concentration was probably in the order of 95 per cent. The viscosity of the propane increased as temperature decreased; however, propane circulation was not impaired in any way even at 91° K. The impurities in the propane caused it to become

somewhat cloudy at the lower temperatures; however, observation of the cell was not seriously affected.

Cooling Rate Control

The manual control of the liquid nitrogen flow rate and thus the cooling rate of the cooling tube was extremely tedious. As stated above the temperature in the liquid bath could be controlled very precisely over an adequate period of time; however, constant attention was required. This function needed to be automated in some manner.

Valves

The gas mixing and storage section was originally constructed with Hoke model R1189 globe valves with Crawford Swagelok tubing fittings. These valves were of 303 stainless steel with 303 stainless steel stems and rubber o-ring packing. Later several valves in the upper manifold, which did not have contact with mercury, were replaced with Hoke model R1193 globe valves. These valves were of brass with 303 stainless steel stems and rubber o-ring packing.

Although the specifications in the Hoke catalog would lead one to believe that these valves are suitable for this particular application, the fact is that they were extremely unsuitable. After limited usuage gas began to leak through nearly every valve.

CHAPTER VI

RESULTS AND CONCLUSIONS

The following results and conclusions have been formulated from this research.

1. The vapor-liquid phase equilibria of mixtures of helium and argon have been measured, as dew points and bubble points, over a temperature range of 100° K to 150° K at pressures below 70 atmospheres. The helium concentration in the liquid phase was less than three per cent and the argon concentration in the vapor phase was greater than 14 per cent throughout these pressure and temperature ranges.

2. The assigned precision of the pressure and temperature measurements of the dew-points and bubble-points is $\pm 0.02^{\circ}$ K and ± 0.15 atm. The uncertainity in the composition of the prepared gas mixtures used is ± 2 per cent of the concentration of the minor constituent.

3. The bubble-points have been measured with a precision of $\pm 0.02^{\circ}$ K, ± 0.15 atm. or ± 2 per cent of the helium concentration except below about 110° K where the uncertainty in the helium concentration may be as much as ± 5 per cent, rising to as much as 20 per cent at the lowest temperature (99.92° K).

4. The dew points have been measured with the same apparent precision in temperature and pressure as given above. However, because of the low argon concentration present at the lower temperatures, the composition of the equilibrium gas is known less accurately. The estimated

overall errors, in terms of the composition limits for the assigned pressure and temperature are:

a. ± 2 per cent of the concentration of the minor component (helium) at temperatures between 135° K and 145° K.

b. ± 5 per cent of the concentration of the minor component (argon or helium) at temperatures between 125° K and 130° K.

c. ± 10 per cent of the concentration of the minor component (argon) at temperatures between 110° K and 120° K.

d. ± 15 per cent of the concentration of the minor component (argon) at 105° K.

5. The vapor pressures of argon have been measured in the temperature range 114.5° K to 150.6° K. These measurements agree with the best available vapor pressure data from the literature to better than $\pm 0.02^{\circ}$ K and ± 0.15 atm.

6. The critical temperature and critical pressure of argon have been determined to be 150.65° K and 47.92 atm. to within $\pm 0.02^{\circ}$ K and ± 0.15 atm.

7. Calculations of the enhancement factor, after the work of Kirk (33) have been used as an aid in evaluating the probable accuracy of the experimental data.

APPENDIX A

EXPERIMENTAL RESULTS SYSTEM HELIUM-ARGON

The results of the experimental dew-point and bubble-point measurements for various known mixtures of helium and argon are given in Table 2. These data have been plotted in Figures 12 and 13 respectively.

The smoothed dew-point curves of Figure 12 were used to obtain the interpolated P - y values (isotherms) and T - y values (isobars) given in Tables 3 and 4, which were used to construct the P - y isotherms and T - y isobars shown in Figures 19 and 22, respectively. The smoothed curves of Figures 19 and 22 were used to obtain the set of interpolated dew-point data at even temperatures and even pressures given in Table 5.

The bubble-point isotherms (P - x values) given in Table 6 and the bubble-point isobars (T - x values) given in Table 7 were interpolated from the smoothed bubble-point curves of Figure 13. This data was used to construct Figures 20 and 23, respectively. The bubble-point data at even temperatures and even pressures given in Table 8 was taken from the smoothed curves of Figures 20 and 23.

The remainder of the experimental data, the observations for pure argon, are given in Appendix E.

Table 2. Tabulation of Experimental Helium-Argon Phase Equilibria Data

Run Number*	Helium Content Mole per cent	Temperature °K	Pressure atm	Type of Measurement
10	1.042	130.47	20.9	dew**
10	1.042	134.50	25.3	dew
10	1.042	140.82	33.1	dew
10	1.042	142.47	35.5	dew
10	1.042	144.53	38.6	dew
10	1.042	147.45	43.7	dew
10	1.042	150.04	48.9	dew
10	1.042	150.48	50.2	dew
10	1.042	149.96	48.5	dew
10	1.042	150.62	52.9	near crit. pt.
15	45.36	110.00	14.0	dew
15	45.36	114.99	19.9	dew
15	45.36	119.31	27.1	dew
15	45.36	123.14	33.6	dew
15	45.36	128.06	43.3	dew
15	45.36	131.87	53.6	dew
15	45.36	135.01	64.2	dew
16	29.70	119.60	18.6	dew
16	29.70	122.42	22.2	dew
16	29.70	127.44	29.2	dew
16	29.70	131.96	37.9	dew
16	29.70	136.54	48.9	dew
16	29.70	140.61	59.9	dew
16	29.70	142.53	67.3	dew
17	2.050	140.37	54.2	bubble
17	2.050	145.85	54.8	bubble
17	2.050	136.26	55.3	bubble
17	2.050	130.77	58.4	bubble
17	2.050	123.24	66.6	bubble
17	2.050	126.17	62.9	bubble

(continued)

*Points are given in chronological order.

**Cell A used in runs 10-18, cell B used in runs 19-25.

Table 2. (Continued)

Run Number	Helium Content Mole per cent	Temperature °K	Pressure atm	Type of Measurement
18	0.746	143.67	42.8	bubble
18	0.746	145.84	45.3	bubble
18	0.746	147.69	47.4	bubble
18	0.746	139.00	37.9	bubble
18	0.746	143.60	42.6	bubble
18	0.746	99.92	43.5	bubble
18	0.746	109.46	36.7	bubble
18	0.746	128.10	31.9	bubble
19	2.656	145.65	61.0	bubble
19	2.656	139.22	62.7	bubble
19	2.656	138.53	63.9	bubble
19	2.656	143.19	60.8	bubble
19	2.656	140.46	62.1	bubble
19	2.656	149.60	60.4	bubble
19	2.656	137.35	66.0	bubble
20	2.353	145.89	59.6	bubble
20	2.353	140.27	60.0	bubble
20	2.353	148.79	59.0	bubble
20	2.353	135.06	62.6	bubble
20	2.353	129.92	68.1	bubble
21	1.632	135.10	47.9	bubble
21	1.632	139.91	48.7	bubble
21	1.632	139.78	48.6	bubble
21	1.632	124.99	51.3	bubble
21	1.632	129.98	48.9	bubble
21	1.632	115.33	68.4	bubble
21	1.632	120.62	55.7	bubble
21	1.632	143.86	51.5	bubble
22	1.460	148.95	53.3	bubble
22	1.460	143.14	48.4	bubble
22	1.460	137.92	46.1	bubble
22	1.460	110.86	69.2	bubble
22	1.460	119.70	49.8	bubble
22	1.460	130.15	45.1	bubble
23	69.52	111.54	32.0	dew
23	69.52	116.65	45.5	dew
23	69.52	121.21	60.6	dew
23	69.52	123.18	70.0	dew
23	69.52	99.89	16.4	dew

(continued)

Table 2. (Concluded)

Run Number	Helium Constant Mole per cent	Temperature °K	Pressure atm	Type of Measurement
24	84.84	106.83	62.9	dew
24	84.84	102.35	46.2	dew
24	84.84	99.88	38.7	dew
25	72.42	115.06	51.8	dew
25	72.42	118.49	67.3	dew
25	72.42	109.91	38.1	dew
25	72.42	104.94	28.4	dew
25	72.42	99.74	19.5	dew

Table 3. Isothermal Dew-Point Data Interpolated from Figure 12 Used to Construct Figure 19.

Temperature °K	Pressure atm	Vapor Composition Mole Per Cent Helium
105	21.7	69.52
105	28.3	75.41
105	55.4	84.84
110	14.0	45.36
110	29.4	69.52
110	38.2	75.41
115	20.0	45.36
115	40.6	69.52
115	51.6	75.41
120	18.9	29.70
120	28.1	45.36
120	56.3	69.52
125	25.8	29.70
125	37.1	45.36
130	34.1	29.70
130	48.4	45.36
135	44.8	29.70
135	64.2	45.36
140	57.9	29.70

Table 4. Isobaric Dew-Point Data Interpolated from Figure 12 Used to Construct Figure 22.

Temperature °K	Pressure atm	Vapor Composition Mole Per Cent Helium
99.9	20	75.41
103.7	20	69.52
115.0	20	45.36
120.8	20	29.70
105.9	30	75.41
110.4	30	69.52
121.1	30	45.36
127.7	30	29.70
100.4	40	84.84
110.7	40	75.41
114.8	40	69.52
126.4	40	45.36
132.9	40	29.70
103.5	50	84.84
114.5	50	75.41
118.1	50	69.52
130.6	50	45.36
137.0	50	29.70
106.2	60	84.84
117.5	60	75.41
121.0	60	69.52
133.8	60	45.36
140.7	60	29.70
108.4	70	84.84
120.1	70	75.41
123.2	70	69.52
136.3	70	45.36
143.4	70	29.70

Table 5. Isothermal Even-Pressure Dew-Point Data Interpolated from Figure 19 and Figure 22.

Temperature °K	Pressure atm	Vapor Composition Mole Per Cent Helium
105	10	42.5
105	15	58.0
105	20	67.3
105	25	73.0
105	30	76.5
105	35	79.0
105	40	81.1
105	45	82.6
105	50	83.8
105	55	84.5
105	60	85.2
105	65	85.6
105	70	85.8
110	10	29.0
110	15	48.0
110	20	58.2
110	25	65.4
110	30	70.6
110	35	73.8
110	40	76.6
110	45	78.7
110	50	80.2
110	55	81.6
110	60	82.6
110	65	83.2
110	70	84.0
115	10	9.4
115	15	33.0
115	20	45.4
115	25	54.2
115	30	61.0
115	35	65.5
115	40	69.3
115	45	72.0
115	50	74.6
115	55	76.2
115	60	77.6
115	65	78.8
115	70	79.5

(continued)

Table 5. (Continued)

Temperature °K	Pressure atm	Vapor Composition Mole Per Cent Helium
120	15	17.0
120	20	31.5
120	25	40.8
120	30	48.5
120	35	55.4
120	40	60.0
120	45	63.3
120	50	66.4
120	55	68.8
120	60	70.9
120	65	72.6
120	70	73.9
125	17.5	7.9
125	20	16.3
125	25	28.3
125	30	36.7
125	35	43.6
125	40	49.0
125	45	53.4
125	50	57.1
125	55	60.3
125	60	62.8
125	65	65.0
125	70	66.8
130	22.5	7.2
130	25	13.5
130	30	23.7
130	35	31.5
130	40	37.7
130	45	42.7
130	50	46.9
130	55	50.3
130	60	53.4
130	65	55.9
130	70	58.2

(continued)

Table 5. (Concluded)

Temperature °K	Pressure atm	Vapor Composition Mole Per Cent Helium
135	27.5	5.8
135	30	11.1
135	35	18.8
135	40	25.0
135	45	30.0
135	50	34.8
135	55	38.9
135	60	42.6
135	65	45.7
135	70	48.4
140	32.5	2.2
140	35	6.7
140	40	13.4
140	45	18.8
140	50	23.4
140	55	27.4
140	60	31.2
140	65	34.4
140	70	37.5

Table 6. Isothermal Bubble-Point Data Interpolated from Figure 13 Used to Construct Figure 20.

Temperature °K	Pressure atm	Liquid Composition Mole Per Cent Helium
105	39.6	0.746
110	36.3	0.746
115	33.6	0.746
115	58.1	1.460
115	69.5	1.632
120	31.8	0.746
120	49.5	1.460
120	56.7	1.632
125	31.8	0.746
125	46.3	1.460
125	51.4	1.632
125	64.2	2.050
130	32.4	0.746
130	45.1	1.460
130	49.0	1.632
130	59.0	2.050
130	68.0	2.353
135	34.7	0.746
135	45.3	1.460
135	48.0	1.632
135	55.7	2.050
135	62.7	2.353
140	38.9	0.746
140	46.8	1.460
140	48.8	1.632
140	54.2	2.050
140	60.2	2.353
140	62.2	2.656
145	44.3	0.746
145	49.8	1.460
145	54.5	2.050
145	59.6	2.353
145	61.0	2.656

Table 7. Isobaric Bubble-Point Data Interpolated from Figure 13 Used to Construct Figure 23.

Temperature °K	Pressure atm	Liquid Composition Mole Per Cent Helium
104.4	40	0.746
141.1	40	0.746
119.7	50	1.460
127.3	50	1.632
142.2	50	1.632
145.4	50	1.460
114.2	60	1.460
118.2	60	1.632
128.8	60	2.050
140.4	60	2.353
(110.5)	70	1.460
(114.8)	70	1.632
(121.5)	70	2.050
(128.9)	70	2.353
(135.9)	70	2.656

( ) indicates extrapolated value.

Table 8. Isothermal Even-Pressure Bubble-Point Data Interpolated from Figure 20 and Figure 23.

Temperature °K	Pressure atm	Liquid Composition Mole Per Cent Helium
105	10	0.120
105	20	0.325
105	30	0.545
105	40	0.760
105	50	0.910
105	60	1.070
105	70	1.170
110	10	0.090
110	20	0.340
110	30	0.595
110	40	0.850
110	50	1.085
110	60	1.290
110	70	1.440
115	10	0.040
115	20	0.340
115	30	0.630
115	40	0.945
115	50	1.240
115	60	1.500
115	70	1.670
120	20	0.300
120	30	0.680
120	40	1.050
120	50	1.420
120	60	1.710
120	70	1.960
125	20	0.210
125	30	0.665
125	40	1.120
125	50	1.570
125	60	1.910
125	70	2.210
130	30	0.600
130	40	1.160
130	50	1.680
130	60	2.080
130	70	2.430

(continued)

Table 8. (Concluded)

Temperature °K	Pressure atm	Liquid Composition Mole Per Cent Helium
135	30	0.410
135	40	1.115
135	50	1.745
135	60	2.250
135	70	2.620
140	40	0.855
140	50	1.715
140	60	2.425
145	40	0.200
145	50	1.485
145	60	2.575

APPENDIX B

GAS MIXING PROCEDURE

One of the tasks which had to be performed prior to experimental operations was the development of a gas mixing procedure which could be used with confidence to insure that concentration gradients within the gas mixture in the Jerguson gas burets were eliminated. The procedure which was used is described below.

The gases to be mixed were confined in the two larger gas burets, labeled B1 and B3 in Figure 1. (The small gas buret, B2, was filled with mercury and closed during all the mixing operations.) The equilibrium cell, C in Figure 1, was normally open to the upper manifold so that the gas within the cell could be included in the mixing operation. During the mixing procedure the pressure in the cell was never permitted to exceed the dew-point pressure for the existing cell temperature. The cell pressure never exceeded the vapor pressure of argon during mixing of the low helium content gas mixtures. The lowest cell pressure during mixing operations was approximately 50 psig.

The mixing procedure used was as follows:

1. With the equilibrium cell blocked off, one buret (say, B1) was rapidly filled with mercury from the mercury storage vessel, B4, thus trapping the major portion of the gas in the remaining buret (B3). The gas-filled buret was now closed. At this point the equilibrium cell was opened to the manifold.

2. The mercury level in the open buret (B1) was then raised and lowered rapidly five times. This forced gas from the buret (B1) into the equilibrium cell. The rapid entrance of gas into the cell from the capillary tubing caused some turbulence which aided mixing. A portion of the gas trapped in the closed buret (B3) was released during these operations each time the mercury level was at its lowest level. After this operation was complete the closed buret (B3) was opened to release the remainder of the gas into the manifold.

3. At this point steps one and two were repeated with the functions of the burets being reversed.

This mixing procedure was repeated several times when a fresh gas mixture was being prepared and was performed at least once after every equilibrium datum point was obtained.

As an example of the effectiveness of this mixing procedure a series of samples were taken from the gas mixing apparatus prior to mixing and after mixing. In order to obtain samples of various portions of the gas mixture the mercury level in each of the burets was raised and lowered as indicated in Table 9. This is not, of course, an ideal way of sampling at various points in the burets; however, it does give a good indication of how the composition varies within the gas mixture. The samples in each group were taken at five minute intervals.

These samples were analyzed by gas chromatographic analysis as described in Chapter II according to the procedure discussed in Chapter III. The results given in Table 9 are in terms of chromatographic peak height, which is directly proportional to concentration. The gas mixture used in the test which is reported in Table 9 contained approximately three per

cent helium in argon. The peak heights reported represent the concentration of helium in the gas mixture.

Table 9 shows that the gas was initially very poorly mixed. Variations of nearly ten per cent between the peak heights are shown. However, after one repetition of the mixing procedure outlined above the differences between peak heights, which are directly related to composition, were on the order to one quarter of one per cent. This is well within the estimated analytical error.

A number of tests of the mixing procedure were made at various concentration levels. Each time the results were the same as shown above. It is not claimed that this procedure is the most logical or the best possible method of mixing the gases. However, it is claimed that the procedure outlined does give the desired results.

Table 9. Example of Gas Mixing Procedure Results.

A. Gas in Gas Burets Partially Mixed.

Position of Mercury Levels During Sampling			Chromatogram
Buret B1	Buret B2	Buret B3 *	Peak Height
down	up	down	76.8
up	up	down	80.2
up	up	down	76.7
down	up	up	70.1
down	up	up	78.0
down	up	down	79.8

B. Same Gas as Above After One Repetition of the Gas Mixing Procedure.

Position of Mercury Levels During Sampling			Chromatogram
Buret B1	Buret B2	Buret B3 *	Peak Height
down	up	down	80.0
down	up	down	80.2
up	up	down	80.0
up	up	down	79.9
down	up	up	79.8
down	up	up	79.9
down	up	down	80.0

*B1, B2, and B3 refer to symbols on Figure 1.

APPENDIX C

CALIBRATION OF THERMOCOUPLES

Cryostat Thermocouples

The cryostat contained four thermocouples and two temperature difference thermocouples. All these were constructed of 32 gage, double nylon wrapped and enameled, advance alloy wire, manufactured by the Driver-Harris Company; and 34 gage, single cotton wrapped and enameled, copper wire, manufactured by Anaconda Copper Company. The wrapping on these wires was impregnated with insulating varnish prior to use. This wire was taken from the same spools used by Ziegler, et al. (52), to construct the thermocouples described in their low temperature thermal conductivity studies.

The thermocouples were calibrated after they were installed in the cryostat. The ice bath, thermocouple switch, lead lines, reference cell, and potentiometer-detector system used for the calibration were the same as were used for the phase equilibrium experimental work.

To facilitate the thermocouple calibration the glass equilibrium cell was removed from the cryostat and the device shown in Figure 27 was installed in its place. A platinum resistance thermometer purchased from Leeds and Northrup (L and N serial number 709892, NBS test number 1024), which had been calibrated by the National Bureau of Standards on the International Temperature Scale, was used as the temperature reference.

The thermometer was encased in a long glass tube suitable for im-

mersion in a liquid bath. The thermometer was inserted through the center of the calibrating device so that it came to within one quarter inch of the bottom. The top of the glass probe extended through the cryostat main plate and was sealed with Apiezon sealing compound to exclude air from the cryostat. The four thermocouples were securely tied to the glass covering of the resistance thermometer. These thermocouples entered the calibrating device from the bottom and extended at least three-quarters of an inch into the annulus of the lower section of the calibrating device. The resistance thermometer was connected through lead-sheathed wires to a Leeds and Northrup G-2 Mueller bridge.

The cryostat was operated according to normal procedure during the calibration runs. The cryofluid was liquid propane. Since the resistance thermometer gave the more sensitive reading, the temperature drift was initially determined by observing the thermocouple-potentiometer system. When the liquid nitrogen flow rate was set well enough to eliminate noticeable drift in the thermocouple-potentiometer system the resistance thermometer-resistance bridge system was used to detect temperature drift. When the temperature drift was less than 0.001° K per minute as indicated by the Mueller bridge a set of calibration data was taken.

A sample set of calibration data is given in Table 11. As may be seen, the procedure involved taking three readings for each pair of leads from the resistance-thermometer on the Mueller bridge, spaced, in time, around two readings of each of the thermocouples on the potentiometer-detector system. The drift in temperature, as indicated by the resistance thermometer system, during a calibration period was spread evenly through the thermocouple readings.

The complete set of thermocouple calibration data is given in Table 12. A fourth degree ploynomial of the form given below was fitted to the data set for each thermocouple using the method of least squares.

$$E = a + bT + cT^2 + dT^3 + eT^4 \qquad (18)$$

In this equation E represents electrical potential reading in microvolts and T represents temperature in degrees Kelvin. The constants for two of the thermocouples are given below.

Table 10. Constants for Thermocouple Equation

Thermocouple Number	a	b	c x 10^2	d x 10^4	e x 10^6
0	6209.8	-15.243	4.876	-5.4859	1.0382
2	6177.5	-14.212	3.6285	-4.8252	0.90999

Equations were not derived for the other two thermocouples since they were not used in the precision measurements.

The ninety-five per cent confidence interval of the data points about the correlation line as determined by a modified t-test is slightly less than $\pm 0.02^{\circ}$ K. This indicates that the random error due to both the thermocouple-potentiometer-detector system and the resistance thermometer-resistance bridge system, in addition to human error in setting and reading both instruments was less than 0.02° K. Statistically this means that if one hundred more data points were determined that only five would have a random deviation from the line of more than $\pm 0.02^{\circ}$ K.

The procedure used in determining temperatures during the phase equilibrium experiments was identical to that used in the thermocouple calibration experiments, except that one source of error, that of the resistance thermometer-resistance bridge system was eliminated. Therefore it is reasonable to state that the precision of the temperature measurements throughout experimental work was at least as good as $\pm 0.02^{\circ}$ K.

This precision estimate was further tested during the course of the extensive argon vapor pressure measurements and found to be a reasonable estimate.

Gas Mixing and Storage Section Thermocouples

The thermocouples in the gas mixing and storage section were constructed of the same thermocouple wire as those described above. All but one of these thermocouples were used to measure temperature difference.

The one thermocouple used to measure temperature was calibrated in a narrow temperature range near 100° F by immersing it in a stirred hot water bath. A mercury-in-glass thermometer calibrated by the National Bureau of Standards was used as the temperature reference. The calibration was relatively crude but was as good as required for the application.

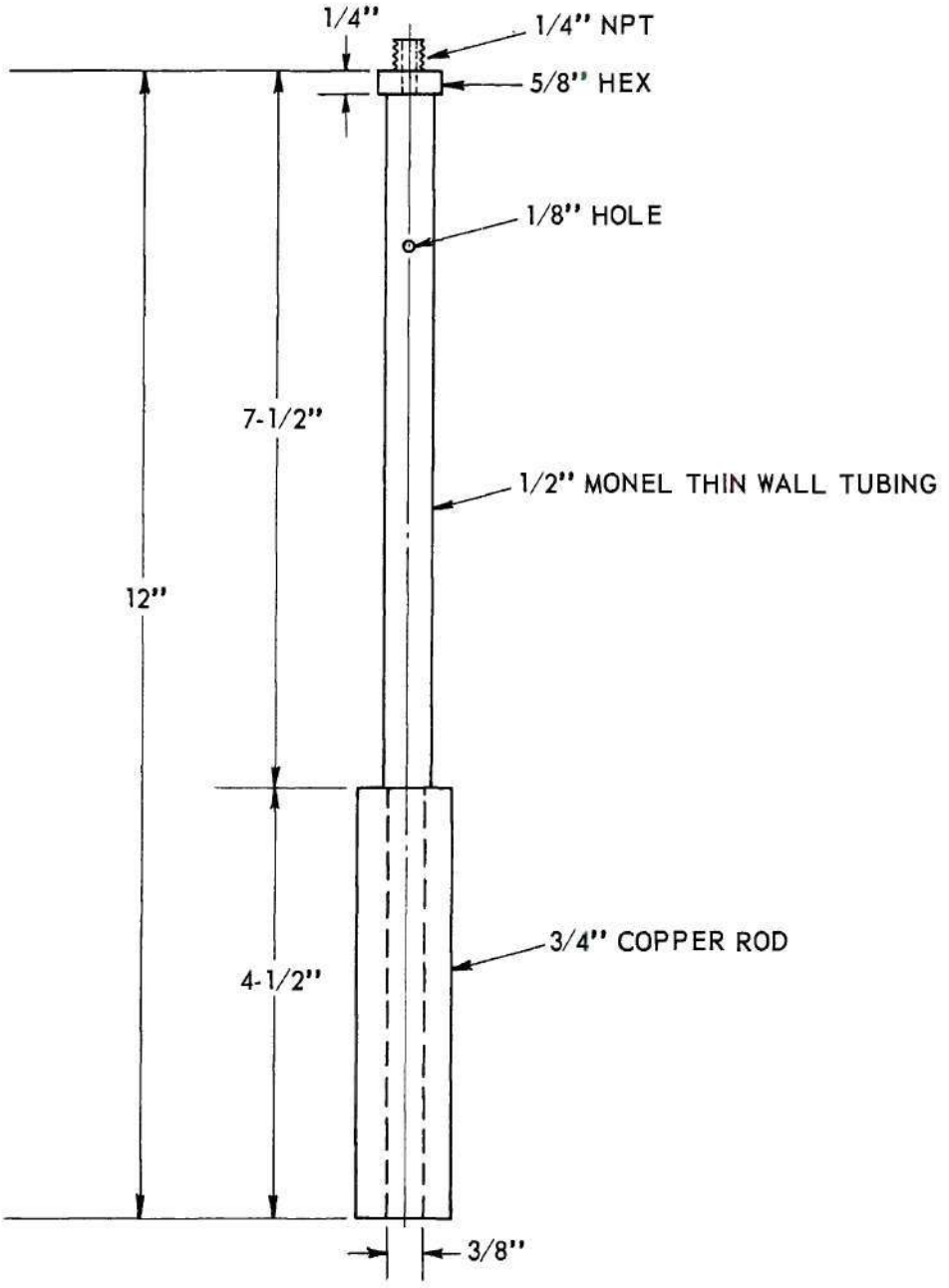

Figure 27. Thermocouple Calibrating Device.

Table 11. Sample Set of Thermocouple Calibration Data, Calibration Run 10B.

Instrument	Units	Switch*	Reading	Temperature** Equivalent °K
Time	seconds		0	
Resistance Bridge	international ohms	N R	7.2566 7.3336	 99.751
Time	seconds		90	
Potentiometer	absolute millivolts	0 1 2 3	4.7325 4.7315 4.7320 4.7302	99.751 99.752 99.752 99.753
Time	seconds		180	
Resistance Bridge	international ohms	R N	7.3336 7.2573	 99.754
Time	seconds		244	
Potentiometer	absolute millivolts	3 2 1 0	4.7301 4.7317 4.7313 4.7324	99.755 99.756 99.756 99.757
Time	seconds		330	
Resistance Bridge	international ohms	N R	7.2576 7.3343	 99.758
Time	seconds		443	

*Switch corresponds to thermocouple number for potentiometer reading.

**T = 273.15 + t, where T = °K and t = °C on International Temperature Scale.

Table 12. Thermocouple Calibration Data.

Thermocouple absolute millivolts	Resistance Thermometer international ohms	Temperature from Resistance Thermometer ^{o}K
THERMOCOUPLE 0		
3.5136	13.54378	157.527
3.5135	13.54410	157.530
3.7066	12.68478	149.465
3.7066	12.68438	149.461
3.8446	12.05159	143.545
3.8445	12.05213	143.550
3.9719	11.44644	137.906
3.9733	11.44002	137.846
3.9734	11.43977	137.843
4.1911	10.34921	127.728
4.1909	10.35070	127.742
4.3566	9.47408	119.658
4.3570	9.47286	119.646
4.4651	8.87594	114.166
4.4654	8.87500	114.157
4.5906	8.15574	107.580
4.5905	8.15688	107.591
4.7325	7.29520	99.752
4.7324	7.29580	99.757
4.8220	6.73002	94.634
4.8215	6.73245	94.656
4.8315	6.66231	94.023
4.8317	6.66338	94.032
4.8733	6.40122	91.666
4.8734	6.39997	91.655
3.1916	14.89735	170.299
3.1919	14.8963	170.289
THERMOCOUPLE 1		
3.5143	13.54374	157.527
3.5141	13.54400	157.529
3.7071	12.68474	149.465
3.7071	12.68443	149.462
3.8451	12.05161	143.545
3.8450	12.05204	143.549
3.9725	11.44623	137.904
3.9738	11.44001	137.846
3.9740	11.43981	137.844

(continued)

Table 12. (Continued)

Thermocouple absolute millivolts	Resistance Thermometer international ohms	Temperature from Resistance Thermometer °K
4.1911	10.34934	127.730
4.1909	10.35053	127.741
4.3570	9.47389	119.656
4.3573	9.47292	119.647
4.4654	8.87588	114.165
4.4655	8.87513	114.158
4.5909	8.15581	107.581
4.5908	8.15673	107.589
4.7315	7.29525	99.752
4.7313	7.29573	99.756
4.8208	6.73026	94.636
4.8204	6.73220	94.654
4.8316	6.66239	94.023
4.8315	6.66324	94.031
4.8731	6.40111	91.665
THERMOCOUPLE 2		
3.5135	13.54371	157.526
3.5134	13.54390	157.528
3.7065	12.68471	149.464
3.7065	12.68447	149.462
3.8444	12.05163	143.545
3.8444	12.05196	143.548
3.9718	11.44602	137.902
3.9731	11.43999	137.846
3.9731	11.43984	137.844
4.1903	10.34947	127.731
4.1902	10.35036	127.739
4.3562	9.47371	119.654
4.3564	9.47298	119.647
4.4647	8.87582	114.164
4.4647	8.87526	114.159
4.5900	8.15588	107.581
4.5899	8.15657	107.588
4.7320	7.29530	99.752
4.7317	7.29566	99.756
4.8214	6.73049	94.639
4.8209	6.73195	94.652
4.8319	6.66247	94.024

(continued)

Table 12. (Concluded)

Thermocouple absolute millivolts	Resistance Thermometer international ohms	Temperature from Resistance Thermometer °K
4.8318	6.66311	94.030
4.8726	6.40099	91.664
4.8726	6.40024	91.658
THERMOCOUPLE 3		
3.5136	13.54367	157.526
3.5136	13.54380	157.527
3.7068	12.68467	149.464
3.7067	12.68451	149.462
3.8446	12.05166	143.546
3.8445	12.05187	143.547
3.9720	11.44581	137.900
3.9733	11.43998	137.845
3.9734	11.43988	137.844
4.1905	10.34960	127.732
4.1905	10.35019	127.737
4.3564	9.47352	119.652
4.3566	9.47304	119.648
4.4649	8.87576	114.164
4.4649	8.87539	114.161
4.5902	8.15596	107.582
4.5901	8.15641	107.586
4.7302	7.29535	99.753
4.7301	7.29559	99.755
4.8197	6.73073	94.641
4.8194	6.73170	94.650
4.8302	6.66254	94.025
4.8302	6.66297	94.029
4.8717	6.40088	91.663
4.8717	6.40038	91.659

APPENDIX D

PRESSURE MEASUREMENT

The primary pressure measuring instrument was a Martin-Decker precision test pressure gage, model GD-10-150. This eight-inch diameter gage had a full scale capacity of 1500 psig. The manufacturer's rating of the gage tolerance was $\pm$0.15 per cent of full scale. Data from the manufacturer's calibration test report are given in Table 13. These data indicate that the gage is at least as good as the manufacturer stated.

As a further test of the gage, it was compared with an Ashcroft, six-inch diameter, 3000 psig, test pressure gage, after installation on the phase equilibria equipment. The Ashcroft gage was rated by the manufacturer at $\pm$0.25 per cent of full scale.

The comparison of these two gages was made primarily to determine if any large shifts had been made in either of the gages during installation. Since both gages were connected to the same manifold, as shown in Figure 1, it was a simple matter to inject nitrogen gas into the manifold to the desired pressures to make the comparison.

The data are shown in Table 14. One can see that in no case does the difference between the pressure readings obtained from the two gages exceed the rated tolerance of the Ashcroft gage; 7.5 psi. In fact, approximately one-half of the pressure differences are within the precision of the Martin-Decker gage; 2.25 psi.

In addition to the above test, extensive argon vapor pressure experiments were performed as described in Chapter V. The results of these experiments are given in Appendix E, Tables 16 and 17. Table 17 shows the deviations of the vapor pressures which were experimentally determined, using the Martin-Decker pressure gage, from the equation of best fit given by Michels (8) for his data. One will note that these deviations are well within the tolerance of the Martin-Decker gage.

The above indicate that the Martin-Decker test pressure gage is as precise a pressure instrument as the manufacturer claims and that the pressure measurements made during the course of the phase equilibrium experiments may be trusted to within 2.25 psi or 0.15 atmosphere.

In addition, the comparison of the two gages showed that the Ashcroft test pressure gage is probably much more precise than the manufacturer rates it. At any rate it may be trusted to within 0.5 atm.

Table 13. Calibration Test Report, Martin-Decker Corporation, Precision Test Pressure Gage Model GD-10-150, Serial Number 1175.

Nominal Reading psig	Gage Reading-Up Vibrated psig	Gage Reading-Down Vibrated psig
0	0	0
99.908	100.625	101.25
199.817	201.25	201.875
299.725	300.625	301.875
399.528	400.0	401.25
499.410	499.375	500.625
599.073	598.75	600.625
699.173	698.125	700.0
799.055	797.5	799.375
898.822	896.875	898.75
998.819	996.875	998.75
1098.701	1097.5	1099.375
1198.512	1197.5	1199.375
1298.465	1297.5	1298.75
1398.347	1398.125	1398.75
1498.228	1496.875	1496.875

Table 14. Comparison of Test Pressure Gages.

Martin-Decker GD-10-150 psig	Ashcroft 1279THXTDSA psig	Difference psig
886	886	0
876	878	-2
824	828	-4
779	779	0
718	718	0
656	652	4
607	606	1
549	550	-1
495	491	4
439	435	4
395	390	5
345	341	4
296	290	6
248	241	7
198	196	2
148	152	-4
98	101	-3
50	52	-2
24	28	-4

APPENDIX E

EXPERIMENTAL RESULTS PURE ARGON

The experimental pressure and temperature observations along the vapor pressure line for pure argon are shown in Table 16. The dew and bubble points are given, as well as points for which the cell was one-half full of liquid, to illustrate the purity of the argon.

The same observed data are given in Table 17. The deviations given reflect the close fit of the experimental data of this work to the argon vapor pressure equation which Michels, et al. (8), derived from their measurements. This equation is given in Chapter V as equation 17.

Several individual observations of the critical point on two occasions resulted in the values for the critical temperature of 150.65° K and for the critical pressure of 47.92 atm. These observations were made by filling the cell approximately one-half full of liquid argon at approximately 150° K. Then the temperature was slowly increased until the meniscus disappeared. This disappearance upon increasing temperature was not sharp, since diffusion from the bottom of the cell (the previous dense phase) into the upper end of the cell was relatively slow. This resulted in persistant density gradients which slowly dissipated.

However, in every case, there was a sharp and distinct indication of the critical point upon slowly lowering temperature from above the critical temperature (temperature change of less than 0.01° K/minute). A period of critical opalescence, which had a faint purple cast, occurred

and lasted for approximately thirty seconds. This opalescence was broken by the formation of many droplets of liquid throughout the cell which immediately fell to the bottom forming two phases. The temperature and pressure were observed just as the drop formation began.

The only other experimental measurement of the critical temperature and pressure for argon was by Crommelin (9) in 1910. His values were - 122.44° C (150.71°K) and 47.996 international atmospheres. Recently, Michels, et al. (39), have calculated the critical properties by the extrapolation of their compressibility and vapor pressure measurements. Their reported values are - 122.29° C (150.86° K) and 48.34 atmospheres. A tabular comparison is given below.

Table 15. Critical Temperature and Critical Pressure of Argon

Investigation	Critical Temperature °K	Critical Pressure atm
Crommelin (9)	150.71	48.00
Michels (39)	150.86	48.34
This Work	150.65	47.92

Table 16. Experimental Argon Vapor Pressure Measurements.

Temperature* °K	Pressure atm	Type Observation		
		Dew Point	Cell Half Full	Bubble Point
142.16	34.28	X		
142.28	34.45			X
142.16	34.25			X
150.09	46.88	X		
150.11	46.92	X		
150.17	47.02		X	
150.20	47.06		X	
150.27	47.22		X	
150.31	47.26		X	
150.65	47.92		critical point	
150.65	47.92		critical point	
150.63	47.89		X	
115.50	9.31	X		
115.44	9.30	X		
115.44	9.30		X	
115.44	9.30			X
115.46	9.30	X		
114.89	8.97	X		
114.50	8.72	X		
115.07	9.07	X		
115.55	9.32	X		
125.96	16.49	X		
125.96	16.49		X	
125.96	16.49			X
125.11	15.77	X		

*Chronological order over a period of six days

Table 17. Experimental Argon Vapor Pressure, with Deviations from the Argon Vapor Pressure Equation of Michel's et al. (8).

Observed* Temperature ^{o}K	Observed Pressure atm	$P_{expt} - P_{calc}$ atm
142.16	34.28	0.02
142.28	34.45	0.01
142.16	34.25	-0.02
150.09	46.88	-0.02
150.11	46.92	-0.01
150.17	47.02	-0.01
150.20	47.06	-0.02
150.27	47.22	0.01
150.31	47.26	-0.04
150.65	47.92	0.02
150.63	47.89	0.03
115.50	9.31	0.04
115.44	9.30	0.06
115.46	9.30	0.05
114.89	8.97	0.03
114.50	8.72	-0.01
115.07	9.07	0.03
115.55	9.32	0.02
125.96	16.49	0.08
125.11	15.77	0.06

*Chronological order over a period of six days.

APPENDIX F

CALIBRATION OF GAS BURETS

The two model 29-T-30 and one model 19-T-30 Jerguson Transparent Gages were calibrated and found to have a constant bore volume of 4.982 cubic centimeters per scale division. Each scale division was approximately one-half inch in length. The overall volume of the 29-T-30 model burets was approximately 250 cm^3 and of the 19-T-30 model buret was approximately 125 cm^3.

The calibration was performed by adding known volumes of mercury from a National Bureau of Standards calibrated precision buret to each of the three gages at various levels. The buret was contained within the cabinet which housed the gages to reduce temperature difference between the buret and the gages. The temperature was approximately 75^{o} F.

The experimental calibration data are given in Table 18. The data are given in five groups as the two larger gages each had two sections which were considered different for calibration purposes.

The standard deviations of the five sets of data were compared using Bartlett's Test, a standard statistical procedure for comparing several variances. This test showed that there was no significant difference between the five standard deviations. Then the means of each of the five sets of data were compared using a modified "t" test and found to have no significant difference. These tests proved that all five gage sections had the same bore area and that the bore area was constant throughout each gage.

Finally all the calibration data were used to calculate an overall bore volume to be used for all five gage sections. This was found to be 4.982 ± 0.024 cm^3 per scale division.

The connections between sections in the two larger gages were calibrated in the same manner as described above and were found to have a volume of 1.44 ± 0.29 cm^3 between the 25.0 scale division on the lower section and the 0.0 scale division on the upper section.

The volumes of the connections from the gages to the valves connecting them to the upper manifold were found to be 7.29 ± 0.58 cm^3 for the left gage, 7.75 ± 0.65 cm^3 for the middle gage, and 6.90 ± 0.51 cm^3 for the right gage.

All interval estimates given above are based on a confidence level of 95 per cent. This means that if the calibration were repeated one hundred times that ninety-five of the results would fall in the interval indicated and that only five would fall outside of the interval due to random effects.

Table 18. Gas Buret Calibration Data.

Section I		Section II		Section III		Section IV		Section V	
Test	Buret	Test	Buret	Test	Buret	Test	Buret	Test	Buret
5.14	1.03	2.44	0.50	4.79	1.00	5.01	1.01	4.96	1.05
4.86	0.99	5.17	1.05	4.88	1.00	5.25	1.09	4.92	0.99
4.80	0.98	4.54	0.95	4.84	1.00	4.78	1.01	5.01	1.03
5.20	1.09	5.31	1.08	5.13	1.05	4.74	0.95	5.16	1.03
5.44	1.07	5.07	1.02	4.43	0.89	4.76	0.95	4.90	0.98
4.46	0.92	4.67	0.91	5.47	1.15	5.55	1.15	4.97	1.02
5.13	1.01	4.99	1.03	5.14	1.01	4.62	0.93	4.88	1.00
5.38	1.08	5.11	1.01	4.44	0.86	5.09	1.01	5.25	1.00
4.78	0.93	5.19	1.01	5.04	0.99	5.07	1.01	5.00	0.98
5.26	1.05	5.13	1.01	5.45	1.06	5.14	1.00	5.10	1.02
4.67	0.94	5.15	1.02	5.46	1.09	5.20	1.00	5.10	1.00
5.31	1.02	5.20	1.00	4.75	0.91	4.99	1.00	5.08	0.98
5.13	1.01	5.22	1.02	4.78	0.98	5.53	1.07	6.12	1.22
4.70	0.94	4.87	0.99	5.08	1.01	4.56	0.89	4.35	0.85
5.25	1.03	5.36	1.04	5.45	1.08	5.02	0.95	5.00	0.95
5.08	1.00	4.80	0.96	4.71	0.92	5.40	1.09	5.25	1.06
4.99	1.01	5.70	1.10	5.04	0.99	5.04	0.99	4.62	0.93
5.02	1.00	4.12	0.85	4.90	1.01	4.76	0.96	5.38	1.06
5.23	1.08	5.19	1.03	4.91	0.98	5.40	1.07	4.57	0.94
4.75	0.92	4.90	1.00	5.18	1.02	4.68	0.93	4.88	0.99
4.74	0.99	4.90	0.97	5.08	1.05	5.20	1.04	4.82	0.98
5.14	1.04	4.97	1.01	5.20	1.05	4.80	0.99	4.90	1.02
4.32	0.90	5.34	1.09	4.65	0.99	4.85	0.97	4.80	1.00
2.30	0.47	1.91	0.43	4.91	1.01	4.54	0.95		
				4.45	0.94				
				4.70	1.00				
				4.90	1.00				
				5.07	1.00				
				4.87	1.00				
				4.96	1.00				
				5.08	1.00				
				5.10	1.00				
				5.22	1.00				
				5.02	1.00				

NOTES:
1. Test gives volume of mercury injected from glass buret in cm^3.
2. Buret gives reading difference on arbitrary scale on gas burets.
3. Section I is right gas buret (B3 in Figure 1), lower section.
4. Section II is right gas buret (B3 in Figure 1), upper section.
5. Section III is left gas buret (B1 in Figure 1), lower section.
6. Section IV is left gas buret (B1 in Figure 1), upper section.
7. Section V is center gas buret (B2 in Figure 1), which has only one section.

APPENDIX G

SUMMARY OF DISCUSSION OF ENHANCEMENT FACTOR CALCULATIONS

This appendix serves two purposes. In the first section the parameters used in the enhancement factor calculations are given in summary form. A more complete description of their use may be found in Chapter IV. The second section contains a compilation of a portion of the results of calculations made to determine the contribution of each of the several terms in the enhancement factor equation.

Parameters Used in Enhancement Factor Calculations

The Kihara core model with 6-12 potential function was used to compute the second virial coefficients, B_{11} and B_{22}, and the second virial interaction coefficient, B_{12}. The parameters from Prausnitz and Myers (42), which were used, are:

Parameter	Units	Argon	Helium
M_o	$\mathring{A}$	2.199	0.0
S_o	$\mathring{A}^2$	0.3848	0.0
V_o	$\mathring{A}^3$	0.02245	0.0
U_o/k	^oK	146.10	9.927
ρ_o	$\mathring{A}$	3.328	2.921

The Lennard-Jones 6-12 potential function was used to compute the third virial coefficients, C_{111} and C_{222}, and the third virial interaction coefficients, C_{112} and C_{122}. Argon parameters were taken from Ziegler, Mullins, and Kirk (53). Parameters for helium were determined in this work.

Parameter	Units	Argon	Helium
e/k	^{o}K	119.3	7.022
b_o	ml/gm mole	50.91	23.16

A linear equation was used to relate the volume of pure liquid argon, v_l, with pressure at constant temperature.

$$v_l = a + bP \tag{9}$$

This equation was fitted to the data of van Itterbeek, Verbeke, and Staes (49) and of Michels, Levelt, and De Graaff (39). The constants derived in this work are given below.

Temperature ^{o}K	a cm^3/gm mole	b cm^3/gm mole, atm
100	30.49	0.00850
105	31.36	0.01050
110	32.33	0.01309
115	33.45	0.01639
120	34.72	0.02034
125	36.24	0.02630
130	38.29	0.03920
135	41.08	0.05779

The vapor pressure of argon, p_{01}, was computed from the equation derived by Michels, Wassennaar, and Zwietering (8) from their argon vapor pressure data.

$$\mathrm{Log}_{10}P = -550.8211/T - 8.7849395\ \mathrm{Log}_{10}T + 0.0174713T + 21.8379 \tag{17}$$

Contribution of the Terms of the Enhancement Factor Equation

The equation used to compute the enhancement factor has been given before as:

$$\ln\phi = \ln \frac{1}{z_{01}} + \frac{(P - p_{01})}{RT}\left[a + \tfrac{1}{2}b(P + p_{01})\right]$$

$$+\left[2\frac{B_{11}}{V_{01}} + \frac{3}{2}\frac{C_{111}}{V_{01}^2}\right] + \ln z_m + \frac{I_b}{V_m} + \frac{I_c}{V_m^2} \qquad (10)$$

As a part of the study of this equation calculations were made to determine the relative contribution of the major terms to the computed value of the enhancement factor. This was done by first performing the calculations with the entire equation. Then the values of these selected terms were subtracted from the right-hand side of equation 10. The contribution of the I_c/V_m^2 term was determined by subtracting this term. Then the set $\ln z_m + I_b/V_m + I_c/V_m^2$ was deleted to determine the effect of the first two of these terms. A portion of the results may be found in Figure 19.

Table 19. Sample Results of Enhancement Factor Calculations.

Temperature °K	Pressure atm	Enhancement Factor, ø		
		Column 3	Column 4	Column 5
90	10	1.103	1.104	0.993
90	50	1.475	1.504	1.164
90	100	2.042	2.183	1.421
110	10	1.061	1.062	0.898
110	50	1.421	1.446	1.035
110	100	1.872	1.982	1.231
125	20	1.073	1.083	0.826
125	50	1.423	1.462	0.916
125	80	1.760	1.858	1.013
135	30	1.081	1.116	0.770
135	50	1.401	1.485	0.825

NOTES: 1. Column three gives the values of enhancement factor as computed with equation 10.

2. Column four gives the values of enhancement factor of column three less the contribution of the term I_c/V_m^2.

3. Column five gives the values of enhancement factor of column three less the contribution of the terms $\ln z_m + I_b/V_m + I_c/V_m^2$.

BIBLIOGRAPHY

1. Benham, A. L. and Katz, D. L., "Vapor-Liquid Equilibria for Hydrogen-Light Hydrocarbon Systems at Low Temperatures", American Institute of Chemical Engineers Journal 3, 33-6 (1957).

2. Bloomer, O. T., Gami, D. C., and Parent, J. D., "Physical-Chemical Properties of Methane-Ethane Mixtures", Institute of Gas Technology Research Bulletin 22, (1953).

3. Bloomer, O. T. and Parent, J. D., "Physical-Chemical Properties of Methane-Nitrogen Mixtures", Institute of Gas Technology Research Bulletin 17, 19-21 (1952). See also: "Liquid-Vapor Phase Behavior of the Methane-Nitrogen System", Chemical Engineering Progress Symposium Series 49, No. 6, 11-24 (1953).

4. Brandt, L. W. and Stroud, L., "Phase Equilibrium in Natural Gas Systems", Industrial and Engineering Chemistry 50, 849-52 (1958).

5. Budenholzer, R. A., Sage, B. H., and Lacey, W. N., "Phase Equilibria in Hydrocarbon Systems", Industrial and Engineering Chemistry 31, 1288-92 (1939).

6. Buzyna, G., Macriss, R. A., and Ellington, R. T., "Vapor-Liquid Equilibrium in the Helium-Nitrogen System", Chemical Engineering Progress Symposium Series 59(44), 101-11 (1963).

7. Cines, M. R., Roach, J. T., Hogan, R. J., and Roland, C. H., "Nitrogen-Methane Vapor-Liquid Equilibria", Chemical Engineering Progress Symposium Series 49, 1-10 (1953).

8. Clark, A. M., Din, F., and Robb, J., and Michels, A., Wassenaar, T., and Zwietering, Th., "The Vapor Pressure of Argon", Physica 17, 876-84 (1951).

9. Crommelin, C. A., "Isotherms of Monatomic Gases and of Their Binary Mixtures. IV. Remarks on the Preparation of Argon. V. Vapour Pressures above - 140°C., Critical Temperature and Critical Pressure of Argon", Communication from the Physical Laboratory of the University of Leiden, No. 115 (1910).

10. Crommelin, C. A., "Isothermals of Monatomic Substances and their Binary Mixtures. XV. The Vapour Pressure of Solid and Liquid Argon, From the Critical Point Down to -206°." Communication from the Physical Laboratory of the University of Leiden, No. 138c (1913).

11. Davis, J. A., Rodewald, N. and Kurata, F., "An Apparatus for Phase Studies Between 20° K and 300° K", Industrial and Engineering Chemistry 55, 36-42 (1963).

12. DeVaney, W. E., Dalton, B. J., and Meeks, J. C., Jr., "Vapor-Liquid Equilibria of the Helium-Nitrogen System", Journal of Chemical and Engineering Data 8, 473-8 (1963).

13. Dodge, B. F. and Dunbar, A., "An Investigation of the Coexisting Liquid and Vapor Phases of Solutions of Oxygen and Nitrogen", Journal of the American Chemical Society 49, 591-610 (1927).

14. Dokoupil, Z., Van Soest, G., and Swenker, M. D. P., "On the Equilibrium Between the Solid Phase and the Gas Phase of the System Hydrogen-Nitrogen, Hydrogen-Carbon Monoxide and Hydrogen-Nitrogen-Carbon Monoxide", Applied Scientific Research A5, 182-240 (1955). See also: Communication from the Physical Laboratory of the University of Leiden No. 297 (1955).

15. Eakin, B. E., Ellington, R. T., and Gami, D. C., "Physical-Chemical Properties of Ethane-Nitrogen Mixtures", Institute of Gas Technology Research Bulletin 26, 29 (1955).

16. Fastovskii, V. G. and Gonikberg, M. G., "Die Löslichkeit von Gasen in Flüssigkeiten bei neidrigen Temperaturen und höhen Drucken. III. Die Löslichkeit von Wasserstoff in flüssigen Methan", Acta Physicochimica (U.R.S.S.) 12, 485-8 (1940). See also: "The Solubility of Gases in Liquids at Low Temperatures. III. Solubility of Hydrogen in Liquid Methane", Journal of Physical Chemistry (U.S.S.R.) 14, 427-8 (1940).

17. Fastovskii, V. G. and Krestinskii, Yu. A., "Solubility of Solid Methane in Liquid Nitrogen and Oxygen", Journal of Physical Chemistry U.S.S.R. 15, 525-31 (1941).

18. Fastovskii, V. G. and Petrovskii, Yu. V., "Liquid and Vapor Equilibriums in the Nitrogen-Methane System", Journal of Physical Chemistry U.S.S.R. 31, 2317-20 (1957).

19. Fedoritenko, A. and Ruhemann, M., "Equilibrium Diagrams of Helium-Nitrogen Mixtures", Zhurnal Tekhnicheskoi Fiziki 4, 36-42 (1937). See also: Ruhemann, M., The Separation of Gases, London, Oxford Press, 2nd Ed., (1949) p. 277.

20. Fedorova, M. F., "Binary Mixtures of Substances Melting at Low Temperatures", Journal of Experimental and Theoretical Physics (U.S.S.R.) 8, 423-35 (1938).

21. Fender, B. E. F. and Halsey, G. D., Jr., "Second Virial Coefficients of Argon, Krypton, and Argon-Krypton Mixtures at Low Temperatures", Journal of Chemical Physics 36, 1881-8 (1962).

22. Freeth, F. A. and Verschoyle, T. T. H., "Physical Constants of the System Methane-Hydrogen", Proceedings of the Royal Society (London) 130A, 453-63 (1930).

23. Gonikberg, M. G. and Fastovskii, V. G., "Solubility of Gases in Liquids at Low Temperatures and High Pressures. II. Solubility of Helium in Liquid Nitrogen at Temperatures from 78.0 to 109.0° K and at pressures up to 295 atmospheres", Acta Physicochimica (U.R.S.S.) 12, 67-72 (1940).

24. Gonikberg, M. G. and Fastovskii, V. G., "Solubility of Gases in Liquids at Low Temperatures and High Pressures. IV. Solubility of Helium in Liquid Methane at 90.3 and 106.0° K and at Pressures up to 160 atmospheres", Acta Physicochimica (U.R.S.S.) 13, 399-404 (1940). See also: Foreign Petroleum Technology 9, 214-19 (1941).

25. Hilsenrath, J., Beckett, C. W., Benedict, W. S., Fano, L., Hoge, H. J., Masi, J. F., Nuttall, R. L., Touloukian, Y. S., and Woolley, H. W., Tables of Thermal Properties of Gases, U. S. Department of Commerce, National Bureau of Standards, Circular 564, issued November 1, 1955, United States Government Printing Office, Washington, D. C.

26. Hirshfelder, J. O., Curtiss, C. F., and Bird, R. B., Molecular Theory of Gases and Liquids, New York, John Wiley and Sons, 1954, pp. 170-72, 1119.

27. Ibid., p. 1110.

28. Hirshfelder, J. O., Curtiss, C. F., and Bird, R. B., Molecular Theory of Gases and Liquids, Addenda and Corrigenda, No. 2, Madison, Wisconsin, September, 1954.

29. Karasz, F. E. and Halsey, G. D., "Solubility of Helium and Neon in Liquid Argon. An Approximation to the Entropy of Lattace Vacancy Formation in Liquid Argon", Journal of Chemical Physics 29, 173-9 (1958).

30. Kharakhorin, F. F., "Liquid-Vapor Equilibrium in the Helium-Methane System", Inzhenerno-Fiziki Zhurnal 2, No. 5, 55-9 (1959).

31. Kharakhorin, F. F., "The Phase Relations in Systems of Liquefied Gases. I. The Binary Mixture Nitrogen-Helium", Zhurnal Tekhnicheskoi Fiziki 10, No. 18, 1533-40 (1940). See also: Foreign Petroleum Technology 9, 397-410 (1940).

32. Kihara, T., "Virial Coefficients and Models of Molecules in Gases", Reviews of Modern Physics 25, 831-43 (1953).

33. Kirk, B. S., Predicted and Experimental Gas Phase Compositions in Pressurized Binary Systems Containing an Essentially Pure Condensed Phase. Phase Equilibrium Data for the Methane-Hydrogen System from 66.88° to 116.53° K and Up to 125 Atmospheres, Ph. D. Thesis, School of Chemical Engineering, Georgia Institute of Technology, 1964.

34. Kirk, B. S., Ziegler, W. T., and Mullins, J. C., "A Comparison of Methods of Predicting Equilibrium Gas Phase Compositions in Pressurized Binary Systems Containing an Essentially Pure Condensed Phase", Advances in Cryogenic Engineering 6, 413-28 (1961).

35. Kurata, F. and Kohn, J. P., "This New Apparatus May Help", Petroleum Processing 11, 57-62 (1956).

36. Levitskaya, E. P., "Equilibrium of Liquid-Gas in the Triple System: Ethane-Methane-Hydrogen", Zhurnal Tekhnicheskoi Fiziki 11, 197-204 (1941).

37. McTaggart, H. A. and Edwards, E., "Composition of the Vapor and Liquid Phases of the System Methane-Nitrogen", Proceedings and Transactions of the Royal Society of Canada 13, III, 57-66 (1919).

38. Michels, A., Dumoulin, E., and Van Dijk, J. J., "Gas Liquid Phase Equilibrium in the System NH_3-A", Physica 27, 886-92 (1961).

39. Michels, A., Levelt, J. M., and De Graaff, W., "Compressibility Isotherms of Argon at Temperatures Between -25° C and -155° C, and at Densities Up to 640 Amagat (Pressures up to 1050 atmospheres)", Physica 24, 659-71 (1958).

40. Milne, W. E., Numerical Calculus, Princeton, Princeton University Press, 1949, 393 pages.

41. Mullins, J. C., Ph. D. Thesis (in preparation), School of Chemical Engineering, Georgia Institute of Technology.

42. Prausnitz, J. M. and Myers, A. L., "Kihara Parameters and Second Virial Coefficients for Cryogenic Fluids and Their Mixtures", American Institute of Chemical Engineers Journal 9, 5-11 (1963).

43. Reamer H. H., Selleck, F. T., Sage, B. H., and Lacey, W. N., "Phase Equilibria in Hydrocarbon Systems", Industrial and Engineering Chemistry 44, 198-201 (1952).

44. Ruhemann, M., "Two Phase Equilibrium in Binary and Ternary Systems. I. The System Methane-Ethane", Proceedings of the Royal Society (London) 171, 121-35 (1939).

45. Sage, B. H. and Lacey, W. N., "Phase Equilibria in Hydrocarbon Systems", Industrial and Engineering Chemistry 31, 1497-507 (1939).

46. Shtekkel, F. A. and Tsin, N. M., "Determination of the Composition Diagram for the Liquid-Gas System Methane-Nitrogen-Hydrogen", Journal of Chemical Industry (U.S.S.R.) 16, No. 8, 24-8 (1939).

47. Stroud, L., Miller, J. E., and Brandt, L. W., "Compressibility of Helium at -10° to 130° F and Pressures to 4000 PSIA", Journal of Chemical and Engineering Data 5, 51-2 (1960).

48. Torocheshnikov, N. S. and Levius, L. A., "The Liquid-Vapor Equilibrium in the System Nitrogen-Methane", Journal of Chemical Industry U.S.S.R. 16, No. 1, 19-22 (1939). See also: Foreign Petroleum Technology 8, 305-315 (1940).

49. Van Itterbeek, A., Verbeke, O., and Staes, K., "Measurements on the Equation of State of Liquid Argon and Methane up to 3000 kg cm^{-2} at Low Temperatures", Physica 29, 742-54 (1963).

50. Vellinger, E. and Pons, E., "Sur la solubilité de l'azote dans le mèthane el le propane liquides", Comptes Rendus des Séances de L'Académie des Sciences 217, 689-91 (1943).

51. White, D., Rubin, T., Camky, P., and Johnston, H. L., "The Virial Coefficients of Helium from 20° K to 300° K", Journal of Physical Chemistry 64, 1607-12 (1960).

52. Ziegler, W. T., Mullins, J. C., and Hwa, S. C. P., Cryogenic Phase of DOD Titanium Sheet Rolling Program. Part II. Thermal Conductivity of Titanium Alloys at Low Temperatures., Final Report, Projects No. A-504 and E-238, Engineering Experiment Station, Georgia Institute of Technology, January 16, 1962. (Purchase Order No. ZKA-0143A, Lockheed Aircraft Corporation, Georgia Division).

53. Ziegler, W. T., Mullins, J. C., and Kirk, B. S., Calculation of the Vapor Pressure and Heats of Vaporization and Sublimation of Liquids and Solids, Especially Below One Atmosphere Pressure. II. Argon., Technical Report No. 2, Project No. A-460, Engineering Experiment Station, Georgia Institute of Technology, June 15, 1962. (Contract No. CST-7238, National Bureau of Standards, Boulder, Colorado).

VITA

William David McCain, Jr. was born in Greenville, Mississippi on February 20, 1933. He attended public schools in Jackson, Mississippi, graduating from Central High School in June, 1951. In June, 1956 he was graduated from Mississippi State University with a Bachelor of Science in Chemical Engineering. He was a part-time graduate student at Louisiana State University during 1956 to 1959. He received the degree of Master of Science in Chemical Engineering from the Georgia Institute of Technology in June, 1961.

The author was employed by Esso Research Laboratories, Baton Rouge, Louisiana, as an engineer and project leader in 1956 to 1959, and for the summer of 1960. He holds two United States patents for his work in petroleum refining process development.

The author was an artilleryman in the United States Army from 1951 to 1953. He was discharged with the rank of Sergeant First Class. He now holds the rank of Captain of Artillery in the Mississippi National Guard and the rank of Captain, Signal Corps, in the United States Army Reserve.

The author is a member of Sigma Xi, Tau Beta Pi, Omicron Delta Kappa, Kappa Mu Epsilon, and Phi Eta Sigma honorary fraternities, and the Society of Petroleum Engineers. He is a Registered Professional Engineer in the State of Mississippi. He was the recipient of the Texas Company Fellowship in 1959-1960 and the Air Reduction Company Cryogenic Engineering Fellowship in 1960-1963 at the Georgia Institute of Technology.

During his graduate study at the Georgia Institute of Technology he taught in the School of Mathematics and in the School of Chemical Engineering. He was a consultant for the Savannah Sugar Refining Corporation, Savannah, Georgia, in 1963.

The author is married and is the father of three children. He and his family now reside in Starkville, Mississippi, where he is an Associate Professor of Petroleum Engineering and an Associate Member of the Graduate Faculty at Mississippi State University.